NTNU – Trondheim
Norwegian University of
Science and Technology

Time Scales for Scour Below Pipelines and Around Vertical Piles in Nonlinear Random Waves and Current

Silje Dyrseth

Marine Technology
Submission date: June 2015
Supervisor: Dag Myrhaug, IMT
Co-supervisor: Muk Chen Ong, IMT

Norwegian University of Science and Technology
Department of Marine Technology

NTNU Trondheim
Norwegian University of Science and Technology
Department of Marine Technology – Group of Marine Structures

MASTER THESIS IN MARINE TECHNOLOGY

SPRING 2015

FOR

STUD. TECHN. SILJE DYRSETH

TIME SCALES FOR SCOUR BELOW PIPELINES AND AROUND VERTICAL PILES IN NONLINEAR RANDOM WAVES AND CURRENT

Pipelines and vertical piles on sandy seabeds are exposed to random waves and current, and consequently these structures are exposed to scour as well as backfilling of scour holes. The assessment of the time-scales for the scour below pipelines and around vertical piles are essential in design of marine pipelines and foundations of vertical piles and in scour protection work.

The student shall:

1. Give an overview of the scour mechanisms below marine pipelines and around vertical piles including the backfilling process around a vertical pile
2. Give the background of time-scales for scour around marine pipelines and around vertical piles on flat seabeds for regular waves as well as backfilling of scour holes around vertical piles in random waves and current.
3. Apply the time-scale formulas discussed in Part 2 together with the Forristall (2000) wave crest height distribution for long-crested (2D) and short-crested (3D) nonlinear random waves to give results for random waves alone and for random waves plus current.
4. Present and discuss results for the time-scales for linear random waves as well as for 2D and 3D nonlinear random waves, including waves alone and waves plus current.

The work scope may prove to be larger than initially anticipated. Subject to approval from the supervisor, topics may be deleted from the list above or reduced in extent.

In the thesis the candidate shall present her personal contribution to the resolution of problem within the scope of the thesis work.

Theories and conclusions should be based on mathematical derivations and/or logic reasoning identifying the various steps in the deduction.

The candidate should utilize the existing possibilities for obtaining relevant literature.

The thesis should be organized in a rational manner to give a clear exposition of results, assessments, and conclusions. The text should be brief and to the point, with a clear language. Telegraphic language should be avoided.

The thesis shall contain the following elements: A text defining the scope, preface, list of contents, summary, main body of thesis, conclusions with recommendations for further work, list of symbols and acronyms, reference and (optional) appendices. All figures, tables and equations shall be numerated.

The supervisor may require that the candidate, in an early stage of the work, present a written plan for the completion of the work. The plan should include a budget for the use of computer and laboratory resources that will be charged to the department. Overruns shall be reported to the supervisor.

The original contribution of the candidate and material taken from other sources shall be clearly defined. Work from other sources shall be properly referenced using an acknowledged referencing system.

The thesis shall be submitted in two copies:

- Signed by the candidate
- The text defining the scope included
- In bound volume(s)
- Drawings and/or computer prints which cannot be bound should be organized in a separate folder.

Advisors: Dr. Muk Chen Ong, Marintek
Professor Dag Myrhaug

Deadline: 10.06.2015

Dag Myrhaug
Supervisor

Abstract

This report presents a stochastic method for predicting the time scale of scour and backfilling, occurring around vertical piles and marine pipelines on the seabed. The erosion occurs due to waves alone or waves combined with a current. Existing formulas for the time scale are expanded allowing input of random waves. The waves are assumed to be stationary and narrow-banded such that the statistical distributions Rayleigh and Forristall (2000) can be employed. When applying the Rayleigh distribution, the waves are assumed to be linear, while Forristall distributes the wave crest heights representing long-crested (2D) and short-crested (3D) waves where the second-order effects sum-frequency and difference-frequency are included. The waves typically exhibit a nonlinear behaviour in severe seastates and in shallow water.

The time scale is calculated based on typical field parameters and presented graphically for linear, nonlinear long-crested and nonlinear short-crested waves. When second-order effects are included, the wave crests appear higher and sharper than to linear sinusoidal waves. This causes the water particle velocity below second-order waves to be higher, resulting in shorter time scale, which is reflected in the results. The results for the time scale of long-crested and short-crested waves are also compared, and all the results display that the $3D$ waves are higher, resulting in lower time scales when the nonlinear effects increase.

Abstract (Norwegian)

Denne avhandlingen presenterer en stokastisk metode for å beregne tidsskalaen av erosjon (scour), som oppstår på havbunnen i sanden rundt marine strukturer. Erosjonen er forårsaket av bølger alene, eller bølger kombinert med strøm. Eksisterende formler for tidsskalaen er omformulert slik at stokastiske bølger kan inkluderes. For å kunne anvende de statistiske fordelingene Rayleigh og Forristall (2000), må bølgene antas å være smalbåndede og stasjonære. I Rayleigh fordelingen er bølgene lineære sinusbølger, mens i Forristall fordelingen kan bølgene beskrives med ulik grad av andre ordens effekter for langkammede (2D) og kortkammede (3D) bølger. Ulineariteten i bølgene øker i kraftige sjøtilstander og på grunt vann der bølgene treffer havbunnen og vokser.

Tidsskalaen er beregnet basert på representative eksempelverdier, og fremstilt grafisk for lineære, ulineære langkammede og ulineære kortkammede bølger. Når andreordens effekter er inkludert, blir bølgetoppene skarpere og høyere, sammenlignet med sinusbølger. Dette vil øke hastigheten under bølgene og dermed resultere i kortere tidsskala, noe som gjenspeiles i alle resultatene. Resultatene for kortkammede og langkammede bølger er også sammenlignet og viser at når ulineære effekter økes, vil de kortkammede bølgene være størst, og dermed føre til kortere tidsskala.

Acknowledgments

This thesis has been written as the final part of a Masters degree at the Norwegian University of Science and Technology (NTNU) in the Department of Marine Technology, during the spring of 2015.

The work has been carried out under the supervision of Professor Dag Myrhaug whom I would like to thank for his patience and for all the time he has spent sharing his knowledge and deep understanding of the mechanism behind scour and the stochastic method. I would also like to thank advisor Dr. Muk Chen Ong for his help and enthusiasm. I am grateful that I got the opportunity to write about this subject under the supervision of such good advisers.

Contents

1 Introduction **1**

2 Background **3**
2.1 The bed shear stress 3
2.1.1 Bed shear stress below regular waves 3
2.2 The equilibrium scour depth 5
2.3 The time scale of scour 6
2.4 The time scale of backfilling 7
2.5 Shields parameter 8

3 Mechanisms of Scour Around Marine Structures **11**
3.1 Scour around slender vertical piles 11
3.1.1 Scour around vertical piles in steady currents 11
3.1.2 Scour around vertical piles below regular waves . . . 13
3.1.3 Scour around piles below irregular waves 17
3.1.4 Scour around piles in combined waves and current . 18
3.2 Scour around large piles 20
3.3 Scour below marine pipelines 24
3.3.1 Scour below marine pipelines due to steady currents 25
3.3.2 Scour below marine pipelines in regular waves 27

4 Statistical Distributions of Wave Heights **31**
4.1 The Rayleigh distribution 31
4.1.1 The truncated Rayleigh distribution 32
4.2 The Forristall distribution 33
4.2.1 The truncated Forristall distribution 38

5 The Time Scale of Scour and Backfilling **39**
5.1 The time scale of scour 40
5.1.1 Method 40
5.1.2 The time scale of scour below pipelines (CASE 1) . 41
5.1.3 The time scale of scour around vertical slender piles (CASE 2) 44
5.2 The time scale of backfilling 45
5.2.1 Method 45

5.2.2 The time scale of backfilling around slender vertical piles below waves when the initial scour hole was generated by current (CASE 3) 46
5.2.3 The time scale of backfilling around slender piles below waves when the initial scour hole was generated by waves (CASE 4) 48
5.2.4 Backfilling around vertical slender piles in combined waves and current when initial scour hole is generated by current (CASE 5) 50
5.2.5 Backfilling around large piles in combined waves and current when initial scour hole is generated by current (CASE 6) 52

6 The Stochastic Method **55**
6.1 The time scale in random waves 55
6.1.1 Linear random waves 56
6.1.2 2D and 3D nonlinear random waves 56
6.1.3 Comparison of nonlinear and linear results 57
6.2 The time scale in random waves plus current 57
6.2.1 Linear random waves plus current 58
6.2.2 2D and 3D nonlinear waves plus current 58

7 Method, Example Values and Limits **61**
7.1 Scour below pipelines in waves (CASE 1) 62
7.2 Scour and backfilling around slender piles below waves (CASE 2 and 3) 63
7.3 Backfilling around a slender pile below waves when the initial hole is generated by waves (CASE 4) 64
7.4 Backfilling in waves plus current (CASE 5 and 6) 65

8 Results and Discussion **67**
8.1 The time scale of scour 68
8.1.1 The time scale of scour below pipelines (CASE 1) . 68
8.1.2 Scour around vertical slender piles (CASE 2) 72
8.2 The time scale of backfilling 78
8.2.1 Backfilling by waves when the initial hole was generated by current (CASE 3) 78
8.2.2 Backfilling by waves when the initial hole was generated by waves (CASE 4) 84

8.2.3 Backfilling around a slender pile by waves and current when initial hole was generated by a current (CASE 5) 88
8.2.4 Backfilling around a large pile by waves and current when initial hole was generated by current (CASE 6) 92

9 Conclusions and Further Work **95**
9.1 Conclusion 95
9.2 Further work 96

References **97**

Appendix A **I**
A. 1- CASE 1 I
A. 2 - CASE 2 II
A. 3 - CASE 3 III
A. 4 - CASE 4 V
A. 5 - CASE 5 VII
A. 6 - CASE 6 IX

Appendix B **XIII**
B. 1- CASE 1 XIII
B. 2- CASE 2 XX
B. 3- CASE 3 XXXI
B. 4- CASE 4 XLIII
B. 5- CASE 5 LI
B. 6- CASE 6 LXIV

List of Figures

2.1 Definition sketch of S below a pipeline, taken from Myrhaug et al. (2009). 5
2.2 Definition sketch of S around a circular vertical pile, taken from Myrhaug et al. (2009). 5
2.3 Definition sketch of S around a vertical pile. (a) Scour hole generated by waves or current. (b) Scour hole after backfilling. Taken from Sumer et al. (2012). 6
2.4 Time development of scour depth. Taken from Sumer and Fredsøe (2002). 7
2.5 The scour depth S_t (cm), given for values of time (s). Time series monitored at the offshore side of the pile during backfilling. Taken from Sumer et al. (2012). 8
2.6 Variation of the equilibrium scour depth normalized by the diameter (S/D) for a pipeline, versus Shields parameter (θ). The initial clearance between the seabed and the pipe is zero. Taken from Sumer and Fredsøe (2002). 9
3.1 Principal sketch of boundary layer flow interacting with vertical pile. Taken from Sumer et al. (1997). 12
3.2 Distributions of amplification factors, α, at the normalized distances (x/D, y/D) from the center of the pile axis. $D =$ 7.5 cm, $U_c = 30\ cm/s$, $\delta = 20\ cm/s$, $\delta/D = 2.7$, $Re_D =$ 23 000. Taken from Sumer et al. (1997). 12
3.3 Formation of horseshoe vortices as a function of KC-number and wave phase. $\circ$ marks flow visualization measurements and + marks the bed shear stress measurement. Taken from Sumer et al. (1997). 14
3.4 Bed shear stress at the horseshoe-vortex side of pile. Taken from Sumer et al. (1997). 15
3.5 Equilibrium depth normalized by the diameter (S/D), versus KC. Eq. (13) represents the solid line. Taken from Sumer et al. (1992). 16
3.6 Equilibrium scour depth normalized by the diameter (S/D), versus KC during backfilling (KC_f). solid line: Eq. (13). Backfilling experiments from initially scoured bed where the initial scour hole was generated by currents ($\circ$) or waves ($\triangleleft$). Taken from Sumer et al. (2012). 17

3.7 Equilibrium scour depth normalized by the diameter (S/D), versus current wave velocity (U_{cw}). Waves and current propagates in the same direction. Taken from Sumer and Fredsøe (2001a). 19
3.8 Equilibrium depth normalized by the diameter (S/D), versus KC. Taken from Sumer et al. (1992). 20
3.9 Sketch of incident, diffracted and reflected wave fronts around a pile. Taken from Sumer and Fredsøe (2002). 21
3.10 Different flow regimes. Taken from Isaacson (1979). 22
3.11 Vector diagram of the period-averaged velocities. Taken from Sumer and Fredsøe (2001b). 23
3.12 S/D versus KC for $D/L = 0.15$. Taken from Sumer and Fredsøe (2001b). 24
3.13 S/D versus D/L for $KC = 0.4$. Taken from Sumer and Fredsøe (2001b). 24
3.14 Pressure distributions for bottom-seated pipe. Taken from Sumer and Fredsøe (2002). 25
3.15 Piping, the break through process. Taken from Sumer and Fredsøe (2002). 26
3.16 Scour development in steady current. Times in minutes. $\theta = 0.098$. Taken from Sumer and Fredsøe (2002). 27
3.17 Lee wake effect. Taken from Sumer and Fredsøe (2002). . . 28
3.18 Equilibrium scour depth. $\theta > \theta_{cr}$. Taken from Sumer and Fredsøe (1990). 29
4.1 Different components of the surface elevation in a simulated time series. Taken from Wist (2003). 33
4.2 The quadratic transfer function for a fixed sum frequency $\omega_1 + \omega_2 = 1 - 12 rad/s$. - - deep water; $\cdot\bullet\cdot\cdot$ $d = 70\,m$; $\cdot\Delta\cdot\cdot$ $d = 42\,m$; $\cdot\Box\cdot\cdot$ $d = 31\,m$; $\cdot+\cdot\cdot$ $d = 16\,m$. Taken from Wist (2003). 35
4.3 Principal sketch of $2D$ and $3D$ waves in deep and finite water. Taken from Hesten (2011). 35
5.1 Non-dimensional plot of time scale against Shields parameter for waves. The bed is originally plane and the gap between the pipe and bed is zero. Taken from Fredsøe et al. (1992). 42

5.2 Non-dimensional plot of time scale against Shields parameter. Steady current and waves. Plane bed, the gap between pipe and bed is zero. The data for the current experiments are obtained in Mao (1986) and Kjeldsen et al. (1973). Wave data and figure are taken from Fredsøe et al. (1992). 43
5.3 Time scale of scour around pile. Taken from Sumer et al. (1992). 44
5.4 Time scale of backfilling. Initial equlibrium scour depth is generated by a current ($KC = \infty$). Taken from Sumer et al. (2012). 47
5.5 Time scale of backfilling. A: Initial equilibrium scour depth generated by current, Eq. (69) B: Initial equilibrium scour depth is generated by waves, Eq. (73). Taken from Sumer et al. (2012). 49
5.6 Time scale of backfilling in combined waves and current. Initial scour hole generated by current. Horizontal lines: Eq. (69), curved lines: Eq.(77). Taken from Sumer et al. (2012). 51
5.7 Time scale of backfilling in combined waves and current around large piles. Initial scour hole generated by current. Taken from Sumer et al. (2012). 53
8.1 Isocurves for the ratios R_1, Eq. (88) and R_2, Eq. (89) for the dimensionless time scale t of scour below a pipeline. a)$R_{1,2D}$ - nonlinear long-crested to linear. b)$R_{1,3D}$ - nonlinear short-crested to linear. c) R_2 - short-crested to long-crested. 70
8.2 The expected value of the time scale T^* of scour below a pipeline for linear and second-order waves. 71
8.3 The expected value of the time scale T (min) of scour below a pipeline for linear and second-order waves. Given for $D = 0.5\,m$, $D = 0.75\,m$ and $D = 1\,m$. 72
8.4 Isocurves for the ratios R_1, Eq. (88) and R_2, Eq. (89) for the dimensionless time scale t of scour around a slender vertical pile. a)$R_{1,2D}$: Nonlinear long-crested to linear. b)$R_{1,3D}$: Nonlinear short-crested to linear. c) R_2: Short-crested to long-crested. 73

8.5 The expected value of the dimensionless time scale T^* of scour around a vertical slender pile for linear and second-order waves for $D = 0.5\,m$, $D = 0.75\,m$ and $D = 1\,m$. a) $\theta_{rms} = 0.07$ b) $\theta_{rms} = 0.13$ and $\theta_{rms} = 0.18$ 75
8.6 The expected value of the time scale T (min) of scour around a vertical slender pile for linear and second-order waves for $D = 0.5\,m$, $D = 0.75\,m$ and $D = 1\,m$. a) $\theta_{rms} = 0.07$. b) $\theta_{rms} = 0.18$. 77
8.7 Isocurves for the ratios R_1, Eq. (88) and R_2, Eq. (89) for the dimensionless time scale t of backfilling around a slender verical pile. a)$R_{1,2D}$: Nonlinear long-crested to linear. b)$R_{1,3D}$: Nonlinear short-crested to linear. c) R_2: Short-crested to long-crested. 79
8.8 The expected value of the time scale T^* of backfilling around a vertical slender pile when the initial hole was generated by a current for $D = 0.5\,m$, $D = 0.75\,m$ and $D = 1\,m$. a) $\theta_{rms} = 0.07$. b) $\theta_{rms} = 0.15$. 81
8.9 The expected value of the time scale T^* of backfilling around a vertical slender pile when the initial hole was generated by a current for $\theta_{rms} = 0.07$, $\theta_{rms} = 0.10$ and $\theta_{rms} = 0.15$. a) $D = 0.5\,m$ b) $D = 1\,m$. 82
8.10 The expected value of the time scale T (min) of backfilling around a vertical slender pile when the initial hole was generated by a current for $D = 0.5\,m$, $D = 0.75\,m$ and $D = 1\,m$. a) $\theta_{rms} = 0.07$. b) $\theta_{rms} = 0.15$. 83
8.11 The expected value T^* of backfilling around a slender vertical pile when the initial hole was generated by $KC_{irms} = 32$, $KC_{irms} = 20$ and $KC_{irms} = 0.11$. a) Linear and nonlinear results for $D = 1\,m$. $KC_{rms} = \infty$ added for comparison. b)Nonlinear results for $D = 0.5\,m$, $D = 0.75\,m$ and $D = 1\,m$. 86
8.12 The expected value T (min) of backfilling around a slender vertical pile when the initial hole was generated by $KC_{irms} = 32$, $KC_{irms} = 20$ and $KC_{irms} = 0.11$. a) $D = 0.5\,m$. b) $D = 1\,m$. 87
8.13 The expected value of the time scale T^* of backfilling around a slender pile in waves and current combined when the initial hole was generated by a current. (KC_{rms1}, θ_{rms1})=(4, 0.07), (KC_{rms2}, θ_{rms2})=(7, 0.07) and (KC_{rms3}, θ_{rms3})=(4, 0.09). a)$D = 0.5\,m$. b) $D = 1.0\,m$. 90

8.14 The expected value of the time scale T (min) for backfilling around a slender pile in waves and current combined when the initial hole was generated by a current for $D = 0.5\,m$, $D = 0.75\,m$ and $D = 1.0\,m$. a) (KC_{rms1}, θ_{rms1})=(4, 0.07). b) (KC_{rms2}, θ_{rms2})=(7, 0.07). 91
8.15 The expected value of the time scale T^* of backfilling around a large pile in waves and current combined when the initial hole is generated by a current. a) $D = 3\,m$. b) $D = 5\,m$. . . 93
8.16 The expected value of the time scale T (min) of backfilling around a large pile in waves and current combined when the initial hole is generated by a current. a) $KC_{rms} = 0.7$. b) $KC_{rms} = 1.5$. 94
9.1 The time scale T^* of scour around a vertical slender pile in current and waves combined for $\theta = 0.07$, $\theta = 0.10$ and $\theta = 0.15$. 96

List of Tables

7.1 Example values for a typical field condition, Myrhaug et al. (2009). 62
7.2 Given values of θ_{rms} for CASE 2 and 3. 63
7.3 Given values of KC_{irms} for CASE 4. 64
7.4 Given values of θ_{rms} and KC_{rms} for CASE 5 and 6. 65
A.1 Given parameters CASE 1 I
A.2 Resulting values CASE 1 I
A.3 Given parameters CASE 2 II
A.4 Resulting values CASE 2 II
A.5 Resulting values CASE 2 III
A.6 Given parameters CASE 3 III
A.7 Resulting values CASE 3 IV
A.8 Resulting values CASE 3 V
A.9 Given parameters CASE 4 V
A.10 Resulting values CASE 4 VI
A.11 Given parameters CASE 5 VII
A.12 Resulting values CASE 5, $D = 0.5\,m$ VII
A.13 Resulting values CASE 5, $D = 0.75\,m$ VIII
A.14 Resulting values CASE 5, $D = 1\,m$ IX
A.15 Given parameters CASE 6 IX
A.16 Resulting values CASE 6, $D = 3\,m$ X
A.17 Resulting values CASE 6, $D = 4\,m$ XI
A.18 Resulting values CASE 6, $D = 5\,m$ XII

List of Symbols

α	amplification factor
α_{2D}	parameter for $2D$ waves in the Forristall distribution
α_{3D}	parameter for $3D$ waves in the Forristall distribution
δ	boundary layer thickness
θ	Shields parameter: the undisturbed dimensionless shear stress
θ_c	normalized Shields parameter,$\theta_c = \theta_m/\theta_{rms}$
θ_{cr}	lower value for motion of sand
θ_f	value of θ during backfilling
θ_{frms}	r.m.s. value of θ during backfilling
θ_m	maximum Shields parameter in waves
θ_{rms}	random mean square (r.m.s.) value of Shields parameter
ϕ	angle between direction of current and waves
σ_u	r.m.s. value of the orbital velocity at the seabed
η_n	nonlinear surface elevation
ρ	water density
ρ_s	density of sediment grains
τ	bed shear stress
τ_∞	undisturbed bed shear stress
$\tau_{max,\infty}$	maximum undisturbed bed shear stress in waves
τ_{rms}	r.m.s. value of undisturbed bed shear stress
ν	kinematic viscosity
ω	angular frequency of waves, $\omega = 2\pi/T_w$
ω_p	frequency of waves in a narrow-banded sea state, $\omega = 2\pi/T_p$
ω_r	relative frequency of waves in a narrow-banded seastate with current
A	maximum near bed horizontal water particle displacement
A_{rms}	r.m.s. value of the maximum near bed horizontal water particle displacement
a	wave amplitude
a_{rms}	r.m.s. value of the linear wave amplitude
$\hat{a}$	normalized wave amplitude
$\hat{a}_{1/n}$	the value of $\hat{a}$ exceeded by the probability $1/n$
$(\hat{a}_1,\ \hat{a}_2)$	lower and upper value of $\hat{a}$ in the truncated distribution
D	diameter of pile or pipeline
d_{50}	median diameter of grain
f	wave frequency, $1/T_w$
f_v	vortex shedding frequency
f_w	seabed friction

g	acceleration of gravity
H_s	significant wave height
h	water depth
KC	Keulegan-Carpenter number
KC_{rms}	r.m.s. value of Keulegan-Carpenter number
KC_i	initial Keulegan-Carpenter number
KC_{irms}	initial r.m.s. value of KC number
KC_f	final Keulegan-Carpenter number (during backfilling)
KC_{frms}	final r.m.s. value of KC number (during backfilling)
k	wave number, $k = 2\pi/L$
k_p	wave number in a narrow-banded seastate
L	wave length
L_p	wave length in a narrow-banded seastate
n	fraction of wave heights in a seastate
Re_D	Pipe/pile Reynolds number
S	equilibrium scour depth
S_t	instantaneous scour depth
S_i	initial scour depth
S_f	scour depth after backfilling
S_1	Wave steepness
s	ratio quartz sand/fluid density
T	the time scale)
T_p	peak period of irregular waves
T_w	wave period
T^*	normalized time scale of scour
t	dimensionless timescale
u	orbital velocity of a water particle due to waves in a water depth z
U	horizontal velocity component of u near the seabed
U_m	maximum near bed horizontal velocity below waves
U_{rms}	rms value of the near bed horizontal velocity below waves
U_c	undisturbed current velocity
U_{cw}	current wave velocity in regular waves
U_{cwrms}	current wave velocity in irregular waves
U_r	Ursells number
U_R	period averaged radial velocity
U_θ	period averaged tangential velocity
$\hat{U}_m$	non-dimensional maximum horizontal water particle velocity
w_c	normalized second-order wave amplitude
$w_{c\,1/n}$	the value of w_c exceeded by the probability $1/n$
$(w_{c1},\ w_{c2})$	lower and upper value of w_c in the truncated distribution
z	depth from mean water level
z_0	bed roughness, $z_0 = d_{50}/12$
(c, d)	coefficients for calculating the seabed friction

1 Introduction

Scour is a type of erosion that occurs around structures on a sandy seabottom due to flow velocities induced by waves, current or a combination. The flows interaction with the seabed creates a boundary layer flow, which interacts with the structure near the bottom, creating complicated flow patterns that will depend on the geometry of the structure. When the seabed is exposed for this three-dimensional flow, the shear stress increases, allowing sand particles to move more easily. When the flow climate is described by one ratio between the orbital fluid particle displacement and the diameter, the scour will develop to a maximum depth where it remains constant. When the flow climate changes, the final depth will also change and backfilling of the initial scour hole may occur.

Scour and backfilling occurs around a variety of marine structures but here it is investigated for offshore piles and pipelines. The main contribution to scour below pipelines and around vertical slender piles occurs due to flow patterns mainly contributed by vortex shedding, while scour around vertical large piles appears due to flow fields related to the diffraction of waves. Pipelines are mainly used to transport hydrocarbons and therefore failures, which might happen due to free spans, which may lead to severe consequences. Free spans allow the flow to surround the whole pipe such that vortex induced vibrations might result. For vertical piles, scour results in decreased stability. Vertical piles are now important as fundaments to many marine structures such as platform legs and wind turbine columns.

The assessment of the time scales for scour and backfilling is of interest in this thesis and it is essential in the the design of marine pipeline and foundations of vertical piles and in scour protection work. The time scale is the time it takes before the scour reaches a certain depth. The time scale of scour created due to the presence of waves is of special interest because during a storm, it may occur quickly and thereby be critical.

The formulas of the time scale are obtained by linear fit of experimental data. For the time scale of scour in regular waves, empirical formulas were proposed in Fredsøe et al. (1992) for pipelines and in Sumer et al. (1992) for vertical slender piles. The time scale of backfilling around piles by irregular waves and current were presented in Sumer et al. (2012). These formulas are expanded with the stochastic method, allowing input of random waves.

The waves are assumed to be stationary and narrow-banded such that the statistical distributions by Rayleigh and Forristall (2000) can be employed. When applying the Rayleigh distribution, the waves are assumed to be linear while Forristall distributes the wave crest heights representing short-crested (2D) and long-crested (3D) waves where the second-order effects sum-frequency and difference-frequency are included. The waves typically exhibit a nonlinear behaviour in severe seastates and in shallow water.

The purpose of this thesis is to derive the formulas for the time scale with the stochastic method and thereby present the time scale graphically for linear, nonlinear long-crested and nonlinear short-crested waves.

2 Background

The theory in this chapter is taken from Sumer and Fredsøe (2002) unless otherwise mentioned.

2.1 The bed shear stress

A requirement for scour to occur is that sand particles must be transported. The seabeds shear stress describes the ability of sediment transport. The presence of a structure will change the flow field and therefore increase the bed shear stress such that sediment transport may occur close to the structure. The increase can be described by the amplification factor:

$$\alpha = \frac{\tau}{\tau_\infty} \tag{1}$$

where τ_∞ is the bed shear stress of the undisturbed flow meaning the shear stress that occurs due to a flow unaffected by the structure. τ is the actual value of the shear stress in the bed created by the disturbed flow. Scour will continue to develop until a depth where $\tau = \tau_\infty$. This depth is referred to as the equilibrium scour depth, S.

In this thesis, the undisturbed value of the shear stress will be applied when calculating the time scale. The reason for this is that the method proposed is based on formulas derived from laboratory experiments where the scour depth is measured versus its corresponding undisturbed shear stress, which is found based on the incoming waves. A result of this is that in a real life scenario, the time scale can be predicted when the sea state is given. However, the distribution of the actual value of the shear stress around the structure is of importance when it comes to the mechanisms of scour and will therefore be elaborated in Ch. 3.

2.1.1 Bed shear stress below regular waves

The shear stress is dependent on the velocity of the incoming flow. The incoming flow is due to current, waves, or a combination. When the flow is caused by waves, the undisturbed maximum shear stress is expressed

as:

$$\tau_{max,\infty}/\rho = \frac{1}{2} f_w U_m^2 \tag{2}$$

where ρ is the density of the seawater and U_m is the maximum horizontal velocity of the water particles on the seabed during one wave period. The maximum shear stress is of interest because it will contribute most to scour. From linear wave theory, the water particle velocity u in a water depth z is given by Faltinsen (1993) as:

$$u = \omega a \frac{\cosh k(h+z)}{\sinh(kh)} \sin(\omega t - kx) \tag{3}$$

where ω is the frequency, a is the linear wave amplitude, k is the wave number and h is the water depth. Close to the sea bottom $z \approx -h$ such that the maximum value of the horizontal velocity near the sea bottom during a wave cycle is:

$$U_m = \omega \frac{a}{\sinh(kh)} = \omega A \tag{4}$$

where A is the maximum horizontal distance the water particle moves during one wave period. k is the wave number and it is expressed $k = 2\pi/L$ where L is the wavelength. It can be found by the dispersion relation:

$$\omega^2 = gk \tanh(kh) \tag{5}$$

where g is the acceleration of gravity. The shear stress is as shown in Eq. (2) linear to the friction f_w. The following friction factor given by Soulsby (1997) is:

$$f_w = c(\frac{A}{z_0})^{-d} \tag{6}$$

where

$$(c, d) = (1.39, 0.52) \quad \text{for} \quad 10 \leq \frac{A}{z_0} \leq 10^5 \tag{7}$$

where c and d are coefficients based on best fit to data and $z_0 = d_{50}/12$ is an expression for the roughness of the sand where d_{50} is the median sand grain diameter. Myrhaug et al. (2001) divided the interval of A/z_0 from Eq. (7) in 3 subintervals with different coefficients c and d for each. These

could be applied in this thesis but for simplicity, Eq. (7) is chosen. From Eq. (6), it can be seen that for a given z_0, the wave friction increases when A decreases. This can be explained by increased turbulence at the sea bottom when A is small. Eqs. (6) and (7) are valid for sinusoidal waves and rough turbulent flow. They are obtained based on laboratory measurements without the presence of a structure and can thereby be applied to find the undisturbed shear stress below waves given by Eq. (2).

2.2 The equilibrium scour depth

The scour process will evolve in different stages where the scour depth increases until it reaches its final value S; the equilibrium scour depth. At this stage, the sediment transport into the scour hole equals the sediment transport out of the hole, Myrhaug and Ong (2012). Definition sketches of S are given for a pipeline in Fig. 2.1 and for a vertical pile in Fig. 2.2.

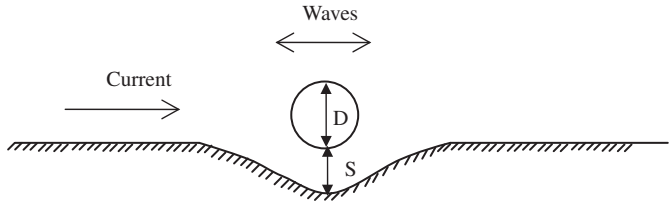

Figure 2.1: Definition sketch of S below a pipeline, taken from Myrhaug et al. (2009).

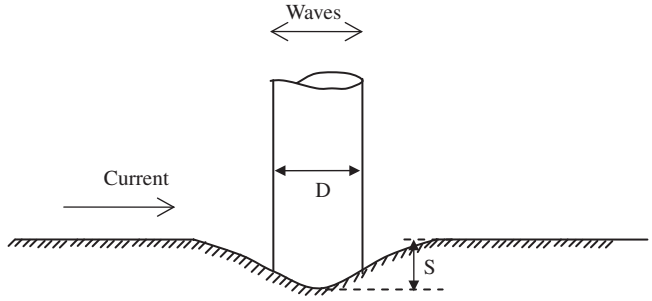

Figure 2.2: Definition sketch of S around a circular vertical pile, taken from Myrhaug et al. (2009).

The value of S is dependent on the flow climate, which changes over time. An important parameter describing this is the Keulegan-Carpenter number (KC). It is defined as:

$$KC = \frac{U_m T_w}{D} \tag{8}$$

where D is the diameter of the structure and T_w is the wave period. Under the assumption of linear theory, U_m from Eq. (8) can be substituted with Eq. (4), resulting in:

$$KC = \frac{2\pi A}{D} \tag{9}$$

For very large KC numbers the flow of each half period resembles a current, while for small KC numbers the movements of the water particles are small relative to D. If the flow climate changes such that the KC number is decreased, the value of S decreases and backfilling of the initial scour hole occurs. This is illustrated in Fig. 2.3

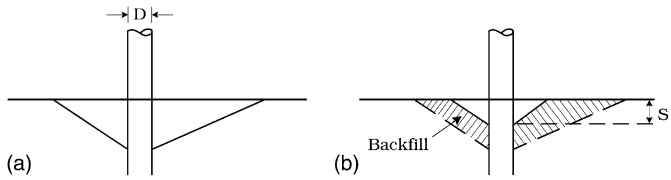

Figure 2.3: Definition sketch of S around a vertical pile. (a) Scour hole generated by waves or current. (b) Scour hole after backfilling. Taken from Sumer et al. (2012).

The value of S can be determined by empirical formulas, that are functions of the KC number. The formulas will vary for different marine structures such as pipelines and vertical piles.

2.3 The time scale of scour

The time scale T is the time it takes for scour to reach a certain depth. It is defined from the value of the equilibrium depth S:

$$S_t = S(1 - e^{-\frac{t}{T}}) \tag{10}$$

where S_t is the instantaneous scour depth at the time t. The equation is presented by Fig. 2.4 where the time scale is the value of t made by the cross section of the tangent to S_t in $t = 0$ and the equilibrium scour depth S. The time scale can therefore be predicted by calculating the slope of the line tangent to the $S_t(t)$ curve at $t = 0$, or by integrating $S_t(t)$ over time. Note that the time scale is defined before the equilibrium scour depth is reached.

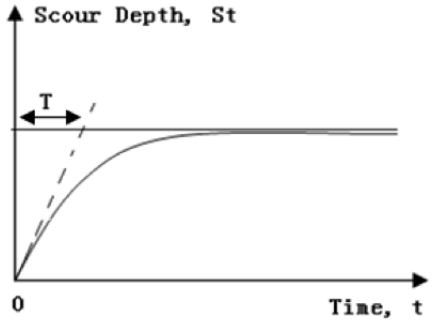

Figure 2.4: Time development of scour depth. Taken from Sumer and Fredsøe (2002).

2.4 The time scale of backfilling

The time scale T is also defined as the time it takes before backfilling has reached a certain depth. It is a function of the equilibrium scour depth S and is given by Sumer et al. (2012) as:

$$S_t = S + (S_i - S)\, e^{-\frac{t}{T}} \tag{11}$$

where S_i is the initial scour depth and S is the equilibrium scour depth when the backfilling is completed. The equation is presented by Fig. 2.5 where the time scale is the value of T made by the cross section of the tangent to S_t in $t = 0$ and S.

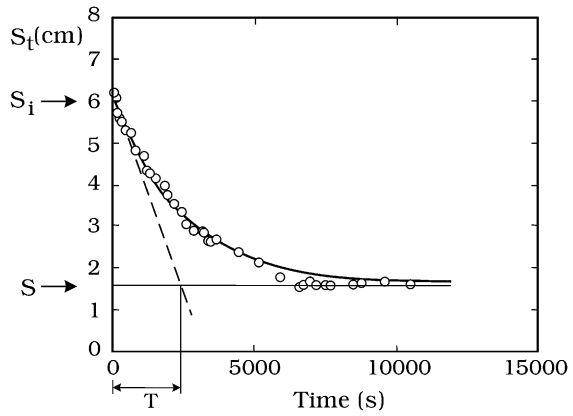

Figure 2.5: The scour depth S_t (cm), given for values of time (s). Time series monitored at the offshore side of the pile during backfilling. Taken from Sumer et al. (2012).

2.5 Shields parameter

The ability of sediment transport is as mentioned in Section 2.1, dependent of the shear stress. The shear stress can be defined dimensionless by the Shields parameter:

$$\theta = \frac{\tau_\infty/\rho}{g(s-1)d_{50}} \tag{12}$$

where $s = \rho_s/\rho$ is the ratio between the sediment (ρ_s) and fluid (ρ) density. For a given grain type and fluid (seawater), the denominator in Shields parameter is constant while the nominator given by Eq. (2) increases with U_m in second power and linearly with f_w. Figure 2.6 presents a relation between the equilibrium scour depth and the Shields parameter obtained by experiments done for a pipeline. It can be seen that the scour depth increases quickly when θ is increased from zero to approximately 0.05. In this case, sediment transport will only take place near the structure and it is referred to as clear water scour.

In this thesis it is assumed that the Shields parameter is above this value, indicating a live bed regime. This is valid for all the figures shown where this information is relevant, except Fig. 2.6 which shows the transition from clear water scour to live bed scour. From this figure it can be seen that in the case of live bed regime an increase in Shields parameter will

not result in a much bigger scour depth. However, it will result in a higher shear stress causing more sediment transport, but note that the sediment transport into the scour hole equals the sediment transport out of the hole.

The value θ_{cr} is used to define the limit between the two scour regimes. When the seabed is sloping the effect of sediment gravity may increase or decrease θ_{cr}, but in this thesis the seabed will always be considered horizontal such that $\theta_{cr} = 0.05$. This value is valid for both pipelines and vertical piles.

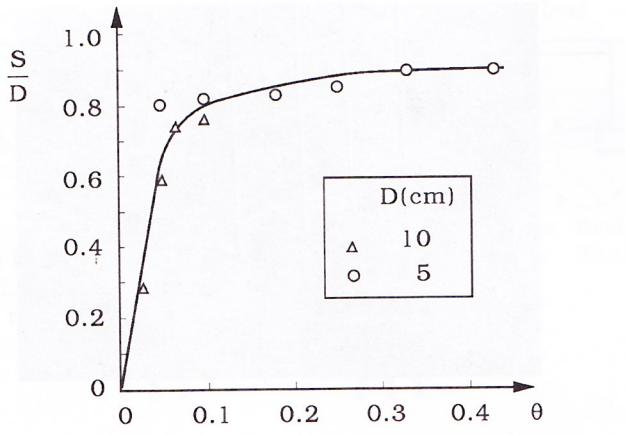

Figure 2.6: Variation of the equilibrium scour depth normalized by the diameter (S/D) for a pipeline, versus Shields parameter (θ). The initial clearance between the seabed and the pipe is zero. Taken from Sumer and Fredsøe (2002).

3 Mechanisms of Scour Around Marine Structures

This section will elaborate the mechanisms of scour around vertical piles and below pipelines. The different behaviour of scour will be described when the incoming flow is due to currents, regular waves, irregular waves or waves plus current. The mechanisms of scour in current or waves will be quite similar, but in the case of waves or a varying current the process will happen on both sides of the structure.

The theory in this chapter is taken from Sumer and Fredsøe (2002) unless otherwise mentioned.

3.1 Scour around slender vertical piles

In the slender pile regime, separation of the flow occurs because the velocity is high relative to the diameter. Separation leads to the formation of vortices that create scour.

3.1.1 Scour around vertical piles in steady currents

When a vertical slender pile is placed on the seabed scour may occur around it due to two main mechanisms, the horseshoes vortices in front, and the lee-wake vortices downstream the pile. Compared to a pipe, the pile is taller resulting in exposure to the whole boundary layer thickness (δ) of the flow field, illustrated in Figure 3.1. This boundary layer causes a rotation of the incoming flow downwards resulting in a flow rotating away from the surface of the pile. This spiral vortex around the structure is defined as the horseshoe vortex. The size of the horseshoe vortices increase with increased δ/D. If it is too small the boundary layer may not separate and no vortex will be shed. The separation is also dependent on the Reynolds number given as $Re_D = U_c D/\nu$ for a cylinder shape, where ν is the kinematic viscosity of the water and U_c is the current velocity. If Re_D decreases to the laminar regime the boundary layer faces more resistance to separation, such that the horseshoe vortices get smaller. No separation will happen if the horseshoe vortex is too small.

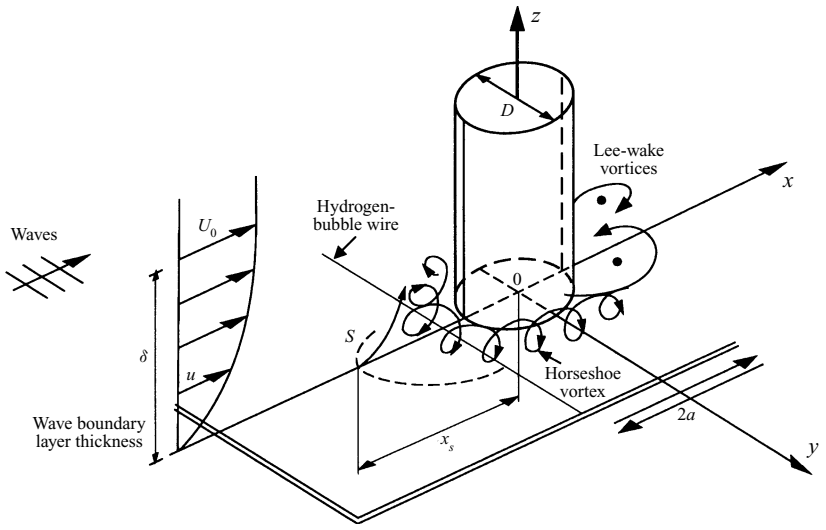

Figure 3.1: Principal sketch of boundary layer flow interacting with vertical pile. Taken from Sumer et al. (1997).

Fig. 3.2 shows the distribution of the amplification factor, α given by Eq. (1), at the normalized distances $(x/D, y/D)$ from the center of the pile axis. It shows that α can be 11 at the middle of the front and side edge of the pipe. This is due to the combined action of the horseshoe vortex and the contraction of the flow.

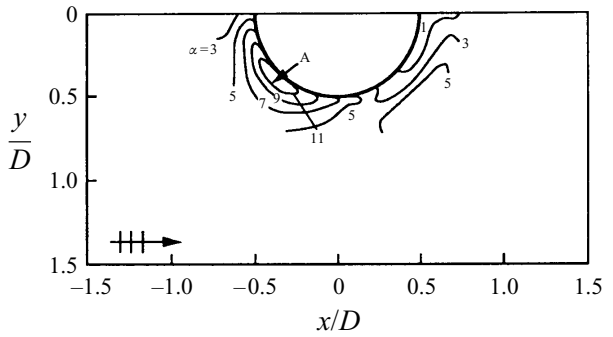

Figure 3.2: Distributions of amplification factors, α, at the normalized distances (x/D, y/D) from the center of the pile axis. $D = 7.5$ cm, $U_c = 30$ cm/s, $\delta = 20$ cm/s, $\delta/D = 2.7$, $Re_D = 23\,000$. Taken from Sumer et al. (1997).

3.1.2 Scour around vertical piles below regular waves

When the pile is exposed to waves, or a varying current such as tidal flows, the downstream section that now has been described, occurs at both sides of the pile. In this case the scour is in addition to $Re_D = U_m D/\nu$ and δ/D also dependent on the KC number as expressed in Eq. (8). For large KC numbers the flow of each half period resembles a current, while for small KC numbers the movement of the water particles is small compared to the diameter of the pile such that the horseshoe vortices may not have time to form.

Fig. 3.3 displays the results of Sumer et al. (1997) regarding the criterion for formation of horseshoe vortices at the upstream and the downstream side of the pile for different wave phases. $0° < \omega t \leq 180°$ indicates the time interval for the wave half-cycle of the wave crest while $180° < \omega t \leq 360°$ is the time interval of the wave half-cycle for the trough. It can be seen that a criterion for formation of horseshoe vortices is $KC > 6$. However, scour also occurs for lower KC-numbers due to other mechanisms which will be described in 3.2. The test was performed with $Re_D = O(10^3)$. The differences in the results for the upstream and the downstream part are due to asymmetry in wave troughs and crests. This phenomenon is explained more in detail in Section 4.2. However, scour will occur when $KC < 6$ due to other mechanisms than the horseshoe vortex, which will be elaborated in Ch. 3.2 under the large pile regime.

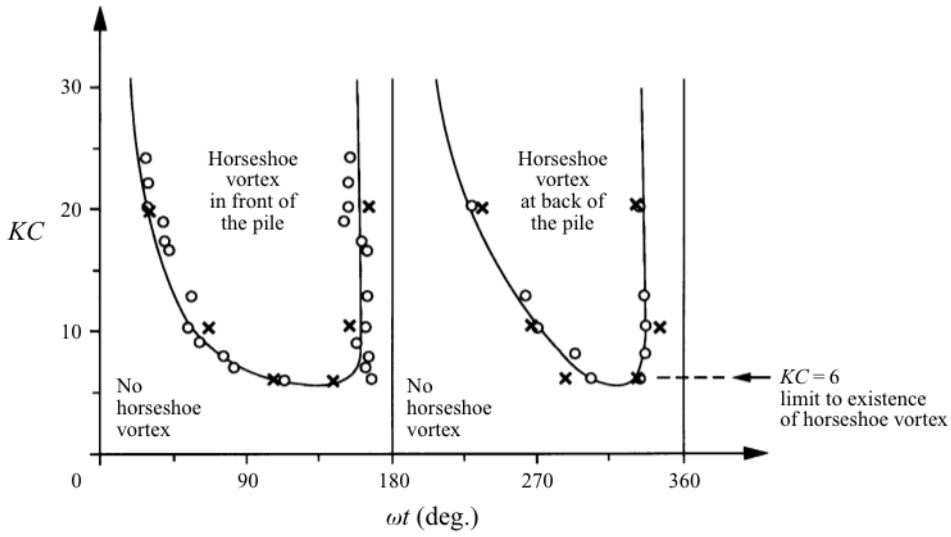

Figure 3.3: Formation of horseshoe vortices as a function of KC-number and wave phase. ∘ marks flow visualization measurements and + marks the bed shear stress measurement. Taken from Sumer et al. (1997).

From Fig. 3.1 it can be seen that lee-wake vortices will be formed behind the pile. They are caused by the separation of the boundary layer on the surface of the pile. The lee wake vortices are essential for the scour characteristics below waves, but the KC number is the governing factor.

Fig. 3.4 shows the amplification factor given by Eq. (1), with varying KC numbers for different values of x, where $x = 0$ is the center of the pile. α increases with increasing KC because the horseshoe vortices grow with increasing KC. The figure also shows that the shear stress is higher during the crest half-period compared to the trough half-period, which is a consequence of the increased horseshoe vortex in the crest half-period, as shown in Fig. 3.3. Although Fig. 3.4 e) shows the amplification factor of the shear stress for currents, it is included in this figure for waves as it clearly illustrates the difference between these conditions. The bed shear stress underneath the horseshoe vortex in front of the pile can be 5 times larger than the undisturbed shear stress.

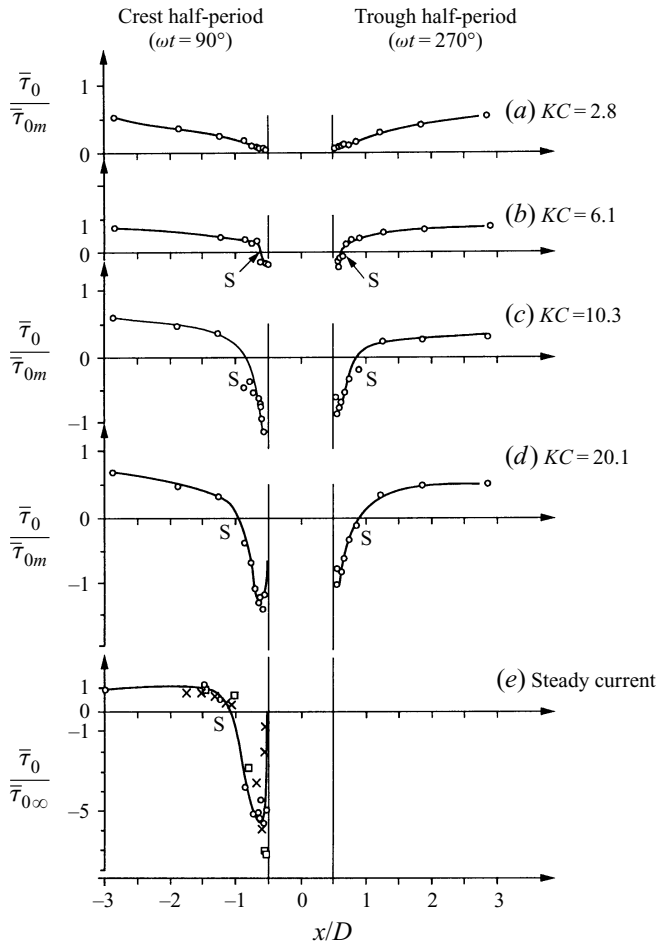

Figure 3.4: Bed shear stress at the horseshoe-vortex side of pile. Taken from Sumer et al. (1997).

At the same time as the shear stress grows with increased KC, the amount of sediment that must be transported also increases. This results in a bigger scour hole for a given D, as revealed in Fig. 3.5. When KC is around 100 the scour is almost equal to the depth generated by a current, while it reaches the current depth around $KC = 300$. Sumer et al. (1992) developed the following empirical expression for the data in Fig. 3.5 for regular waves:

$$\frac{S}{D} = C(1 - e^{-q(KC-r)}) \quad \text{for} \quad KC \geq r \tag{13}$$

where:

$$(C, q, r) = (1.3, 0.03, 6) \tag{14}$$

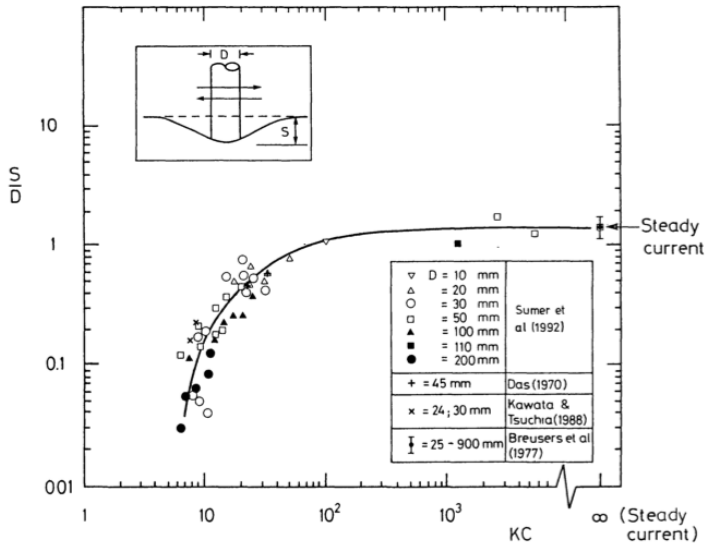

Figure 3.5: Equilibrium depth normalized by the diameter (S/D), versus KC. Eq. (13) *represents the solid line. Taken from Sumer et al. (1992).*

As previously mentioned in Ch. 2.2, the value of S will be reduced if the KC number decreases. In this case the initial scour hole S_i will be backfilled and will end up with the final depth S_f. Fig. 3.6 displays S/D plotted versus KC_f. The squares show scour experiments performed with an initially flat bed, while the the circles and the triangles are the result of backfilling experiments from an initially scoured bed. The solid line in Fig. 3.6 represents Eq. (13) and therefore implies that regardless of the initial scour hole geometry, the equilibrium scour depth of the backfilling process will be the same as for the scour process for the same value of KC. This means that the final depth is not affected by whether the initial bed is flat or scoured, or whether the initial scour hole is generated by current or waves. However, the time scale will be influenced by these factors. This

is implied in Eqs. (10) and (11) where it can be seen that the time scales dependency on S are different for backfilling and scour.

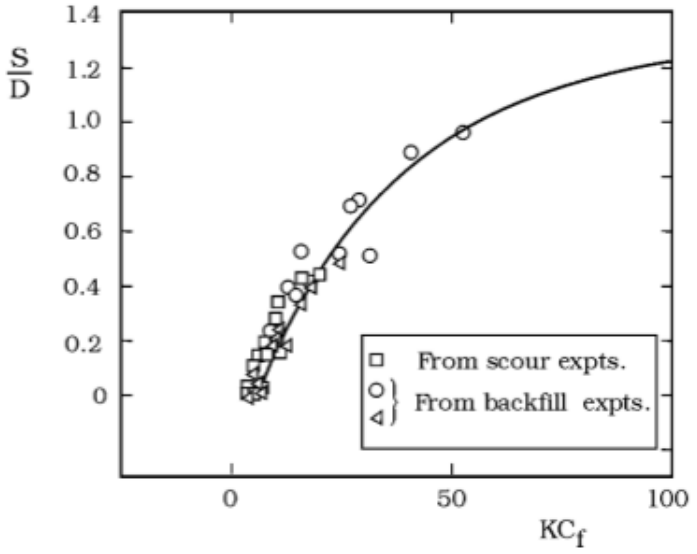

Figure 3.6: Equilibrium scour depth normalized by the diameter (S/D), versus KC during backfilling (KC_f). solid line: Eq. (13)*. Backfilling experiments from initially scoured bed where the initial scour hole was generated by currents (∘) or waves (◁). Taken from Sumer et al. (2012).*

3.1.3 Scour around piles below irregular waves

Sumer and Fredsøe (2001a) studied the effect of irregular waves on scour. They used North Sea storm conditions in their laboratory experiments described by the JONSWAP spectrum. Sumer and Fredsøe (2002) compared results of S/D for irregular waves with Eq. (13) where the KC number was calculated in six different ways. They found that replacing KC with KC_{rms} defined as:

$$KC_{rms} = \frac{U_{rms} T_p}{D} \tag{15}$$

gave the best representation of the scour depth in irregular waves. T_p is the peak period and U_{rms} is the random mean square (r.m.s.) value of the velocity below irregular waves defined as:

$$U_{rms} = \sqrt{2}\sigma_U \tag{16}$$

where σ_U is the r.m.s. value of the orbital velocity U at the bed,

$$\sigma_U^2 = \int_0^\infty S(f)df \tag{17}$$

where $S(f)$ is the power spectrum of U and f is the wave frequency given by $1/T_w$.

3.1.4 Scour around piles in combined waves and current

Fig. 3.7 presents experimental results from Sumer and Fredsøe (2001a), and it shows S/D versus the current wave velocity for regular waves, U_{cw}, which is expressed as:

$$U_{cw} = \frac{U_c}{U_c + U_m} \tag{18}$$

U_c is the undisturbed current velocity $D/2$ from the bed. The figure implies that for small KC numbers, even a small current will cause the scour depth to increase significantly. This is due to the strong horseshoe vortex in front of the pile in the case of a current. It can be seen that when $U_{cw} \approx 0.7$, the scour depth approaches the value representing current alone.

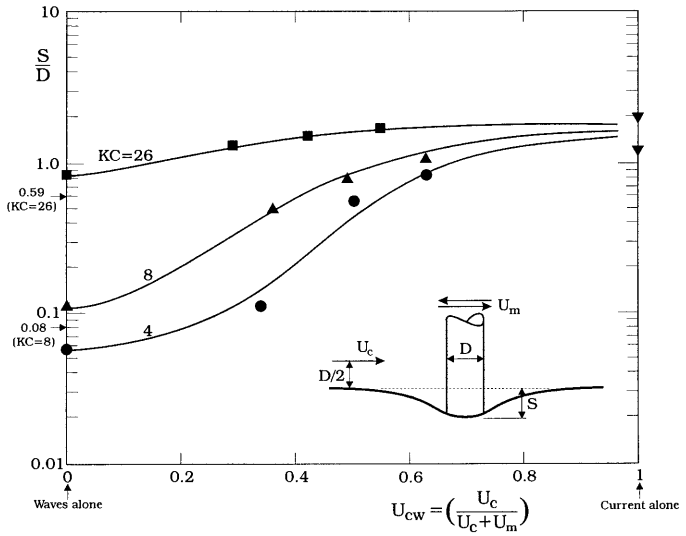

Figure 3.7: Equilibrium scour depth normalized by the diameter (S/D), versus current wave velocity (U_{cw}). Waves and current propagates in the same direction. Taken from Sumer and Fredsøe (2001a).

Sumer and Fredsøe (2001a) did experiments for irregular waves plus current. Sumer and Fredsøe (2002) found that Eq. (13) can be used for irregular waves plus current if KC is replaced by KC_{rms}, Eq. (15) and the coefficients q and r in Eq. (14) are replaced by:

$$q = 0.03 + 0.75U_{cwrms}^{2.6} \tag{19}$$

$$r = 6\exp(-4.7U_{cwrms}) \tag{20}$$

where U_{cwrms} is expressed as:

$$U_{cwrms} = \frac{U_c}{U_c + U_{rms}} \tag{21}$$

Eqs. (19) and (20) are given for wave dominated seastates, meaning $0 \leq U_{cwrms} \leq 0.4$. For waves plus current with an angle ϕ, the dispersion relation becomes:

$$\omega = kU_c \cos\phi + (gk \tanh kh)^{1/2} \tag{22}$$

Sumer and Fredsøe (2002) found that KC_{rms} reduces to the ordinary KC number in the case of regular waves because $\sqrt{2}\sigma_U \rightarrow U_m$ and $T_p \rightarrow T_w$. Eq. (15) and Eq. (21) given for irregular waves plus current then result in Eq. (8) and Eq. (18) given for regular waves plus current.

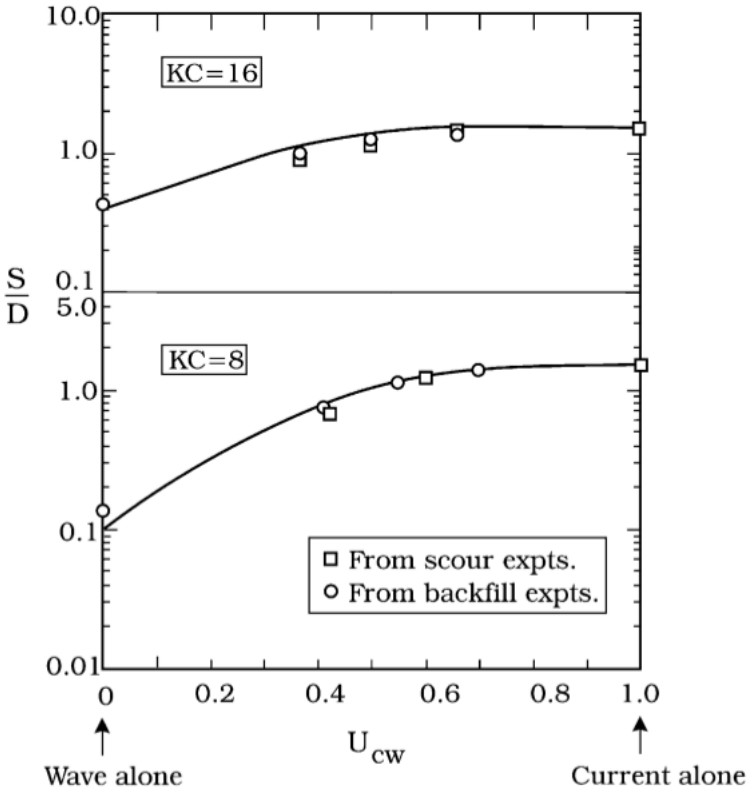

Figure 3.8: Equilibrium depth normalized by the diameter (S/D), versus KC. Taken from Sumer et al. (1992).

3.2 Scour around large piles

When the diameter of the pile becomes large the body will affect the incoming waves, such that the waves become reflected and diffracted, see

Fig. 3.9. Reflection and diffraction are often just referred to as diffraction, and it becomes important when $D/L > 0.2$, Isaacson (1979). In the diffraction regime the value of D/L will affect the flow, and therefore the scour process.

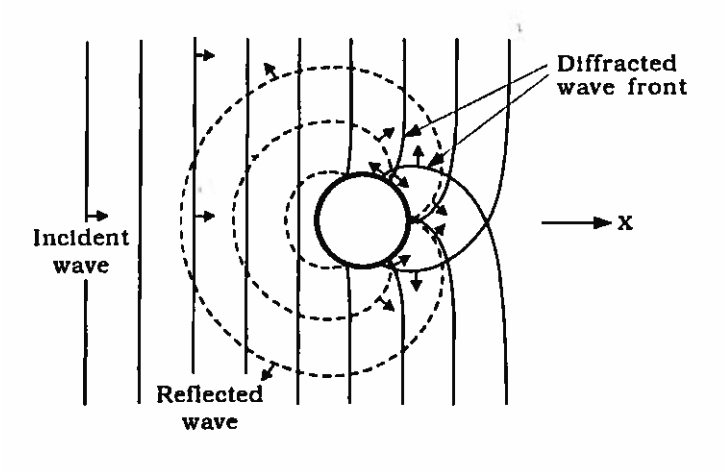

Figure 3.9: Sketch of incident, diffracted and reflected wave fronts around a pile. Taken from Sumer and Fredsøe (2002).

No separation, and therefore no vortex shedding, will exist in the diffraction regime. Fig. 3.10 shows that diffraction occurs within low KC numbers. This is because the period is too short compared to D, such that the direction of the incoming flow changes before separation has time to occur. The dotted line defines the maximum steepness of the waves given by Isaacson (1979) as $\left(\frac{H}{L}\right)_{max} = 0.14 \tanh(kh)$.

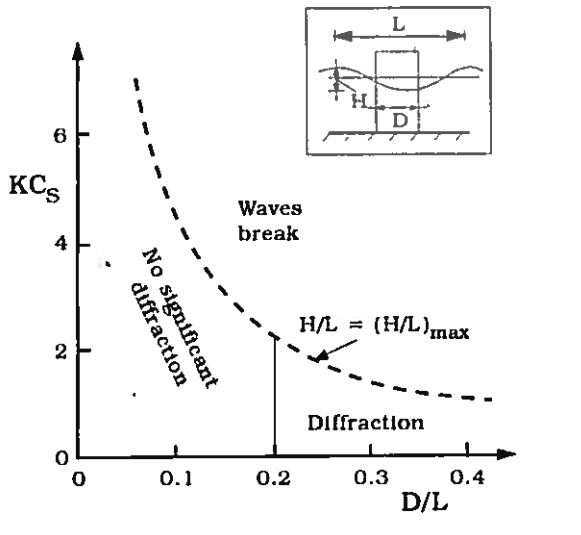

Figure 3.10: Different flow regimes. Taken from Isaacson (1979).

In the diffraction regime there are other flow processes that cause scour compared to the slender pile regime, where scour is related to the vortex shedding. The flow patterns that occur are described as phase-resolved flow and steady streaming, and their mechanisms and contribution to scour will be described in the following.

The phase-resolved flow is an outer flow occurring around the pile due to the interacting wave field. In the front of the pile the incident waves interact with the reflected waves, while behind the pile the diffracted waves interact with reflected waves. This causes velocities near the pile, which can be up to twice as large as the undisturbed wave velocity, causing the Shields parameter to increase, such that sediments are stirred up from the seabottom.

The boundary layer over the bed will be affected by the interacting waves, and this will result in steady streaming. Fig. 3.11 shows the period averaged resultant velocities 4 cm above the bed, defined as $\sqrt{U_R + U_\theta}$, where U_R is the period-averaged radial velocity and U_θ is the period-averaged tangential velocity. Three areas are defined in the Fig. 3.11; region A where the flow is directed towards the front of the pile and region B and C where the flow components are directed outwards. In region B the radial velocities are likely to occur as a response of the bed boundary

layers interaction with the reflected waves. It should be noted that this flow picture occurs when the bed is plane. The streaming will experience a constant adjustment as scour develops.

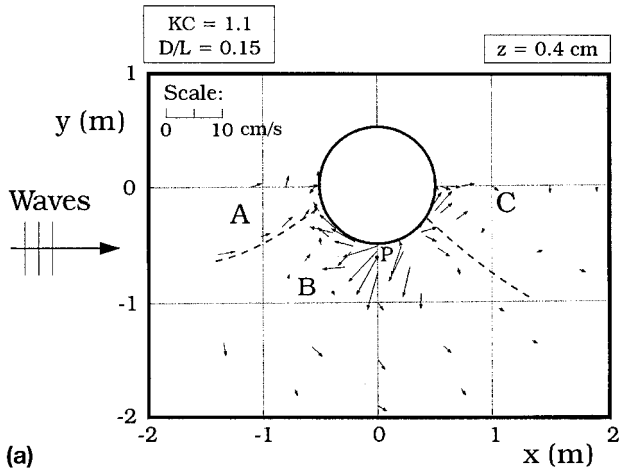

Figure 3.11: Vector diagram of the period-averaged velocities. Taken from Sumer and Fredsøe (2001b).

Figs. 3.12 and 3.13 show that S/D increases with increased KC and D/L, which can be explained by a stronger steady streaming. When KC increases for a given water depth, diameter and period, the wave height grows resulting in larger incoming waves and therefore larger reflected and diffracted waves, causing more steady streaming. When D/L is large, the reflected and diffracted waves becomes stronger, which also results in more steady streaming. However, Sumer and Fredsøe (2001b) suggest that when D/L is above 0.15, the phase-resolved velocity decreases, preventing the sand to be transported as far away from the bed as it would be for smaller D/L. Therefore, the sand will not be exposed to the same steady streaming.

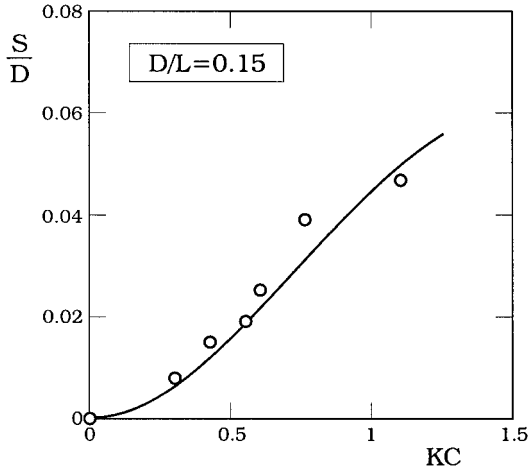

Figure 3.12: S/D versus KC for $D/L = 0.15$. Taken from Sumer and Fredsøe (2001b).

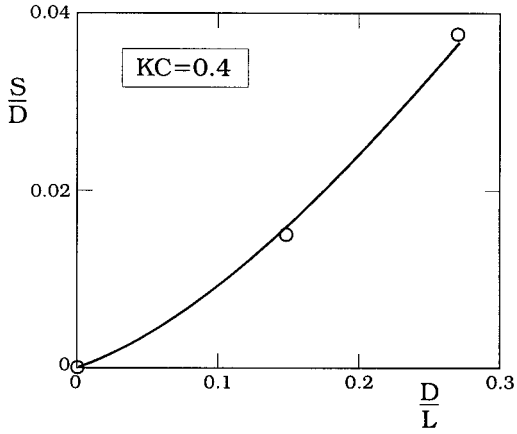

Figure 3.13: S/D versus D/L for $KC = 0.4$. Taken from Sumer and Fredsøe (2001b).

3.3 Scour below marine pipelines

The development of scour below pipelines can be divided in four stages, which are onset of scour, tunnel erosion, lee-wake erosion and the equilib-

rium stage.

3.3.1 Scour below marine pipelines due to steady currents

The first process is the onset of scour and it is caused by piping. Piping happens due to the pressure difference at the upstream and downstream side of the pipe. When a transverse water flow hits the pipe, the velocity decreases near the bottom of the pipe such that the pressure increases. This can be seen in Fig. 3.14(b). The downstream side has a low pressure such that the water will try to flow underneath the pipe from the upstream to the downstream side. The sand is not impermeable, and there will be water in the sand moving slowly. This will cause sand to build up on the downstream side of this pipe, see Fig. 3.15(b). When a certain amount is removed, the remaining sand can not hold the pressure difference and water seeps through, Fig. 3.15(c).

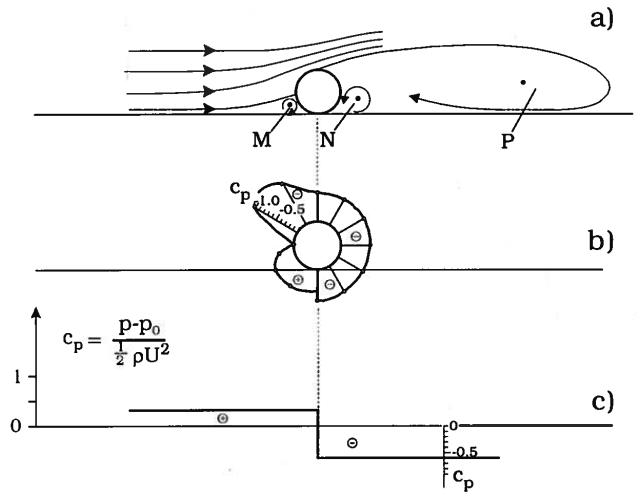

Figure 3.14: Pressure distributions for bottom-seated pipe. Taken from Sumer and Fredsøe (2002).

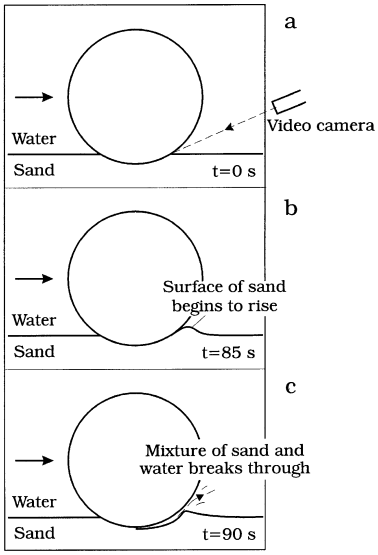

Figure 3.15: Piping, the break through process. Taken from Sumer and Fredsøe (2002).

The second stage of the scour development is tunnel erosion. Right after the onset of scour, the gap between the pipe and the seabed is small. This results in high velocities in the gap, causing a high bed shear stress, Eq. (2), such that the sediment transport is large and scour occurs violently. When the gap is sufficiently large, the velocity has decreased to an extent that indicates tunnel erosion is over.

The next stage is the lee-wake erosion which happens due to vortex shedding. Vortex shedding begins when the gap between the pipeline and the seabed reaches a certain value. Measurements from the bed shear stress show that Shields parameter may increase up to four times during the vortex shedding period. This results in a high sediment transport at the downstream side of the pipeline so the sand dunes behind the pipe get more distributed, and may disappear. This results in a less steep slope of the scour downstream than upstream.

After the lee-wake erosion the scour process reaches the equilibrium stage, where the depth is termed S. At this stage the bed stress underneath the pipe equals the undisturbed shear stress τ_∞.

Fig. 3.16 presents the results of a typical scour test where a fixed pipe

is exposed to a steady current. The numbers on the slopes are the times it takes before the dune develops, given in minutes. It can be seen how fast the scour depth evolves in the beginning, where tunnel erosion occurs. Later the sand dune downstream the pipe gets more distributed.

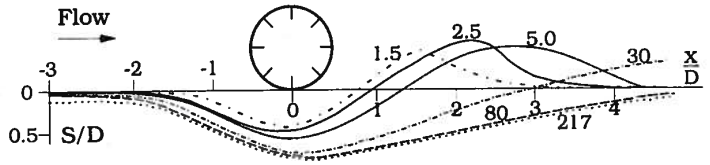

Figure 3.16: Scour development in steady current. Times in minutes. $\theta = 0.098$. Taken from Sumer and Fredsøe (2002).

3.3.2 Scour below marine pipelines in regular waves

When the pipeline is exposed to waves the downstream section that now has been described occurs at both sides of the pipe. This is illustrated in Fig. 3.17(b). In this case the KC number, Eqs. (8) and (9), must also be considered.

When KC is small, the orbital motion of the water particles is small relative to the diameter, and the separation behind the pipe may not occur due to the short length of the lee-wake erosion. Large KC numbers mean that water particles travel large distances relative to the diameter, resulting in longer lee-wake, such that separation and probably vortex shedding occur. For very large KC number, the scour characteristics resemble the situation for current because of the long period.

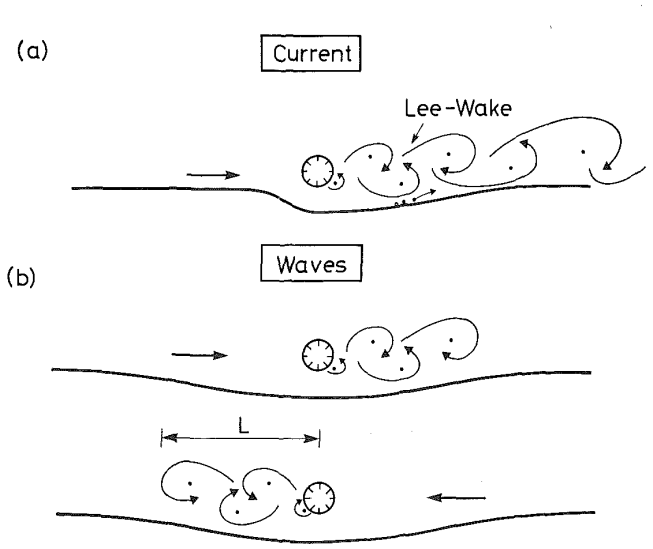

Figure 3.17: Lee wake effect. Taken from Sumer and Fredsøe (2002).

Fig. 3.18 depicts experimental data from Sumer and Fredsøe (1990) where a pipeline was exposed to regular waves in live-bed conditions. It shows the scour depth normalized by the diameter versus the KC number. For waves, the normalized scour depth is linearised by the solid line in the figure expressed as:

$$\frac{S}{D} = 0.1\sqrt{KC} \tag{23}$$

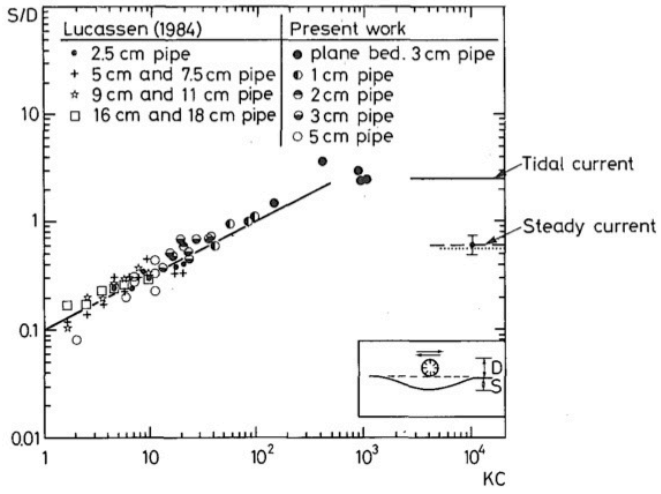

Figure 3.18: Equilibrium scour depth. $\theta > \theta_{cr}$. Taken from Sumer and Fredsøe (1990).

4 Statistical Distributions of Wave Heights

The scour depth and the resulting time scale were described in the previous chapters as highly dependent on the incoming flow to the structure. Therefore, the origin of this flow is of interest, and is in this thesis considered to be caused by waves alone, or waves and current combined.

The description of waves can be done statistically based on stochastic processes such that the waves can be seen as random variables. In this thesis the Rayleigh and the Forristall (2000) distributions are used. Rayleigh assumes each random variable to be a linear wave, while in Forristall each random variable is a second-order wave.

In mild to moderate sea states the linear approach gives good results but in severe sea states and shallow water the nonlinear effects become more important, and Forristall is just one example of a model that can be used to include such effects, Wist (2003). To use these distributions two assumptions must be made:

- The waves are stationary, resulting in a constant variance of the energy spectrum of the wave elevations.
- The waves are narrow-banded. A stochastic process is narrow-banded when most of the energy in the wave spectrum is concentrated around one frequency; the peak frequency ω_p. This means that all the frequencies can be approximated to be equal this frequency, Myrhaug (2004).

4.1 The Rayleigh distribution

Longuet-Higgins (1952) showed that if the sea surface is assumed to be the sum of many regular waves in a random phase and the wave spectrum is narrow-banded, the wave amplitudes are distributed according to Rayleigh. The wave crests and troughs are then equally distributed below and above the mean water level over time, referred to as a Gaussian distribution. The distribution of the normalized wave amplitude is of interest when employing the stochastic method that will be presented in the following chapters. It is given as:

$$\hat{a} = \frac{a}{a_{rms}} \tag{24}$$

where a_{rms} is the r.m.s. value of the wave amplitude, given according to the Rayleigh distribution as:

$$a_{rms} = \frac{H_s}{2\sqrt{2}} \tag{25}$$

where H_s is the significant wave height, which can be found from a time series of wave elevations as the mean value of the 1/3 highest waves. The cumulative distribution function (cdf) of the normalized linear wave amplitude $\hat{a}$ is given as:

$$P(\hat{a}) = 1 - e^{-\hat{a}^2} \quad \text{for} \quad \hat{a} \geq 0 \tag{26}$$

The probability density function (pdf) is obtained by derivation of the cumulative distribution function in Eq. (26) such that $p(\hat{a}) = dP(\hat{a})/d\hat{a}$:

$$p(\hat{a}) = 2\hat{a}e^{-\hat{a}^2} \quad \text{for} \quad \hat{a} \geq 0 \tag{27}$$

4.1.1 The truncated Rayleigh distribution

If $\hat{a}$ is defined within an interval $\hat{a}_1 \leq \hat{a} \leq \hat{a}_2$, this is accounted for by letting $\hat{a}$ follow the truncated Rayleigh distribution where the cdf is given as:

$$P(\hat{a}) = \frac{e^{-\hat{a}_1^2} - e^{-\hat{a}^2}}{e^{-\hat{a}_1^2} - e^{-\hat{a}_2^2}} \quad \text{for} \quad \hat{a}_1 \leq \hat{a} \leq \hat{a}_2 \tag{28}$$

The pdf is obtained by derivation of Eq. (28) such that $p(\hat{a}) = dP(\hat{a})/d\hat{a}$:

$$p(\hat{a}) = \frac{2\hat{a}e^{-\hat{a}^2}}{e^{-\hat{a}_1^2} - e^{-\hat{a}_2^2}} \quad \text{for} \quad \hat{a}_1 \leq \hat{a} \leq \hat{a}_2 \tag{29}$$

4.2 The Forristall distribution

The weakness of the Rayleigh distribution is that real waves do not have a perfectly Gaussian distributed surface. The crests are higher and sharper than expected from a summation of sinusoidal waves with random phases, and the troughs are shallower and flatter, Cataño-Lopera and García (2007). This can be seen in Fig. 4.1 that shows a part of a simulated time series. Eq. (4) shows that the maximum near bed velocity U_m increases linearly with the wave amplitude. This results in a higher velocity below the crest and therefore a higher bed shear stress given by Eq. (2), leading to more scour.

Fig. 4.1 shows how a second order wave can be split in different parts. It has contribution from the the second order sum-frequency and difference frequency parts. Note that most of the wave is built up by the linear term. The sum frequency increases the wave amplitude and the difference frequency reduces this effect, and thereby they are also termed wave set-up and wave set-down effects. The biggest contributions from the second order terms appear in the highest wave amplitudes. This means that the nonlinearity of the waves will increase with increasing crest height and trough depth, Wist (2003).

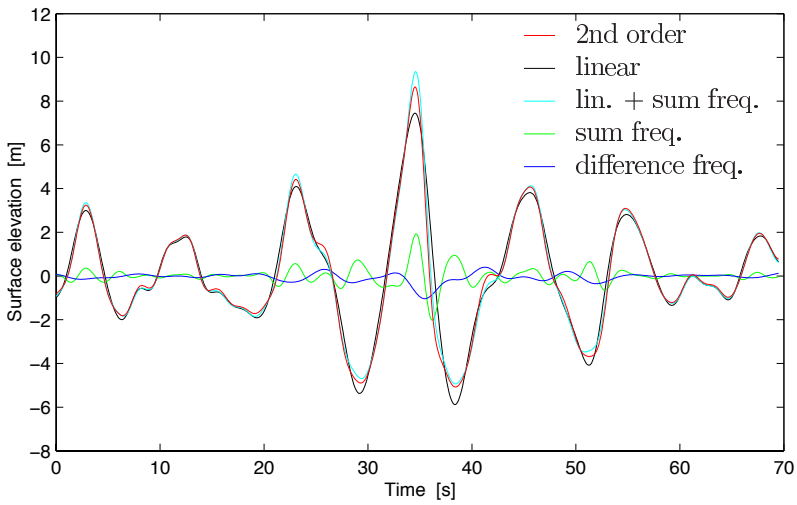

Figure 4.1: Different components of the surface elevation in a simulated time series. Taken from Wist (2003).

Fig. 4.2 is based on field data from the Draupner field and shows the relative magnitude between sum-frequency and difference-frequency for waves with varying water depth. Due to the assumption of a narrow-banded process, $\omega_2 = \omega_1 = \omega_p$. The positive values of the quadratic transfer function describe the sum-frequency, while the negative values describe the difference frequency. It can be seen that when the water depth is large the sum-frequency, and the difference frequency effect are small. The difference frequency becomes smaller relative to the sum-frequency and Forristall (2000) states that the difference frequency effect can be neglected for long-crested ($2D$) and short-crested ($3D$) waves in deep water. $3D$ waves are characterized by a three-dimensional wave spectrum dependent on the frequencies and the propagation angles of the waves. $2D$ waves are only dependent on the frequency spectrum, and therefore propagate in the same direction.

From Fig. 4.2 it can be seen that when the water depth decreases the difference-frequency gets more negative, while the sum-frequency gets more positive, meaning the second order effects increase. Fig. 4.3 shows that in finite water depth the difference-frequency is most significant for $2D$ waves, resulting in a smaller $2D$ wave compared to $3D$. In deep water the total $2D$ wave ends up being larger than the $3D$ because the difference frequency effect is neglected, as earlier stated.

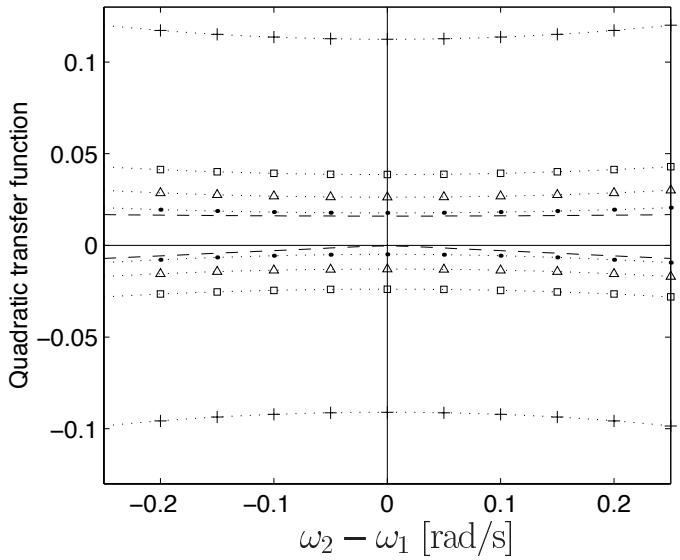

Figure 4.2: The quadratic transfer function for a fixed sum frequency $\omega_1 + \omega_2 = 1 - 12 rad/s$. *- - deep water;* $\cdot \bullet \cdot \cdot$ $d = 70\,m$; $\cdot \Delta \cdot \cdot$ $d = 42\,m$; $\cdot \square \cdot \cdot$ $d = 31\,m$; $\cdot + \cdot \cdot$ $d = 16\,m$. *Taken from Wist (2003).*

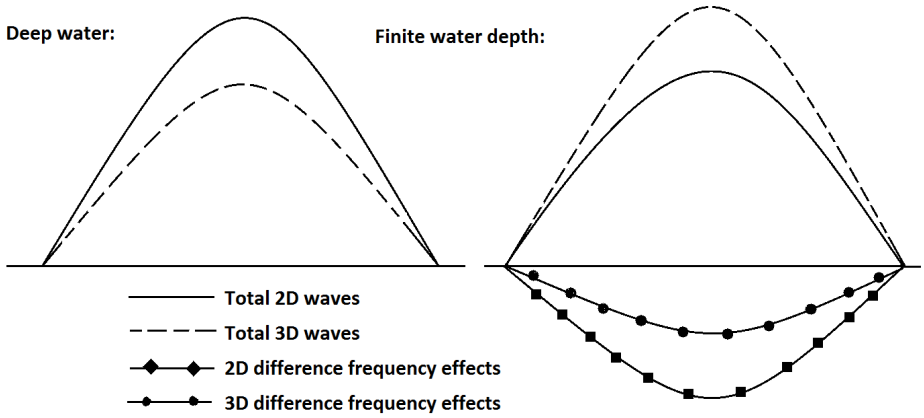

Figure 4.3: Principal sketch of $2D$ *and* $3D$ *waves in deep and finite water. Taken from Hesten (2011).*

Forristall (2000) includes the second-order effects by using a two-parameter Weibull distribution based on the assumption of the surface elevations as a stationary narrow-banded process. The distribution of the normalized wave crests, w_c, is of interest because they contribute more to scour as they are higher than the trough.

The nonlinear crest height is given by $w_c = \eta_n/a_{rms}$ where η_n is the nonlinear surface elevation. At a fixed point in a sea state with stationary narrow-banded waves, consistent with Stokes second-order regular waves in finite water depth, w_c and $\hat{U}_m$ are given by Dean and Dalrymple (1984) as:

$$w_c = \hat{a} + O(k_p a_{rms}) \tag{30}$$

$$\hat{U}_m = \hat{a} + O(k_p a_{rms}) \tag{31}$$

where $\hat{U}_m = U_m/U_{rms}$ is the the non-dimensional nonlinear maximum horizontal particle velocity at the seabed. $O(k_p a_{rms})$ is the second-order terms which are proportional to the characteristic wave steepness $k_p a_{rms}$, where k_p is the wave number in a narrow-banded seastate. Eq. (30) can be reorganized such that $\hat{a} = w_c - O(k_p a_{rms})$. Substitution of this into Eq. (31) results in $\hat{U}_m = w_c + O(k_p a_{rms})$. When comparing this result with Eq. (31), it appears that $\hat{a}$ can be replaced by w_c in the linear term of $\hat{U}_m$, because the error involved is of second order, Myrhaug and Ong (2014):

$$\hat{a} = w_c \tag{32}$$

Even though $\hat{a}$ is assumed to equal to w_c, the distribution of them will be different. Eq. (25) will be employed when using the Forristall distribution to find necessary statistical parameters. Forristall (2000) derived the following cumulative distribution function:

$$P(w_c) = 1 - e^{-(\frac{w_c}{\sqrt{8}\alpha})^{\beta}} \quad \text{for} \quad w_c \geq 0 \tag{33}$$

where α and β are Weibull parameters. These are obtained by simulations based on Sharma et al. (1981) theory that includes the second order sum-frequency and difference-frequency effects. Forristall (2000) expressed the

Weibull parameters α and β for long-crested (2D) and short-crested (3D) waves:

$$\alpha_{2D} = 0.3536 + 0.2892S_1 + 0.1060U_r \tag{34}$$

$$\beta_{2D} = 2 - 2.1597S_1 + 0.0968{U_r}^2 \tag{35}$$

$$\alpha_{3D} = 0.3536 + 0.2568S_1 + 0.0800U_r \tag{36}$$

$$\beta_{3D} = 2 - 1.7912S_1 - 0.5302U_r + 0.284{U_r}^2 \tag{37}$$

where S_1 is the wave steepness, and U_r is the Ursell number. These parameters characterize the degree of nonlinearity in the waves. When $S_1 = U_r = 0$, the waves become sinusoidal such that the Forristall distribution reduces to the Rayleigh distribution. The wave steepness and the Ursell number are defined as:

$$S_1 = \frac{2\pi}{g}\frac{H_s}{T_1^2} \tag{38}$$

$$U_r = \frac{H_s}{k_1^2 h^3} \tag{39}$$

where T_1 is the mean wave period, and k_1 is the corresponding wave number. The seastate is narrow-banded such that $T_1 = T_p$, which by the dispersion relation, Eq. (5), implies that $k_1 = k_p$. The Forristall distribution is based on simulations for $U_r \leq 1$. The value of the wave steepness is given as $S_1 < 0.1412$ to avoid breaking waves.

The pdf is obtained by derivation of Eq. (33) such that $p(w_c) = dP(w_c)/dw_c$:

$$p(w_c) = \frac{\beta}{\sqrt{8}\alpha}(\frac{w_c}{\sqrt{8}\alpha})^{\beta-1} e^{-(\frac{w_c}{\sqrt{8}\alpha})^{\beta}} \quad \text{for} \quad w_c \geq 0 \tag{40}$$

4.2.1 The truncated Forristall distribution

If w_c is defined within the interval $w_{c1} \leq w_c \leq w_{c2}$, this is accounted for by letting w_c follow the truncated Forristall distribution, where the cdf is given as:

$$P(w_c) = \frac{e^{-(\frac{w_{c1}}{\sqrt{8}\alpha})^\beta} - e^{-(\frac{w_c}{\sqrt{8}\alpha})^\beta}}{e^{-(\frac{w_{c1}}{\sqrt{8}\alpha})^\beta} - e^{-(\frac{w_{c2}}{\sqrt{8}\alpha})^\beta}} \quad \text{for} \quad w_{c1} \leq w_c \leq w_{c2} \tag{41}$$

The pdf is obtained by derivation of Eq. (41) such that $p(w_c) = dP(w_c)/dw_c$:

$$p(w_c) = \frac{(\frac{1}{\sqrt{8}\alpha})^\beta \beta w_c^{\beta-1} \, e^{-(\frac{w_{c1}}{\sqrt{8}\alpha})^\beta}}{e^{-(\frac{w_{c1}}{\sqrt{8}\alpha})^\beta} - e^{-(\frac{w_{c2}}{\sqrt{8}\alpha})^\beta}} \quad \text{for} \quad w_{c1} \leq w_c \leq w_{c2} \tag{42}$$

5 The Time Scale of Scour and Backfilling

This chapter derives a method where empirical empirical formulas for the time scale of scour and backfilling are presented and reformulated, such that random waves can be included. This allows the time scale to be found for a given seastate in linear or nonlinear waves. The empirical formulas were obtained by linear fit of experimental data, which can be found in Sumer and Fredsøe (2002) and Sumer et al. (2012). They presented the time scale non-dimensionally as T^*, which is independent of the diameter and related to real time by:

$$T = T^* \frac{D^2}{\sqrt{g(s-1)d_{50}^3}} \tag{43}$$

Note that all the experiments were performed in live bed conditions. The data were plotted as functions of θ and KC in waves, and the additional parameter U_{cw} in waves plus current. For each experiment the parameters have been calculated based on the properties of the incoming waves, current and the sand grains. The corresponding S was measured with necessary instrumentation such that T could be found from the slope method or the area method by the formulas $S_t = S(1 - e^{-t/T})$ and $S_t = S + (S_i - S)^{e^{-t/T}}$, given in Eq. (10) and (11).

The formulas for the time scale will vary depending on the different scenarios, which will be referred to as CASE 1- CASE 6. In CASE 1- CASE 4, scour is caused by random waves alone, while in CASE 5 and 6, backfilling is caused by currents and waves combined. The first section will present the time scale of scour. The formulas are taken from Fredsøe et al. (1992) and Sumer et al. (1992) where the experiments were performed in regular waves. The second section presents the time scale of backfilling taken from Sumer et al. (2012) where the vertical pile were subjected to irregular waves during the experiments.

5.1 The time scale of scour

5.1.1 Method

The following method is used to express KC and θ by their r.m.s. values and the normalized wave height:

The maximum value of the Shields parameter below waves is obtained by substituting τ_∞/ρ in Eq. (12) with $\tau_{max,\infty}/\rho$ from Eq. (2):

$$\theta_m = \frac{\tau_{max,\infty}/\rho}{g(s-1)d_{50}} \tag{44}$$

When Eq. (44) is divided by its r.m.s. value, Shields parameter is expressed non-dimensionally as:

$$\theta_c = \frac{\theta_m}{\theta_{rms}} \tag{45}$$

where

$$\theta_{rms} = \frac{\tau_{rms}/\rho}{g(s-1)d_{50}} \tag{46}$$

When combining Eqs. (44) - (46) the normalized Shields parameter equals:

$$\theta_c = \frac{\tau_{max,\infty}/\rho}{\tau_{rms}/\rho} \tag{47}$$

By substituting Eq. (6) into Eq. (2) the following is obtained:

$$\tau_{max,\infty}/\rho = \frac{1}{2}c(\frac{A}{z_0})^{-d}U_m^2 \tag{48}$$

τ_{rms}/ρ is expressed similarly, but A and U are replaced by A_{rms} and U_{rms}:

$$\tau_{rms}/\rho = \frac{1}{2}c(\frac{A_{rms}}{z_0})^{-d}U_{rms}^2 \tag{49}$$

Eqs. (47) - (49) result in the following expression for the normalized Shields parameter:

$$\theta_c = (\frac{A}{A_{rms}})^{-d}(\frac{U_m}{U_{rms}})^2 \tag{50}$$

By the assumption of a narrow banded process, the following relation of the ratio of U_m/U_{rms} can be seen from Eq. (4):

$$\frac{U_m}{U_{rms}} = \frac{A\omega}{A_{rms}\omega_p} = \frac{A}{A_{rms}} = \frac{a}{a_{rms}} \tag{51}$$

By combining Eqs. (24), (32), (50) and (51), the normalized Shields parameter becomes:

$$\theta_c = \frac{\theta_m}{\theta_{rms}} = \hat{a}^{2-d} = w_c^{2-d} \tag{52}$$

such that

$$\theta_m = \theta_{rms}\hat{a}^{2-d} = \theta_{rms}w_c^{2-d} \tag{53}$$

The normalized Keulegan Carpenter number is found by dividing the KC-number, Eq. (8), by its r.m.s. value, Eq. (15). Under the assumption of a narrow banded sea state the following relation is obtained:

$$KC_c = \frac{KC}{KC_{rms}} = \frac{U_m T_w}{U_{rms} T_p} = \frac{U_m}{U_{rms}} = \hat{a} = w_c \tag{54}$$

such that

$$KC = KC_{rms}\hat{a} = KC_{rms}w_c \tag{55}$$

Note that even though the linear normalized wave amplitude $\hat{a}$ and the nonlinear normalized wave crest w_c are equal, they are distributed differently. In the following formulas the time scales will be presented by w_c, but T^* will also be calculated for linear waves.

5.1.2 The time scale of scour below pipelines (CASE 1)

Fredsøe et al. (1992) showed that the time scale of scour below pipelines can be expressed as a function of only the Shields parameter in waves and currents. They did experiments with varying KC numbers, presented in Fig. 5.1, and concluded that the dependency of KC could be neglected.

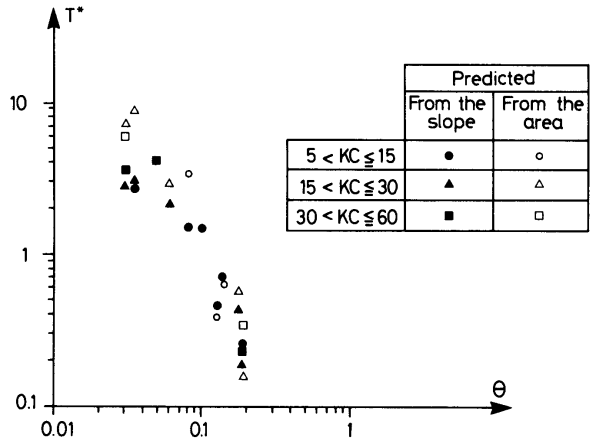

Figure 5.1: Non-dimensional plot of time scale against Shields parameter for waves. The bed is originally plane and the gap between the pipe and bed is zero. Taken from Fredsøe et al. (1992).

Fig. 5.2 shows that the data sets for steady currents and waves correlate. By linear fit to the data, Fredsøe et al. (1992) obtained the following expression:

$$T^* = r_1 \theta^{-s_1} \tag{56}$$

where $r_1 = 1/50$ and $s_1 = 5/3$. The tests were performed within $0.05 \leq \theta \leq 0.19$.

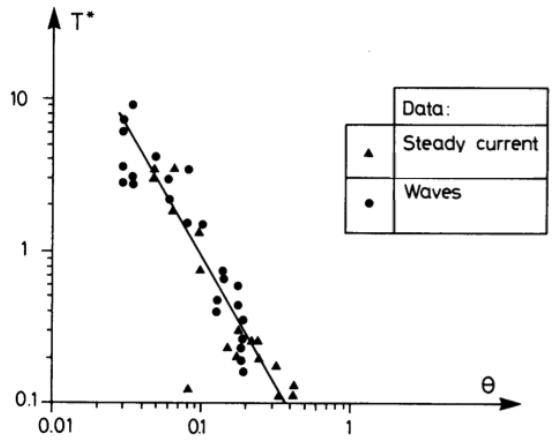

Figure 5.2: Non-dimensional plot of time scale against Shields parameter. Steady current and waves. Plane bed, the gap between pipe and bed is zero. The data for the current experiments are obtained in Mao (1986) and Kjeldsen et al. (1973). Wave data and figure are taken from Fredsøe et al. (1992).

By substituting θ_m in Eq. (56) with the expression for θ_m given in Eq. (53), the dimensionless time scale becomes:

$$T^* = r_1 \theta_{rms}^{-s_1} \, w_c^{-s_1(2-d)} \tag{57}$$

Eq. (57) can be reorganized and expressed by the dimensionless constant t:

$$t = \frac{T^*}{r_1 \theta_{rms}^{-s_1}} = w_c^{-s_1(2-d)} = w_c^{-v} \tag{58}$$

where

$$v = s_1(2-d) \tag{59}$$

The purpose of defining t is that it is easier to compare the scour characteristics for linear, nonlinear 2D and nonlinear 3D solutions of the time scale by this value. The ratio of t will reflect the ratio of T^* for a given value of θ_{rms} and KC_{rms} (CASE 2 - 4). It is possible to derive t in CASE 1 - CASE 4, where the only value that will differentiate the cases is v, making the calculation simple.

5.1.3 The time scale of scour around vertical slender piles (CASE 2)

Sumer et al. (1992) investigated the time scale of scour around vertical piles and concluded that T^* decreases with increasing θ_m, consistent with the results obtained for pipelines. This can be seen in Fig. 5.3, which also shows the time scales dependency on the KC number. As seen from Fig. 3.5, higher KC-numbers result in higher equilibrium scour depths S for a given D, and therefore, more sediment must be transported to reach S. This results in longer time. Based on their results, they obtained the relation:

$$T^* = r_1 (\frac{KC}{\theta_m})^{s_1} \tag{60}$$

where $r_1 = 10^{-6}$ and $s_1 = 3$. The tests were performed within $7 \leq KC \leq 34$ and $0.07 \leq \theta \leq 0.19$.

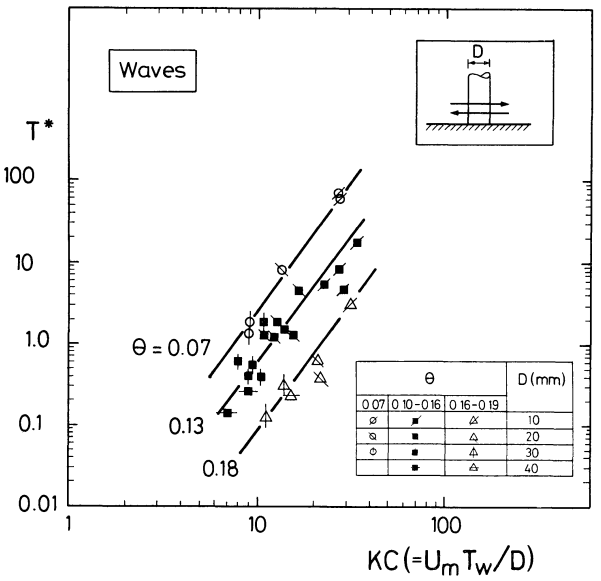

Figure 5.3: Time scale of scour around pile. Taken from Sumer et al. (1992).

By substituting θ_m and KC in Eq. (60) with the expressions for θ_m and

KC given in Eqs. (53) and (55), the dimensionless time scale becomes:

$$T^* = r_1 \Big(\frac{KC_{rms}}{\theta_{rms}} \Big)^{s_1} w_c^{-s_1(1-d)} \tag{61}$$

where

$$t = \frac{T^*}{r_1 {KC_{rms}}^{s_1} \theta_{rms}^{-s_1}} = w_c^{-s_1(1-d)} = w_c^{-v} \tag{62}$$

such that

$$v = s_1(1-d) \tag{63}$$

5.2 The time scale of backfilling

The formulas of the time scale for backfilling were derived by Sumer et al. (2012) for irregular waves, and therefore presented by KC_{rms}, θ_{rms} and U_{cwrms}. However, in this thesis it is assumed that these parameters can be reduced to KC, θ, and U_{cw} in the formulas for the time scale in the event of regular waves alone or regular waves plus current. A similar assumption were made by Sumer and Fredsøe (2002). They found that S/D from Eq. (13) was valid for irregular waves plus current when KC was replaced by KC_{rms} and q and r by Eqs. (19) and (20), represented by U_{cwrms}. They stated that these formulas could be applied in regular waves plus current by replacing KC_{rms} and U_{cwrms} with KC and U_{cw}.

5.2.1 Method

As mentioned in the introduction, the equations from Sumer et al. (2012) were assumed to be valid for regular waves plus current. Now it is further assumed that these equations are valid for individual waves in an irregular narrow-banded seastate. This results in the following:

$$KC = \frac{U_m T_p}{D} \tag{64}$$

The expressions for θ_m will be similar to Eq. (44), where $\tau_{max,\infty}/\rho$ is replaced by Eq. (2) containing f_w, which is replaced by Eq. (6), where

$A = U_m/w_p$ under the assumption of individual waves in a narrow-banded sea state:

$$\theta_m = \frac{0.5\, c\, (z_0\omega_p)^d\, {U_m}^{(2-d)}}{g(s-1)d_{50}} \tag{65}$$

Eqs. (64) and (18) are multiplied with U_{rms}/U_{rms} and Eq. (65) with $(U_{rms}/U_{rms})^{2-d}$. By using the relation $U_m/U_{rms} = w_c$ from Eq. (54), KC and θ_m end up beeing equal to Eqs. (53) and (55). U_{cw} becomes:

$$U_{cw} = \frac{U_c}{(U_c + w_c U_{rms})} \tag{66}$$

By re-arranging U_{cwrms} given in Eq. (21), the following is obtained:

$$U_c = \frac{U_{cwrms} U_{rms}}{1 - U_{cwrms}} \tag{67}$$

which is substituted into Eq. (66) resulting in:

$$U_{cw} = \frac{U_{cwrms}}{w_c(1 - U_{cwrms}) + U_{cwrms}} \tag{68}$$

5.2.2 The time scale of backfilling around slender vertical piles below waves when the initial scour hole was generated by current (CASE 3)

Sumer et al. (2012) defined the non-dimensional time scale for backfilling in the same manner as for scour; linear fit to data of experimental results. The time scale for each experiment was obtained by the tangent method according to the definition in Eq. (11). Fig. 5.4 presents results where the initial scour depth (S_i) was generated by current and the final depth (S_f) was caused by waves alone, characterized by KC_f on the x-axis. In the further context, the index i will always present the initial conditions for the scour hole, while the index f describes the waves causing backfilling.

From Fig. 3.5 it was seen that when $KC = \infty$ (the current situation), S/D reaches its highest possible value. When backfilling begins the time is dependent on KC_f as this will indicate how big the final depth is. If

KC_f is high the final scour hole is closer to the initial hole, resulting in less backfilling and therefore shorter time. The time scale decreases with increasing θ_f due to the same reason as described earlier; increased θ causes faster sediment transportation.

Definitions of KC_f and θ_f by Sumer et al. (2012) are r.m.s. values such that their equation for the time scale becomes:

$$T^* = (\theta_{frms}^{s_1} \, KC_{frms})^{-s_2} \tag{69}$$

were $s_1 = 2$ and $s_2 = 1.45$. The experiments were performed within $5 < KC_{frms} < 53$ and $0.07 < \theta_{frms} < 0.15$.

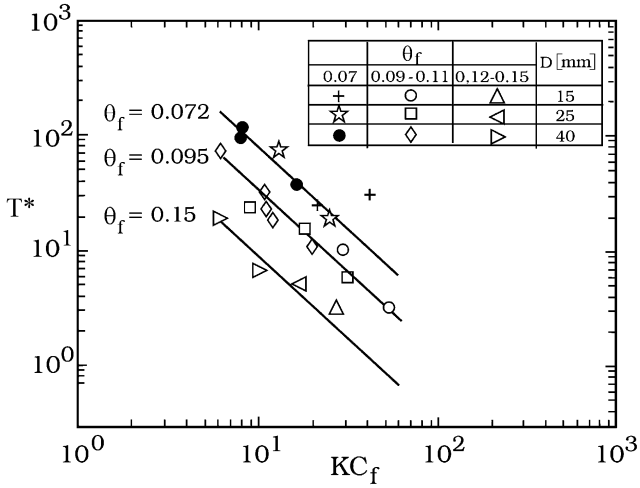

Figure 5.4: Time scale of backfilling. Initial equlibrium scour depth is generated by a current ($KC = \infty$). Taken from Sumer et al. (2012).

θ_{rms} and KC_{rms} in Eq. (69) reduce to θ_m and KC under the assumption of individual waves in a narrow-banded seastate. They are thereby replaced with Eqs. (53) and (55) such that the dimensionless time scale becomes:

$$T^* = (\theta_{frms}^{s_1} KC_{frms})^{-s_2} w_c^{-s_2(s_1(2-d)+1)} \tag{70}$$

where

$$t = T^*(\theta_{frms}^{s_1} KC_{frms})^{s_2} = w_f^{-s_2(s_1(2-d)+1)} = w_c^{-v} \tag{71}$$

such that

$$v = s_2(s_1(2-d)+1) \tag{72}$$

5.2.3 The time scale of backfilling around slender piles below waves when the initial scour hole was generated by waves (CASE 4)

In this case of backfilling around a slender vertical pile the initial scour hole is generated by waves. Sumer et al. (2012) performed experiments on this presented in Fig. 5.5. For a given value of $\theta^2 KC_f$, a smaller value of KC_i causes a smaller initial hole and the time it takes to reach the final value will therefore be shorter. Definitions of KC_f and θ_f by Sumer et al. (2012) are r.m.s. values such that their equation for the time scale becomes:

$$T^* = (r_1 \frac{KC_{frms}}{KC_{irms}} \theta_{frms}^{s_1})^{-s_2} \tag{73}$$

where $r_1 = 70$, $s_1 = 2$ and $s_2 = 1.45$. The experiments were performed in the ranges: $11 \leq KC_{irms} \leq 32$, $4 \leq KC_{frms} \leq 25$ and
$0.07 \leq \theta_{frms} \leq 0.15$, resulting in $0.02 \leq \theta_{frms}^2 KC_{frms} \leq 0.56$.

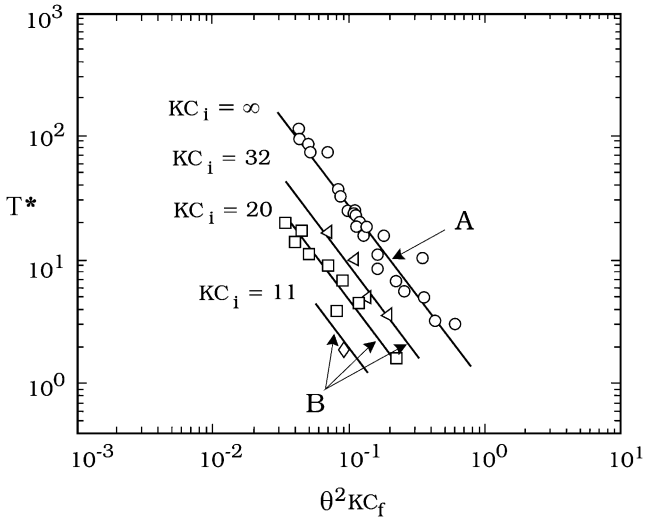

Figure 5.5: Time scale of backfilling. A: Initial equilibrium scour depth generated by current, Eq. (69) *B: Initial equilibrium scour depth is generated by waves, Eq.* (73)*. Taken from Sumer et al. (2012).*

θ_{rms} and KC_{rms} in Eq. (73) reduce to θ_m and KC under the assumption of individual waves in a narrow-banded sea state, and are thereby replaced with Eqs. (53) and (55) such that the dimensionless time scale becomes:

$$T^* = (r_1 \frac{KC_{frms}\theta_{frms}^{s_1}}{KC_{irms}})^{-s_2} w_c^{-s_2(s_1(2-d)+1)} \tag{74}$$

where

$$t = T^*(r_1 \frac{KC_{frms}\theta_{frms}^{s_1}}{KC_{irms}})^{s_2} = w_c^{-s_2(s_1(2-d)+1)} = w_c^{-v} \tag{75}$$

such that

$$v = s_2(s_1(2-d)+1) \tag{76}$$

5.2.4 Backfilling around vertical slender piles in combined waves and current when initial scour hole is generated by current (CASE 5)

Fig. 5.6 shows the time scale of backfilling around a slender pile by current and waves combined when the initial hole was generated by a current. From Fig. 3.5 it was seen that the scour depth increases with increasing KC until it reaches a constant value corresponding to the depth generated by current. This means that the stronger the current, corresponding to higher U_{cw}, the bigger is the final depth, which results in less time of backfilling. Therefore, the time scale approaches zero when the current-wave ratio is $U_{cw} > 0.7$. Sumer et al. (2012)s definition of KC_f, θ_f, and U_{cw} are as mentioned r.m.s. values, resulting in the following empirical expression based on the experiments presented in the figure:

$$T^* = 1.9 - (\frac{0.65}{(\theta_{frms}^{s_1} KC_{frms} - 0.01)^{s_2}} + 2)(U_{cwrms} - 0.7) \text{ for } U_{cwrms} < 0.7 \tag{77}$$

where $s_1 = 2$ and $s_2 = 1.68$. The tests were performed within $4 \leq KC_{frms} \leq 20$ and $0.07 \leq \theta_{frms} \leq 0.11$.

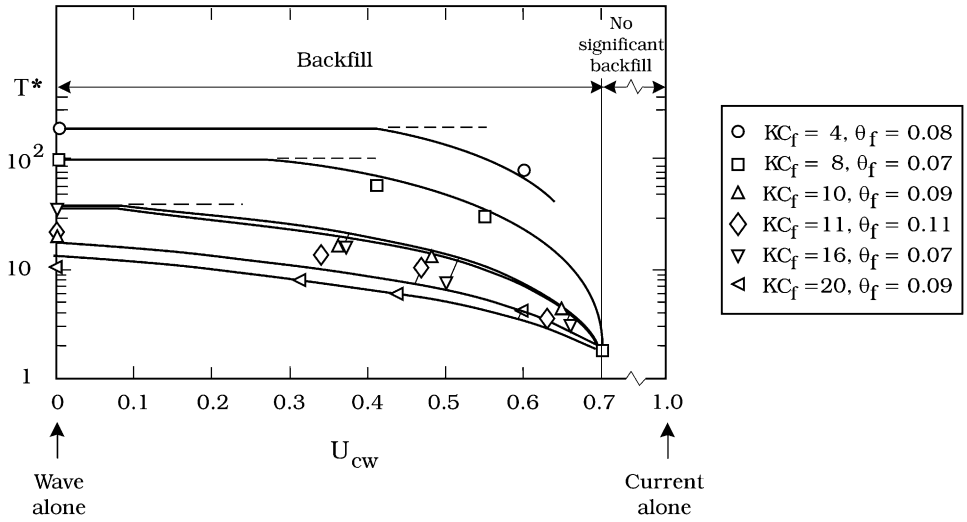

Figure 5.6: Time scale of backfilling in combined waves and current. Initial scour hole generated by current. Horizontal lines: Eq. (69)*, curved lines: Eq.*(77)*. Taken from Sumer et al. (2012).*

KC_{rms}, θ_{rms}, and U_{cwrms} in Eq. (77) are reduced to KC, θ, and U_{cw} given in Eqs. (55), (53), and (68), under the assumption of individual waves in a narrow-banded sea state. This results in:

$$T^* = 1.9 - \left(\frac{0.65}{\left(w_c^{s_1(2-d)+1}\theta_{frms}^{s_1}KC_{frms} - 0.01\right)^{s_2}} + 2\right)\left(\frac{U_{cwrms}}{w_c(1-U_{cwrms}) + U_{cwrms}} - 0.7\right) \tag{78}$$

It was seen in Eq. (77) that the validity is within $U_{cwrms} < 0.7$, resulting in the following criterion for Eq. (78):

$$\frac{U_{cwrms}}{w_c(1-U_{cwrms}) + U_{cwrms}} < 0.7 \tag{79}$$

5.2.5 Backfilling around large piles in combined waves and current when initial scour hole is generated by current (CASE 6)

Fig. 5.7 shows the time scale of backfilling around a large pile by current and waves combined when the initial hole was generated by a current. Similarly to Fig. 5.6, the time scale decreases when the current becomes stronger because the final depth increases, resulting in less time of backfilling. It should be noted that the amount of data is limited such that extrapolation must be done with caution. The scour will not vary with any significance when the diffraction parameter D/L changes from 0.07 to 0.12, Sumer and Fredsøe (2002), as seen in Fig. 3.13. This is due to the small variation in the flow pattern. However, in Fig. 3.12 it can be observed that S/D changes between $KC_f = 0.7$ to $KC_f = 1.5$. Sumer et al. (2012) present the following empirical expression based on their experiments presented in Fig. 5.7:

$$T^* = -\frac{15.15}{KC_{frms}^{s_1}}(U_{cwrms} - 0.7) \quad \text{for} \quad U_{cwrms} < 0.7 \tag{80}$$

where $s_1 = 2.38$. The experiments were performed within $0.7 \leq KC_{frms} \leq 1.5$ and $0.101 \leq \theta_{rms} \leq 0.105$.

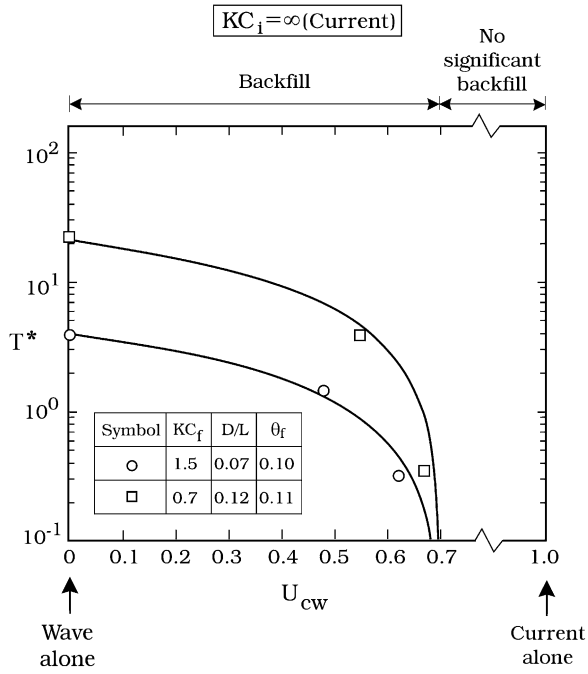

Figure 5.7: Time scale of backfilling in combined waves and current around large piles. Initial scour hole generated by current. Taken from Sumer et al. (2012).

KC_{rms} and U_{cwrms} in Eq. (80) can be replaced by KC and U_{cw} given in Eqs. (55) and (68) under the assumption of individual waves in a narrow-banded sea state. This results in:

$$T^* = -\frac{15.15}{(KC_{frms}w_c)^{s_1}}\left(\frac{U_{cwrms}}{w_c(1-U_{cwrms})+U_{cwrms}} - 0.7\right) \qquad (81)$$

where Eq. (79) must be fulfilled.

6 The Stochastic Method

In this Chapter, a stochastic method for calculating the expected value of time scale of scour and backfilling is described. As seen in Ch. 5 and 5.2.4, the formulas of the timescale expressed by the normalized wave crest were derived, allowing input of random waves, which will be distributed by the Rayleigh and Forristall pdfs shown in Ch. 4.

This stochastic approach is based on the following assumptions:

- In a given sea state, only the $1/n$'th highest waves contribute to scour.
- The seastate has lasted longer than the timescale of the scour.
- The method is only valid for live-bed conditions. This assumption appears because the formulas for the time scale are obtained based on experiments where $\theta > \theta_{cr}$.
- The surface elevation is a stationary narrow-banded random process. This assumption is connected to the probability distributions that were shown Ch 4. Now they will be used to find the time scale.

Myrhaug and Ong (2011) found that the scour depth and width below pipelines caused by the (1/10)'th highest waves represent the upper values of the random wave-induced scour, and suggest that this can be used for design purposes. $n = 10$ is therefore applied in this thesis. $\theta_{cr} = 0.05$ when the seabed is flat, which is assumed here.

6.1 The time scale in random waves

The time scales caused by random waves were derived in Ch. 5.1.1 as CASE 1-4. All the formulas of the dimensionless time scale T^* could be expressed by t as the only parameter dependent on the distribution of the wave amplitudes/crests. This is used in the following method to calculate the expected value of the time scale of scour or backfilling.

6.1.1 Linear random waves

The expected value of the dimensionless time scale t for linear waves is expressed as:

$$E[t(\hat{a})|\hat{a} > \hat{a}_{1/n}] = n \int_{\hat{a}_{1/n}}^{\infty} t(\hat{a}) p(\hat{a}) d\hat{a} \tag{82}$$

where $p(\hat{a})$ is the probability density function given by Eq. (27) and $t(\hat{a})$ is the normalized dimensionless time scale from Eqs. (58), (62), (71) and (75), given as $t(\hat{a}) = \hat{a}^{-v}$. By inserting $t(\hat{a})$ and $p(\hat{a})$ into Eq. (82), the expected value of the dimensionless time scale is found as:

$$E[t(\hat{a})|\hat{a} > \hat{a}_{1/n}] = n \int_{\hat{a}_{1/n}}^{\infty} 2\hat{a}^{(1-v)} e^{-\hat{a}^2} d\hat{a} \tag{83}$$

where $\hat{a}_{1/n}$ is the linear normalized wave height exceeded by the probability $1/n$. It is found by substituting $\hat{a}$ by $\hat{a}_{1/n}$ in the cdf from Eq. (26) such that $1 - P(\hat{a}_{1/n}) = 1/n$ can be solved with respect to $\hat{a}_{1/n}$. This results in:

$$\hat{a}_{1/n} = \sqrt{\ln n} \tag{84}$$

6.1.2 2D and 3D nonlinear random waves

The expected value of the time scale for nonlinear waves is expressed:

$$E[t(w_c)|w_c > w_{c1/n}] = n \int_{w_{c1/n}}^{\infty} t(w_c) p(w_c) dw_c \tag{85}$$

where $p(w_c)$ is the probability density function given by Eq. (40) and $t(w_c)$ is the normalized dimensionless time scale given by Eqs. (58), (62), (71) and (75) as $t(w_c) = w_c^{-v}$. By inserting $t(w_c)$ and $p(w_c)$ into Eq. (85), the expected value of the dimensionless time scale is found as:

$$E[t(w_c)|w_c > w_{c1/n}] = n\beta \int_{w_{c1/n}}^{\infty} \frac{w_c^{\beta-1-v}}{(\sqrt{8}\alpha)^{\beta}} * e^{-(\frac{w_c}{\sqrt{8}\alpha})^{\beta}} dw_c \tag{86}$$

where $w_{c1/n}$ is the normalized nonlinear wave height exceeded by the probability $1/n$. It is found by substituting w_c by $w_{c1/n}$ in the cdf from Eq. (33) such that $1 - P(w_{c1/n}) = 1/n$ can be solved with respect to $w_{c1/n}$. This results in:

$$w_{c1/n} = \sqrt{8}\alpha(\ln n)^{1/\beta} \tag{87}$$

6.1.3 Comparison of nonlinear and linear results

The time scales T^* in CASE 1 - CASE 4 for linear, nonlinear 2D, and nonlinear 3D waves can be compared by the non-dimensional time scale t. t is independent of KC_{rms} and θ_{rms}, but the ratio of t will represent the ratio of T^* for given values of θ_{rms} and KC_{rms}. For linear waves, $t(\hat{a})$ will be constant for each case, while for nonlinear waves $t(w_c)$ will vary with only U_r and S_1.

The ratio of the expected values of t for the nonlinear Forristall distribution and the linear Rayleigh distribution is obtained by dividing Eq. (86) by Eq. (83):

$$R1 = \frac{n\beta \int_{w_{c,1/n}}^{\infty} \frac{w_c^{\beta-1-v}}{(\sqrt{8}\alpha)^{\beta}} * e^{-(\frac{w_c}{\sqrt{8}\alpha})^{\beta}} dw_c}{n \int_{\hat{a}_{1/n}}^{\infty} 2\hat{a}^{(1-v)} * e^{-\hat{a}^2} d\hat{a}} \tag{88}$$

The expected value for the nonlinear solution can be solved by assuming long-crested or short-crested waves. The ratio of the $3D$ and $2D$ solution is found by substituting α and β in Eq. (86) with α_{3D}, β_{3D}, α_{2D}, and β_{2D} from Eqs. (34) - (37):

$$R2 = \frac{n\beta_{3D} \int_{w_{c,1/n}}^{\infty} \frac{w_c^{\beta_{3D}-1-v}}{(\sqrt{8}\alpha_{3D})^{\beta_{3D}}} * e^{-(\frac{w_c}{\sqrt{8}\alpha_{3D}})^{\beta_{3D}}} dw_c}{n\beta_{2D} \int_{w_{c,1/n}}^{\infty} \frac{w_c^{\beta_{2D}-1-v}}{(\sqrt{8}\alpha_{2D})^{\beta_{2D}}} * e^{-(\frac{w_c}{\sqrt{8}\alpha_{2D}})^{\beta_{2D}}} dw_c} \tag{89}$$

6.2 The time scale in random waves plus current

The time scales for random waves plus current were derived in Ch. 5.2.4 and the final expressions for T^* are shown in Eqs. (78) and (81). In these

equations, it is not possible to express the w_cs as one factor in T^*. Due to this, the whole expression of T^* must be included in the integral. A truncated distribution must be applied because there exists a lower limit of w_c due to the criterion $U_{cw} < 0.7$.

6.2.1 Linear random waves plus current

The expected value of the non-dimensional time scale of scour or backfilling in linear waves is found by the following formula:

$$E[T^* \mid \hat{a} > \hat{a}_{1/n}] = n \int_{a_{1/n}}^{\infty} T^*(\hat{a}) p(\hat{a}) d\hat{a} \tag{90}$$

where $p(\hat{a})$ is the truncated pdf for the Rayleigh distribution given in Eq. (29). By inserting $\hat{a}_2 = \infty$ as the upper value, the following pdf is obtained:

$$p(\hat{a}) = 2\hat{a} e^{\hat{a}_1^2 - \hat{a}^2} \tag{91}$$

The $1/n$ highest waves in the truncated Rayleigh distribution is found by solving
$1 - P(\hat{a} \leq \hat{a}_{1/n}) = 1/n$ where the cdf is given by Eq. (28) where $\hat{a}_2 = \infty$, such that:

$$\hat{a}_{1/n} = \sqrt{\ln n + \hat{a}_1^2} \tag{92}$$

$\hat{a}_1$ is the smallest value the linear non-dimensional wave amplitude can have in order to make Eq. (78) valid. This value is found by solving Eq. (79) with respect to $\hat{a}_{1/n}$ (shown as w_c) for each value of U_{cwrms}.

6.2.2 2D and 3D nonlinear waves plus current

The expected value of the non-dimensional time scale for scour or backfilling in nonlinear waves is found by the following formula:

$$E[T^* \mid w_c > w_{c1/n}] = n \int_{w_{c1/n}}^{\infty} T^*(w_c) p(w_c) dw_c \tag{93}$$

where $p(w_c)$ is the truncated pdf for the Forristall distribution given in Eq. (42). By inserting $w_{c2} = \infty$ as the upper value the following pdf is obtained:

$$p(w_c) = \left(\frac{1}{\sqrt{8}\alpha}\right)^{\beta} \beta w_c^{\beta-1}\, e^{\left(\frac{w_{c1}}{\sqrt{8}\alpha}\right)^{\beta} - \left(\frac{w_c}{\sqrt{8}\alpha}\right)^{\beta}} \tag{94}$$

The $(1/n)$'th highest waves in the truncated Forristall distribution is found by solving $1 - P(\omega_c \leq \omega_{c1/n}) = 1/n$ where the cdf is given by Eq. (41) for $w_2 = \infty$, such that:

$$w_{c1/n} = \sqrt{8}\alpha \left[\left(\frac{w_{c1}}{\sqrt{8}\alpha}\right)^{\beta} + \ln n\right]^{1/\beta} \tag{95}$$

w_{c1} is the smallest value the nonlinear non-dimensional wave amplitude can have in order to make Eq. (78) valid. This value is found by solving Eq. (79) with respect to w_c for each value of U_{cwrms}.

7 Method, Example Values and Limits

To calculate the dimensionless time scale T^* by the Forristall distribution, some example values of parameters have to be given. This is because the pdf is dependent on α and β, which are functions of S_1 and U_r, Eqs. (38) and (39), expressed by the parameters H_s, T_p, k_p and h. H_s and h are constant through the example calculations shown along with the other fixed parameters in Table 7.1. The procedure for finding T_p and k_p will vary in the different cases and will be described in this chapter. All the calculations are performed in MATLAB.

Caution must be taken when applying different parameters. Some limits appear through the method and are described earlier. They are summarized below:

- Different validity areas of KC and θ are given for each case of T^*. θ_{rms} and KC_{rms} are replaced directly.
- Ursells criterion: $U_r \leq 1$
- $(c, d) = (1.39,\ 0.52)$ for $10 \leq \frac{A_{rms}}{z_0} \leq 10^5$

The criteria check is performed in Microsoft Excel and the resulting parameters can be found in Appendix A as tables given for each case.

Due to the Ursell criterion, an upper limit of KC_{rms} appears and substitutes the initial upper limit given for the time scale if it is higher. By applying the criterion and inverting the expression for U_r given in Eq. (39), a lower value of k_p results when inserting the example values from Table 7.1:

$$k_p \geq \sqrt{\frac{H_s}{h^3}} = 0.0548 \tag{96}$$

U_{rms} is obtained when replacing a, k and ω in Eq. (4) with its r.m.s. values:

$$U_{rms} = \frac{\omega_p a_{rms}}{\sinh(k_p h)} \tag{97}$$

When U_{rms} is substituted into Eq. (15) where T_p is replaced by $2\pi/\omega_p$, the following is obtained:

$$KC_{rms} = \frac{2\pi a_{rms}}{D \sinh(k_p h)} \tag{98}$$

a_{rms} is calculated in accordance with the Rayleigh distribution given in Eq. (25) as $H_s/2\sqrt{2}$. When replacing k_p in Eq. (98) with k_p from Eq. (96), an upper value of KC_{rms} appears for each of the diameters given in Table 7.1. The time scale for the different diameters will be compared such that the lowest upper value must be used. For the slender pile regime (diameters given in row 3), the upper values of KC_{rms} becomes 23, 15 and 12. The upper values given by the validity area of the formulas are always higher than 12, meaning that this limit will be applied. In the large pile regime (diameters given in row 4), the upper limits of KC_{rms} are 4,3 and 2. However, the upper limit of the initial validity area of T^* is $KC_{rms} = 1.5$ and therefore this value must be applied.

Given parameters	
Water depth (h)	$10\,m$
Significant wave height (H_s)	$3\,m$
Diameter (D)	(0.5, 0.75, 1.0) m (CASE 2-5)
Diameter (D)	(3, 4, 5) m (CASE 6)
Ratio quartz sand/fluid density (s)	2.65
Median grain diameter (d_{50})	$0.001\,m$ (CASE 1 and 4)
Constant from friction formula (c)	1.39
Constant from friction formula (d)	0.52
a_{rms}	$1.061\,m$

Table 7.1: Example values for a typical field condition, Myrhaug et al. (2009).

7.1 Scour below pipelines in waves (CASE 1)

θ_{rms} is the only varying parameter in the equation for the time scale of scour below pipelines, given in Eq. (57). An interval of θ_{rms} is given such that the corresponding k_p and ω_p can be found. This is done in the following procedure: the expression for θ_{rms} is found by substituting U_m and z_0 with U_{rms} and $d_{50}/12$ in Eq. (65). The equation is inverted and expressed as U_{rms}:

$$U_{rms} = \Big(\frac{2 * 12^d \, \theta_{rms} \, g(s-1){d_{50}}^{(1-d)}}{{\omega_p}^d \, c}\Big)^{1/(2-d)} \tag{99}$$

To make the dispersion formula, Eq. (5), valid for a narrow-banded seastate, which is one of the assumptions of the method, k and ω are replaced by k_p and ω_p resulting in:

$$\omega_p = \sqrt{g k_p \tanh(k_p h)} \tag{100}$$

When requiring Eq. (99) to equal Eq. (97) and inserting Eq. (100) for ω_p in both of the equations, k_p will be the only unknown for the given θ_{rms}, and can therefore be found. Further, ω_p is calculated by the dispersion formula such that U_r and S_1 can be solved.

The limit A_{rms}/z_0 is controlled for each value of θ_{rms}. A_{rms} is found as U_{rms}/ω_p and z_0 is given as $d_{50}/12$ where d_{50} is found in Tab. 7.1. All the resulting parameters can be found in Appendix A. 1.

7.2 Scour and backfilling around slender piles below waves (CASE 2 and 3)

An interval of of KC_{rms} and three example values of θ_{rms} are given, see Table 7.2, along with the other parameters from Tab. 7.1.

CASE	Shields parameter (θ_{rms})
2	(0.07, 0.13, 0.18)
3	(0.07, 0.10, 0.15)

Table 7.2: Given values of θ_{rms} for CASE 2 and 3.

k_p is found for each value of the given KC_{rms} by inverting Eq. (98):

$$k_p = \frac{1}{h}\sinh^{-1}\Big(\frac{2\pi a_{rms}}{KC_{rms}D}\Big) \tag{101}$$

The frequency is found from Eq. (100) such that U_r and S_1 can be calculated for each value of KC_{rms}. Note that θ_{rms} will not affect the values of U_r and S_1 but they will affect T^*.

It remains to check the criterion A_{rms}/z_0 for each value of the three given values of θ_{rms}. θ_{rms} is given by Eq. (65) when replacing U_m with U_{rms}, resulting in:

$$\theta_{rms} = \frac{0.5\, c\, (z_0 \omega_p)^d\, {U_{rms}}^{(2-d)}}{g(s-1)d_{50}} \tag{102}$$

When evaluating Eq. (102), it can be seen that a consequence of holding θ_{rms} constant is that z_0 must change accordingly to fulfil the equation. z_0 is obtained when replacing d_{50} with $12z_0$ such that the equation can be reorganized and expressed:

$$z_0 = \left(\frac{24}{{w_p}^d} \frac{\theta_{rms} g(s-1)}{c\, U_{rms}^{(2-d)}} \right)^{\frac{1}{d-1}} \tag{103}$$

When calculating the real time, Eq. (43), the change in z_0 must be accounted for in each value of KC_{rms}. All the resulting parameters can be found in Appendices A. 2 and A. 3.

7.3 Backfilling around a slender pile below waves when the initial hole is generated by waves (CASE 4)

CASE 4 is plotted for different values of $\theta_{rms}^2 KC_{rms}$. The procedure is quite similar as for CASE 2 and 3 described in the previous section; KC_{rms} is given and the corresponding k_p is found from Eq. (101) such that ω_p and thereby U_r and S_1 are found. However, in this case, θ_{rms} is not given, allowing z_0 to hold its constant value given in Tab. 7.1. θ_{rms} is found from Eq. (102) for each value of KC_{rms}.

To be able to find T^*, values for KC_{irms} are given, see Table 7.3.

CASE	Keulegan-Carpenter number (KC_{irms})
4	(11, 20, 32)

Table 7.3: Given values of KC_{irms} for CASE 4.

7.4 Backfilling in waves plus current (CASE 5 and 6)

The time scale of backfilling in current plus waves will be given for different values of U_{cwrms}, Eq. (21). For each plot of the time scale, values of KC_{rms} and θ_{rms} are given, see Table 7.4.

CASE	Keulegan-Carpenter number (KC_{rms})	Shields parameter (θ_{rms})
5	(4, 8, 11)	(0.08, 0.07, 0.09)
6	(0.7, 1.5)	(0.101, 0.105)

Table 7.4: Given values of θ_{rms} and KC_{rms} for CASE 5 and 6.

The wave number is calculated by Eq. (101) and will now represent the wave number for waves and current combined. The frequency obtained by the dispersion formula from Eq. (100) is now relative:

$$\omega_r = \sqrt{gk_p \tanh(k_p h)} \tag{104}$$

Further, U_{rms} is calculated by Eq. (97) such that U_c can be calculated for the given interval $U_{cwrms} = [0, 0.7]$ by Eq. (67). The absolute frequency can now be found for each value of U_c:

$$\omega_p = k_p U_c + \sqrt{gk_p \tanh(k_p h)} \tag{105}$$

The Ursell number will be constant in each of the three plots, since k_p is constant. S_1 is varying with the absolute frequency.

The criterion z_0/A_{rms} is controlled by calculating z_0 given by Eq. (103). Similarly as for CASE 2 and 3, a consequence of holding θ_{rms} constant is that z_0 changes. It should be mentioned that the time scale T^* for CASE 6 is not dependent on θ_{rms}, it is only used to check the criterion, while T^* for CASE 5 is directly dependent on the value of θ_{rms}. When finding the real time T given by Eq. (43), both of the cases are dependent on θ_{rms} through z_0.

8 Results and Discussion

This chapter presents the expected value of the time scale for scour and backfilling, calculated by the stochastic method and displayed graphically with its dependency of KC_{rms}, θ_{rms} and U_{cwrms}. The time scale is given non-dimensionally as T^*, and in real time by T given in minutes. Comparisons are made between linear, second-order long-crested and second-order short-crested waves in all cases.

It was described in Ch. 4.2 that when applying the Forristall distribution, second-order effects are included resulting in higher and sharper wave crests compared to the linear sinusoidal waves represented by the Rayleigh distribution. This results in a faster scour process and therefore less time before the equilibrium scour depth is reached when applying Forristall, which will be seen in all the results.

The water depth regime for the different cases will decide whether the short-crested or the long-crested waves give the shortest time scale. From Fig. 4.2 it is seen that the second-order effects almost cease in deep water. The difference frequency effect becomes so small that Forristall neglects it, resulting in higher $2D$ waves as illustrated in Fig. 4.3. However, most of the results lie within the finite water depth regime where the difference frequency effect causes the $3D$ waves to be higher than the $2D$ waves, resulting in a decreased time scale. This is physically sound because when the waves are directionally spread, the waves will hit each other and therefore form shapes that are unlikely to be linear sinusoidal waves. The water regime of each case can be found in Appendix A where $h/L < 0.05$ characterize shallow water waves, $0.05 < h/L < 0.5$ is the intermediate region and $h/L > 0.5$ is deep water, Pettersen (2004).

An assumption for all the formulas of the time scale is the live-bed criterion ($\theta > \theta_{cr}$). In this project, the initial bed is always flat resulting in $\theta_{cr} = 0.05$. From Fig. 2.6 it can be seen that when the Shields parameter is above this value, the equilibrium scour depth will not increase even though θ increases. This means that for all the cases, an increase in θ will result in higher sediment transport and therefore shorter time, but not a bigger scour depth.

All the results for vertical piles are plotted for various numbers of KC_{rms}. Fig. 3.4 shows that the bed shear stress increases around the pile when the KC-number increases such that the amount of sediment that must be

transported also increases. This results in a bigger scour hole for a given D, as illustrated in Fig. 3.5, and therefore a longer time in the event of scour.

For the stochastic method proposed in this project, it was seen that for a given sea state, only the (1/10)th highest waves were assumed to contribute to scour. This means that the random waves included in the formulas for the time scale, are quite high resulting in lower time scales than those seen from the original formulas.

The time scale T^* presented by Sumer et al. (1992), Fredsøe et al. (1992) and Sumer et al. (2012) are independent of D. In the previous chapter it was seen that the dependency on the diameter appears through the KC-number, Eq. (98), which is inverted to find k_p and thereby ω_p in order to solve U_r and S_1. This will however not influence the Rayleigh pdf such that T^* calculated by the Rayleigh distribution is independent of D for all the cases.

Note that each case has its own validity area of KC_{rms} and θ_{rms}, presented along with T^* in Chs. 5 and 5.2.4. The intervals on the x-axes are chosen accordingly. The upper value of KC_{rms} is limited by the Ursell criterion as 12 for CASE 2-5 as seen in Ch. 7.

8.1 The time scale of scour

8.1.1 The time scale of scour below pipelines (CASE 1)

Fig. 8.1 shows the isocurves of the ratios R_1 and R_2 for the dimensionless time scale t for scour below a pipeline. Figs. 8.1a and 8.1b display $R_{1,2D}$ and $R_{1,3D}$ given in Eq. (88) where $R_{1,2D}$ gives the ratio of the dimensionless time scale t for nonlinear long-crested to linear waves, while $R_{1,2D}$ gives the ratio of t for nonlinear short-crested to linear waves. Fig. 8.1c gives the ratio of t for short-crested and long-crested waves, given in Eq. (89). As seen from the equations, the solutions are dependent on α and β, which are determined by U_r and S_1. Note that t, and therefore R_1 and R_2 are independent of θ_{rms} and KC_{rms}, but the ratio of t will represent the ratio of T^* for given values of θ_{rms} and KC_{rms}. The distribution of the wave amplitude/crest is the only parameter that will vary when giving different values of U_r and S_1.

In Figs. 8.1a and 8.1b it appears that R_1 decreases with increased S_1 and U_r. This is physically sound because increasing S_1 and U_r means increasing the second-order effects, resulting in flow structures with higher intensity. This causes a lower time scale for the nonlinear solution, while the linear one obviously remains constant.

With high nonlinearity, the nonlinear time scale is 40% as low as the linear time scale for $R_{1,2D}$, while for $R_{1,3D}$ the nonlinear solution is even lower. When comparing one value of an isocurve in the two plots, the $R_{1,3D}$ curve generally appears more to the left. This means that the $3D$ solution gives a lower time scale for a given value of U_r and S_1. However, when studying the isocurves in $R_{1,2D}$ they appear linear, while the $R_{1,3D}$ curves are bent and have a steeper slope. A result of this is that the isocurves for $R_{1,2D}$ appear more to the left compared to $R_{1,3D}$ when S_1 is high and U_r is low. This can be seen more clearly in Fig. 8.1c where this area has positive isocurves showing that the time scale for $2D$ waves is lowest. It can also be seen in R_2 that the highest nonlinearity indicated by high values of U_r and S_1, gives the biggest difference in the time scale for short crested and long crested waves where $3D$ is 80% of the $2D$ time scale.

The tendencies shown in Fig. 8.1 are also found in Myrhaug and Ong (2014) in Fig. 2, where R_1 and R_2 represent the ratios of the burial depth for nonlinear to linear and short-crested to long-crested waves. In this thesis, the time scale will be shorter for sharper and bigger waves while S/D will on the other hand increase. This means that Fig. 2 in Myrhaug and Ong (2014) shows the opposite of what is seen here; the isocurves in R_2 are generally larger than 1, except for the combination of high values of S_1 and low values of U_r.

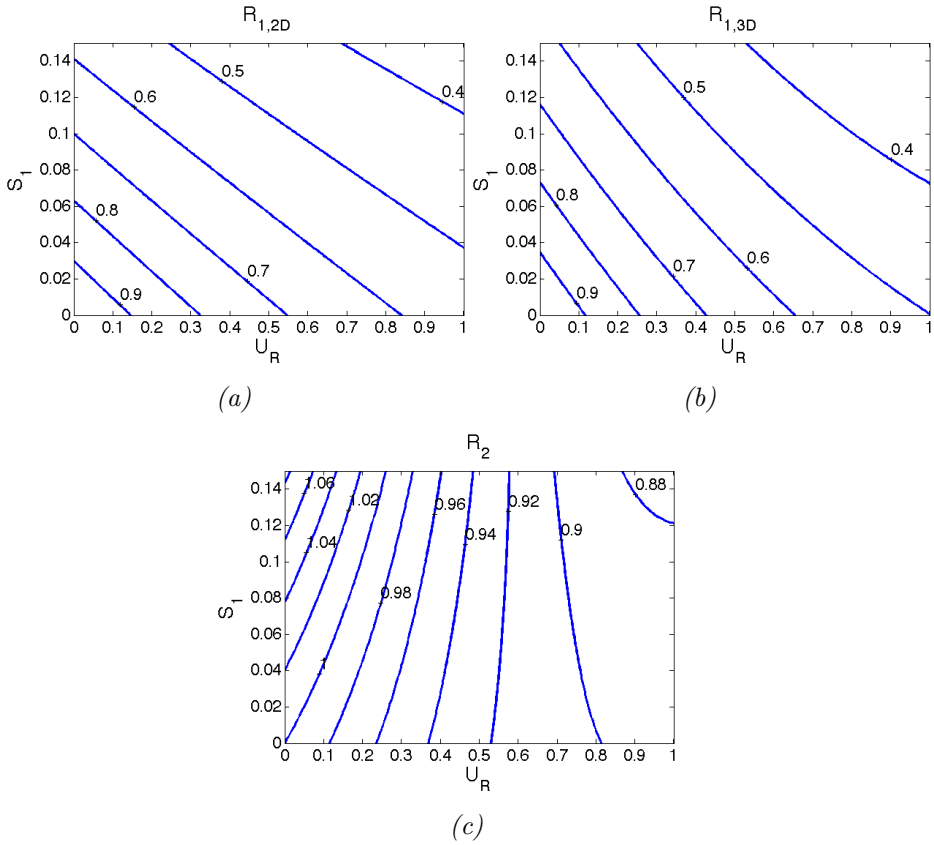

Figure 8.1: Isocurves for the ratios R_1, Eq. (88) and R_2, Eq. (89) for the dimensionless time scale t of scour below a pipeline. a)$R_{1,2D}$ - nonlinear long-crested to linear. b)$R_{1,3D}$ - nonlinear short-crested to linear. c) R_2 - short-crested to long-crested.

Fig 8.2 shows the expected value of the time scale T^* of scour below a pipeline, presented in Eq. (57) and calculated with the stochastic method proposed in Ch. 6.1. It shows that the time scale decreases with increased θ_{rms} due to higher sediment transport. The short-crested waves result in a higher time scale than the long-crested, this is most significant for lower values of θ_{rms}. From Appendix A. 1, Tab. A.2, it can be seen that lower values of θ_{rms} give higher values of h/L_p, indicating deep water waves, which are long relative to the water depth. In this case the wave set-down effects are small, while the set-up effects are larger for $2D$ than $3D$ waves. This is also verified when studying S_1 and U_r from Tab. A.2, revealing

low values of U_r combined with high values of S_1, which result in a lower time scale for $2D$ waves as shown in Fig. 8.1c.

Fig. 8.3 shows the expected value of the time scale T of scour below a pipeline, given in minutes. This is obtained by using the relation between T^* and T from Eq. (43). It can be seen from the figure that an increase in D results in higher time scale. This can be explained by the decreased vortex shedding frequency for higher diameters, which can be seen when studying the Strouhals number, $S = f_v D/U$, where S equals 0.2 within a big velocity area such that the vortex shedding frequency can be expressed as:

$$f_v = \frac{0.2 U_{rms}}{D} \tag{106}$$

From Tab. A.2 it is seen that for a given value of θ_{rms}, U_{rms} is constant, resulting in lower vortex shedding frequency when D increases.

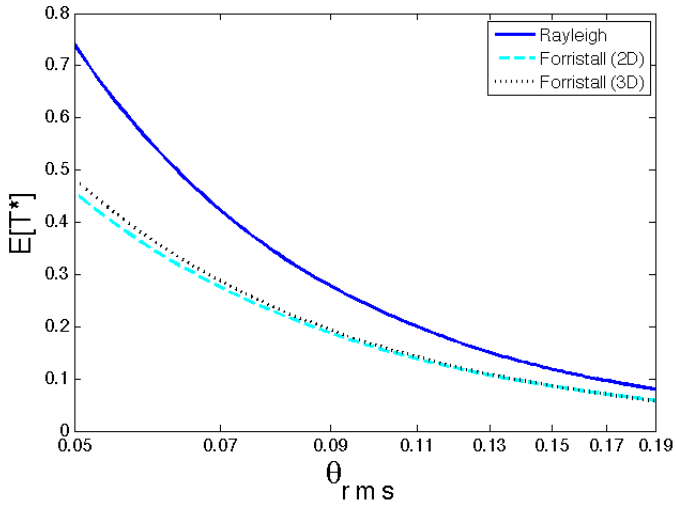

Figure 8.2: The expected value of the time scale T^* of scour below a pipeline for linear and second-order waves.

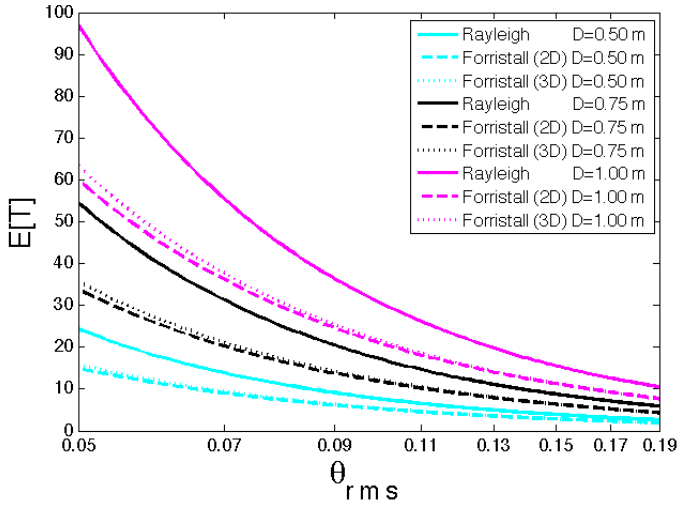

Figure 8.3: The expected value of the time scale T (min) of scour below a pipeline for linear and second-order waves. Given for $D = 0.5m$, $D = 0.75m$ and $D = 1m$.

8.1.2 Scour around vertical slender piles (CASE 2)

Fig. 8.4 displays the isocurves of the ratios R_1 and R_2 for the dimensionless time scale t of scour around a slender vertical pile, plotted versus S_1 and U_r. The trend in these figures is similar to that described for pipelines in the previous section; the isocurves for a given value of $R_{1,3D}$ generally appear more to the left compared to $R1_{2D}$, indicating a lower time scale for a given value of U_r and S_1. The combination of low values of U_r and high values of S_1 also gives shorter time scale for long-crested waves in this case. Keep in mind that these ratios are independent of θ_{rms} and KC_{rms}, the only varying parameters are U_r and S_1.

The highest difference in the time scale t between the short-crested and long-crested waves can be seen from Fig. 8.4c where it appears in the area of highest second-order effects where t for $3D$ waves is 92 % of $2D$ waves.

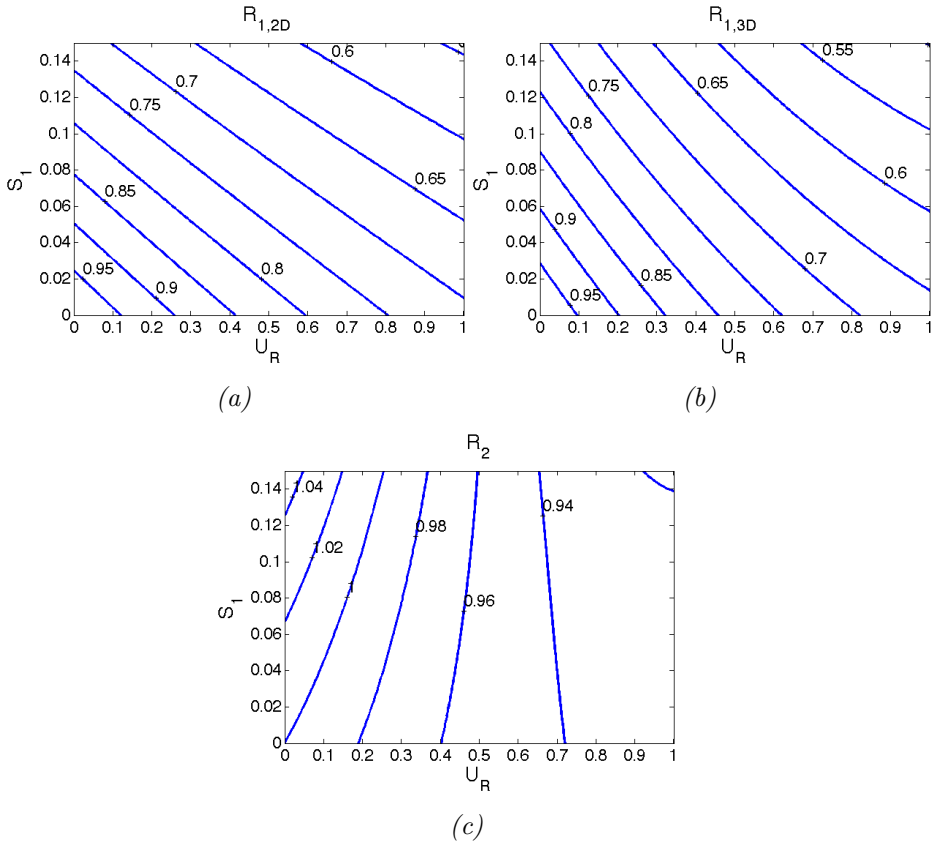

Figure 8.4: Isocurves for the ratios R_1, Eq. (88) and R_2, Eq. (89) for the dimensionless time scale t of scour around a slender vertical pile. a)$R_{1,2D}$: Nonlinear long-crested to linear. b)$R_{1,3D}$: Nonlinear short-crested to linear. c) R_2: Short-crested to long-crested.

Fig. 8.5 shows the expected value of the time scale T^* of scour around a vertical slender pile for $\theta_{rms} = 0.07$, $\theta_{rms} = 0.13$ and $\theta_{rms} = 0.18$, presented by Eq. (61) and calculated by the stochastic method proposed in Ch. 6.1. It shows that the time scale decreases with increased θ_{rms} due to higher sediment transport.

In Appendix A. 2, Tab. A.4, it can be seen that for $D = 0.5\,m$ and $KC_{rms} = 7$, the combination of S_1 and U_r corresponds to an isocurve in Fig. 8.4c where R_2 is just below 1. When KC_{rms} increases, S_1 decreases and U_r increases, moving the point in R_2 downwards to the right. This indicates a lower value of $R2$ and therefore an even lower value of the time scale of the $3D$ solution, compared to the $2D$. This is consistent with Fig.

8.5 where it can be observed that the difference in the time scale for short-crested and long-crested waves increases with KC_{rms}. When comparing the values of S_1 and U_r for a given KC_{rms} for the 3 diameters, it can be seen that higher D always gives a point more downward to the right in R_2, causing a higher difference in $2D$ and $3D$. This is also consistent with Fig. 8.5.

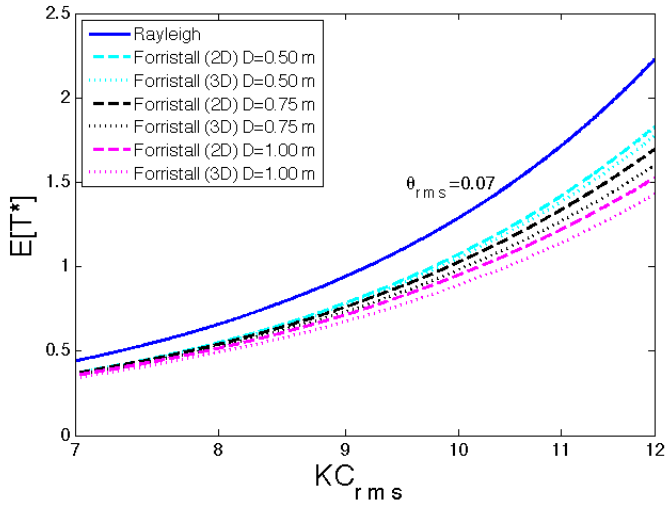

(a)

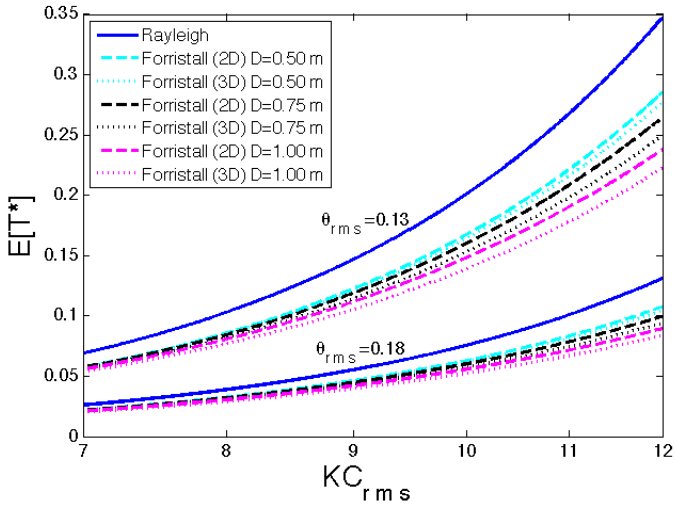

(b)

Figure 8.5: The expected value of the dimensionless time scale T^* of scour around a vertical slender pile for linear and second-order waves for $D = 0.5\,m$, $D = 0.75\,m$ and $D = 1\,m$. a) $\theta_{rms} = 0.07$ b) $\theta_{rms} = 0.13$ and $\theta_{rms} = 0.18$

As earlier mentioned, the time scale T^* for linear waves is independent of D because the Rayleigh distribution function is not dependent on U_r and S_1 such that the distribution of the wave amplitudes therefore is independent of the given KC_{rms}, for details see Ch. 7.2. D will affect the value of S_1 and U_r and is therefore responsible for a small variation in T^* for nonlinear waves. However, D is totally accounted for in the time scale T by the relation $T = T^* D^2 / \sqrt{g(s-1)d_{50}^3}$ from Eq. (43). This means that the variation of the time scale for different diameters should be evaluated in T and not in T^*. Fig. 8.6 shows the time scale T given in minutes and it can be observed that the time scale increases with increased D. This is consistent with the values of f_v in Appendix A. 2, Tab A.4, Col. 9 where it can be seen that for a given KC_{rms}, f_v decreases with increased diameter.

Fig. 8.6 displays T for $\theta_{rms} = 0.07$ and $\theta_{rms} = 0.18$, and it shows the opposite of what would be expected; the highest value of θ_{rms} gives the highest value of the time scale. For a given value of KC_{rms}, h, H_s, D, s, d_{50}, c and d (see Tab. 7.1), this would not be physically sound. However, in this case, a mathematical consequence of holding θ_{rms} at a constant value, is that d_{50} varies for each given KC_{rms} and D. From Appendix A. 2, Tab. A.5, Col. 2,4 and 6, it can be observed that for a given value of KC_{rms}, z_0 decreases when θ_{rms} increases. Tab A.4 shows that for a given KC_{rms} and D, there will be one resulting value of U_{rms} and A_{rms}. This means that the only parameter varying in the equation for the shear stress given by Eq. (2), is z_0. The reduced z_0 for higher θ_{rms} therefore results in a lower shear stress, which explains the increased time scale for higher θ_{rms}. Note that the value of z_0 will not affect T^* but it comes into T through Eq. (43) where d_{50} appears in the denominator.

The problem with the varying z_0 could be avoided if θ_{rms} was calculated for each given value of KC_{rms} with a given z_0, similar to the procedure in CASE 4 described in Ch. 7.3. However, the present results are displayed for a given θ_{rms} for simpler comparison with the results from Sumer et al. (1992).

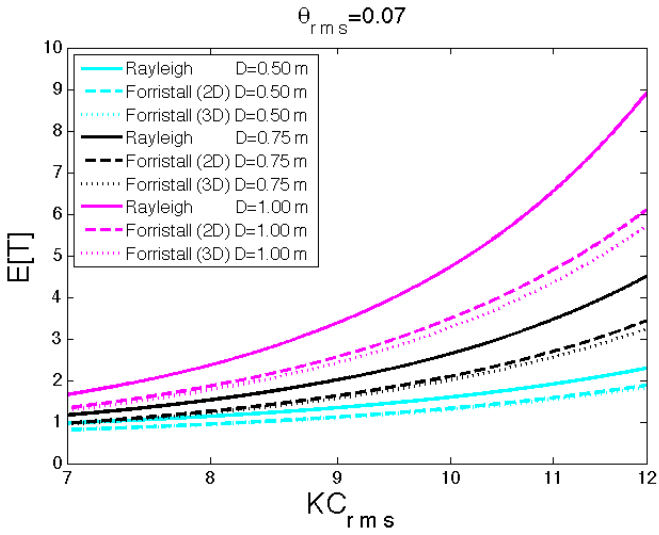

(a)

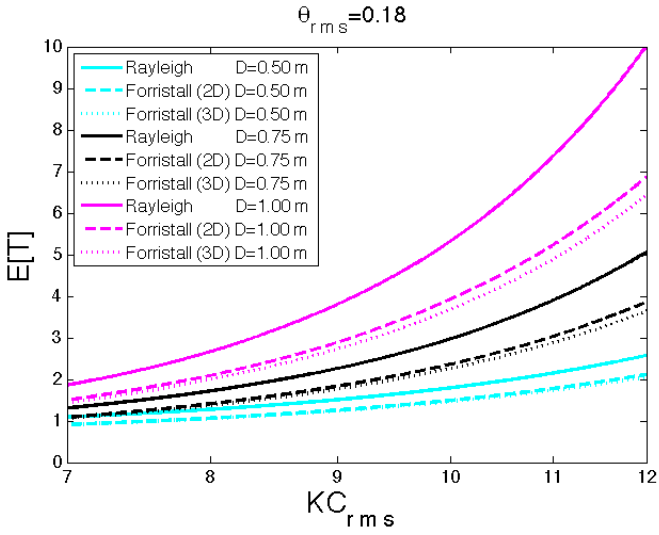

(b)

Figure 8.6: The expected value of the time scale T (min) of scour around a vertical slender pile for linear and second-order waves for $D = 0.5\,m$, $D = 0.75\,m$ and $D = 1\,m$. a) $\theta_{rms} = 0.07$. b) $\theta_{rms} = 0.18$.

8.2 The time scale of backfilling

When KC_{rms} increases for a given D, the scour hole will also increase until a certain depth corresponding to the depth generated by a current. In the cases of backfilling, smaller values of KC_{frms} indicate smaller value of the final scour depth, resulting in longer time.

8.2.1 Backfilling by waves when the initial hole was generated by current (CASE 3)

Fig. 8.7 displays the isocurves for the ratios R_1 and R_2 for the dimensionless time scale t of backfilling around a slender vertical pile, plotted versus S_1 and U_r. The trend in these figures is similar to those described for scour below pipelines and around vertical piles in the previous section. The main difference is that in Figs. 8.7a and 8.7b, the value of t for nonlinear waves is as low as 10 % of the linear t, which is much lower than what is shown for scour where it was $40 - 60$ %, when the nonlinearity is high. The largest difference in the time scale between the short-crested and long-crested waves can be seen from Fig. 8.7c where it is below 0.8 when the second-order effects are high.

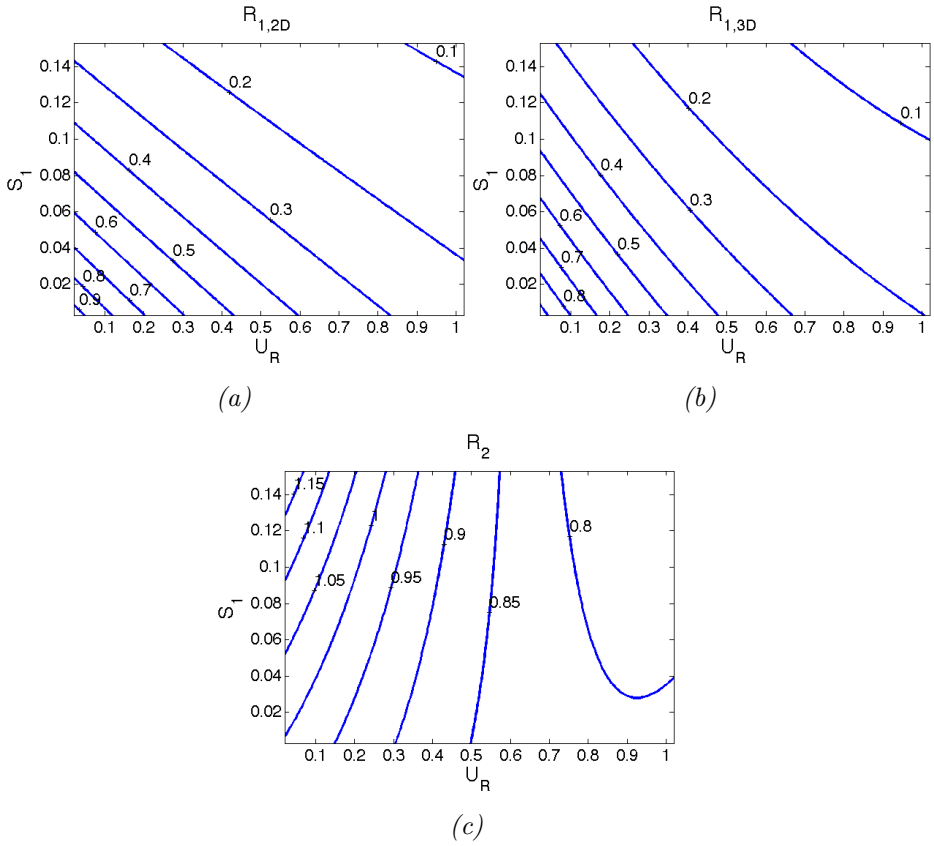

Figure 8.7: Isocurves for the ratios R_1, Eq. (88) and R_2, Eq. (89) for the dimensionless time scale t of backfilling around a slender verical pile. a)$R_{1,2D}$: Nonlinear long-crested to linear. b)$R_{1,3D}$: Nonlinear short-crested to linear. c) R_2: Short-crested to long-crested.

Fig. 8.8 shows the time scale T^* of backfilling by waves around a vertical slender pile where the initial hole was generated by a current, described in Eq. (70) and calculated with the stochastic method proposed in Ch. 6.1. The same tendencies as mentioned earlier can be seen: higher θ_{rms} gives shorter time scale and the nonlinear time scale is shorter than the linear. When studying U_r and S_1 (App. A. 3, Tab. A.7) in relation with the isocurves from 8.7c, it can be seen that R_2 decreases when KC_{rms} becomes higher. This indicates that the difference between the $2D$ and $3D$ solution increases relatively for high values of KC_{rms}, even though it looks like the solutions approach each other in Fig. 8.8 due to the decreased time scale.

Fig. 8.9 shows the variation of T^* with θ_{rms} for $D = 0.5\,m$ and $D = 1\,m$.

When reading the values of U_r and S_1 for $D = 0.5\,m$ (App. A. 3, Tab. A.7), it can be seen from the isocurves in Fig. 8.7c that R_2 is higher than 1 when KC_{rms} is low. Therefore, the time scale in $2D$ waves appear lower than for $3D$ waves when $D = 0.5$ and KC_{rms} is low. This is most visible when $\theta_{rms} = 0.07$ because it gives the highest time scale. Keep in mind that R_2 is independent of θ_{rms}. When $D = 1\,m$, R_2 is lower than 1 for all the values of KC_{rms}, which can be seen in Fig. 8.9b where the $3D$ solution gives the smallest time scale.

Fig. 8.10 shows the expected value of the time scale T given in minutes for $\theta_{rms} = 0.07$ and $\theta_{rms} = 0.15$. Higher values of D give lower vortex shedding frequency (App. A. 3, Tab. A.7), and therefore increased time scales. However, this figure shows that when KC_{rms} is low, $D = 0.5\,m$ gives the highest time scale. This can be explained when considering Tab. A.8, where $D = 0.5\,m$ gives the highest values of A_{rms}/z_0 for low values of KC_{rms}, indicating the lowest friction given by Eq. (6). As KC_{rms} increases, A_{rms}/z_0 becomes smallest for $D = 0.5\,m$, indicating the highest friction and therefore the lowest time scale.

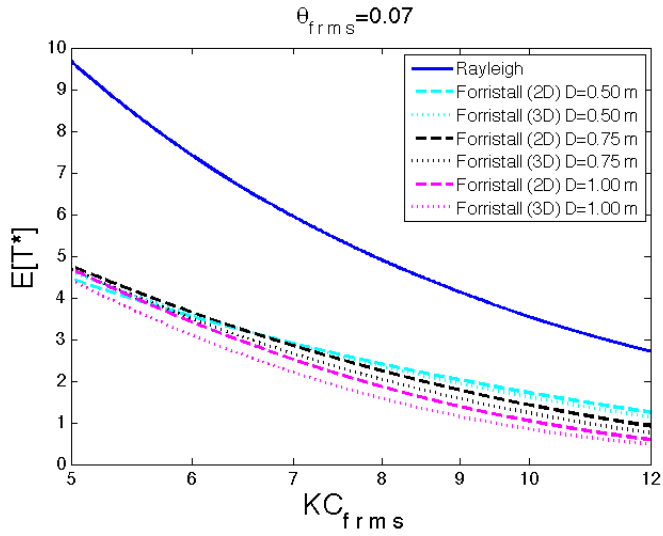

(a)

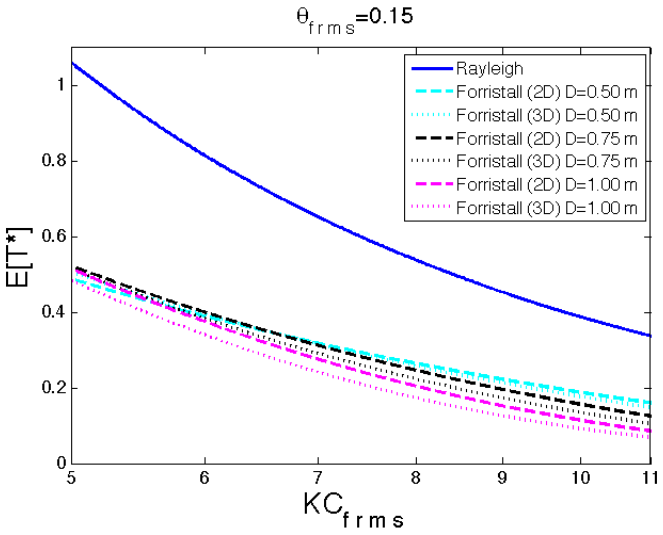

(b)

Figure 8.8: The expected value of the time scale T^* of backfilling around a vertical slender pile when the initial hole was generated by a current for $D = 0.5\,m$, $D = 0.75\,m$ and $D = 1\,m$. a) $\theta_{rms} = 0.07$. b) $\theta_{rms} = 0.15$.

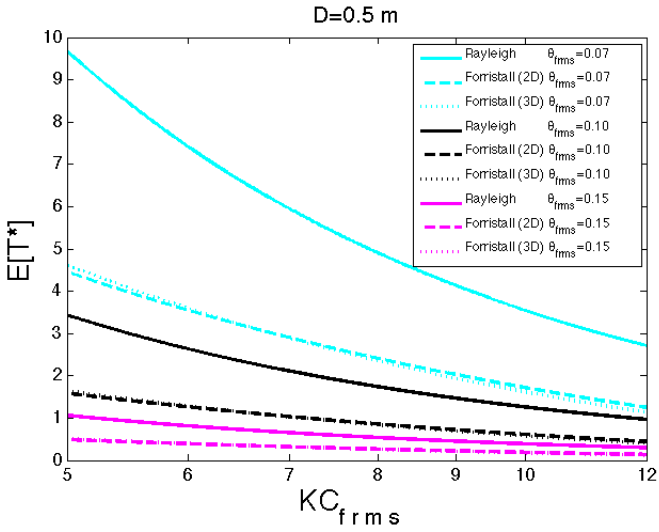

(a)

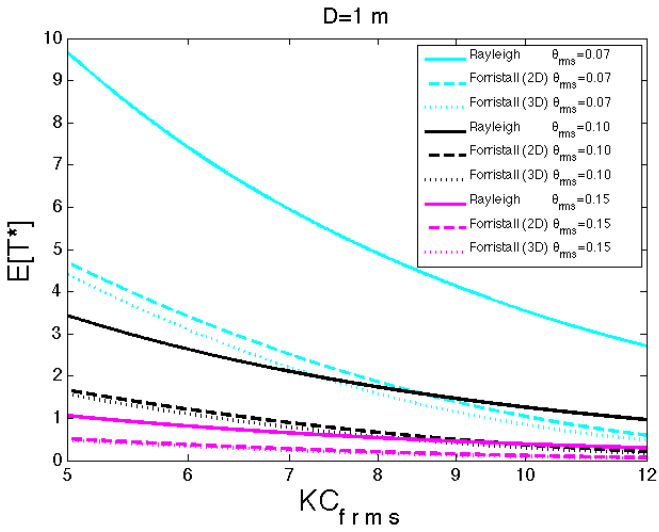

(b)

Figure 8.9: The expected value of the time scale T^* of backfilling around a vertical slender pile when the initial hole was generated by a current for $\theta_{rms} = 0.07$, $\theta_{rms} = 0.10$ and $\theta_{rms} = 0.15$. a) $D = 0.5\,m$ b) $D = 1\,m$.

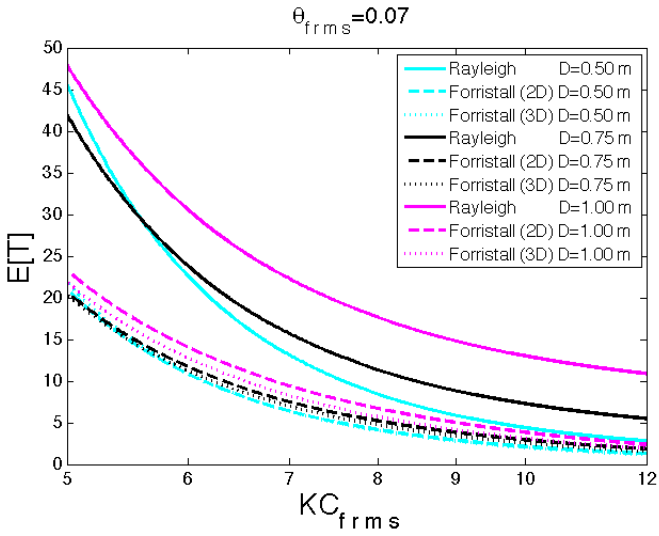

(a)

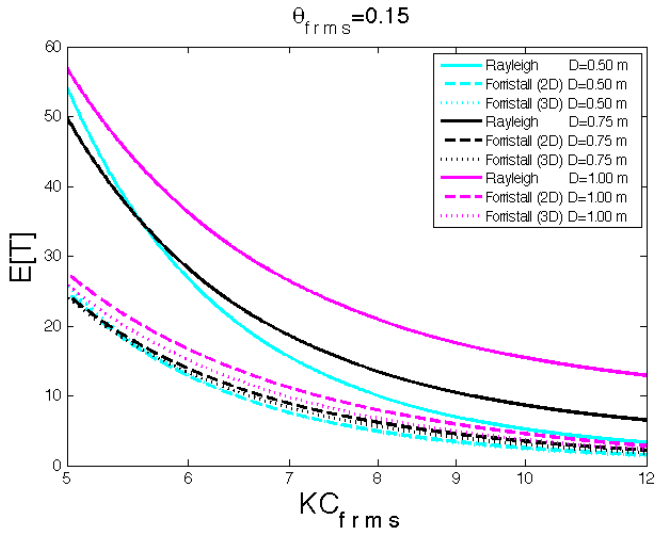

(b)

Figure 8.10: The expected value of the time scale T (min) of backfilling around a vertical slender pile when the initial hole was generated by a current for $D = 0.5\,m$, $D = 0.75\,m$ and $D = 1\,m$. a) $\theta_{rms} = 0.07$. b) $\theta_{rms} = 0.15$.

8.2.2 Backfilling by waves when the initial hole was generated by waves (CASE 4)

This section shows the time scale of backfilling by waves when the initial scour was generated by waves with $KC_{irms} = 32$, $KC_{irms} = 20$ and $KC_{irms} = 0.11$, described by Eq. (74) and calculated by the stochastic method proposed in Ch. 6.1. In this case, the time scale is plotted versus $(\theta^2 KC)_{rms}$. As described in Ch. 7.3, U_r and S_1 were found from the given KC_{rms} in addition to the global parameters. Based on KC_{rms}, θ_{rms} was calculated from Eq. (102) where d_{50} was given. In contrast to CASE 2 and 3, θ_{rms} therefore varies with each value of KC_{rms}.

The experiments of the time scale were performed by Sumer et al. (2012) with the following lower and upper values:

$$4 \leq KC_{rms} \leq 25 \tag{107}$$

$$0.07 \leq \theta_{rms} \leq 0.15 \tag{108}$$

resulting in:

$$0.02 \leq (\theta^2 KC)_{rms} \leq 0.56 \tag{109}$$

The upper limit of KC_{rms} in the stochastic method appears at 12 due to the Ursells criteria, which is lower than the upper limit from Eq. (107). Even so, $(\theta^2 KC)_{frms}$ calculated in this thesis becomes higher than the upper value from Eq. (109). This is because θ_{rms} calculated in this method becomes higher than the upper limit from Eq. (108), for most of the given values of KC_{rms} (see App. A. 4, Tab. A.10). This will result in a smaller validity area, especially when comparing the 3 diameters. For example when $KC_{rms} = 4$, this method results in $(\theta^2 KC)_{rms} = 0.13$ (for $D = 1\,m$) and when $KC_{rms} = 12$, $(\theta^2 KC)_{rms} = 0.54$ ($D = 0.5\,m$). Therefore, extrapolation is performed by using $KC_{rms} = 3$ as the lower value and $KC_{rms} = 13$ as the upper value. This gives the validity area $0.07 \leq (\theta^2 KC)_{frms} \leq 0.55$, which is used in all the following plots.

The isocurves from this case will equal those for CASE 3, because v given by Eqs. (72) and (76), are the same for the two cases.

Fig. 8.11 shows the time scale T^* of backfilling around a slender vertical pile when the initial hole was generated by waves corresponding to a given initial value of the Keulegan-Carpenter number; denoted KC_{irms}. When KC_{rms} is small, the initial scour depth for a given D is small and therefore it takes shorter time to reach the final depth. Fig. 8.11a displays the time scale for nonlinear waves when $D = 1\,m$ and for linear waves, which are independent of D. Fig. 8.11b shows that the variation of T^* for different values of D is small for nonlinear waves.

Fig. 8.12 shows the time scale T given in minutes for backfilling around a vertical slender pile when the initial hole was generated by waves for $D = 0.5\,m$ and $D = 1\,m$. When studying S_1 and U_r (App. A. 4, Tab. A.10) for $D = 0.5\,m$, in relation with the isocurves from Fig. 8.7c, it can be seen that R_2 is higher than 1 until $KC_{rms} = 7$, which corresponds to $(\theta^2 KC)_{rms} = 0.2$. This is consistent with Fig. 8.12a where it can be seen that after this point, the time scale for the short-crested waves becomes smaller than for the long-crested waves. Note that R_2 is equal for the plots having the same D, but the tendency is more visible when T^* is high. When considering $D = 1\,m$, R_2 is lower than 1 already at $KC_{rms} = 4$, corresponding to $(\theta^2 KC)_{rms} = 0.13$. Fig. 8.12 also shows that the time scale is higher when D increases due to the reduced vortex shedding frequency (App. A. 4, Tab. A.10), consistent with previous results.

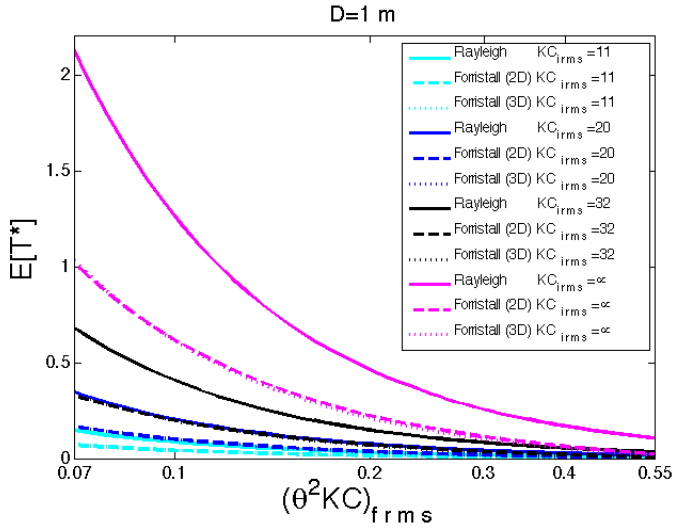

(a)

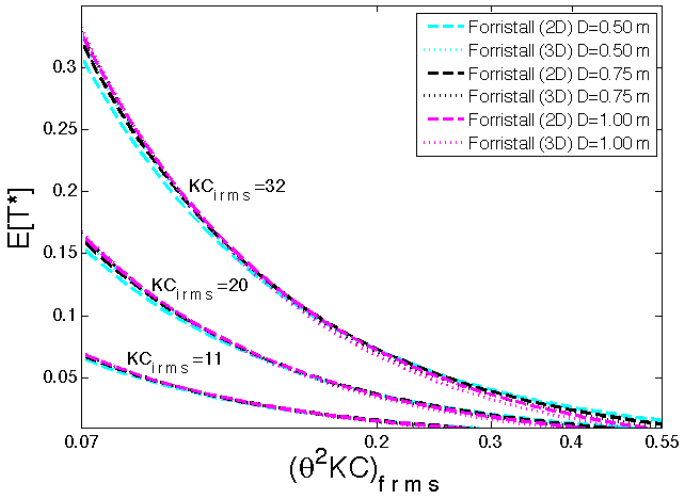

(b)

Figure 8.11: The expected value T^* of backfilling around a slender vertical pile when the initial hole was generated by $KC_{irms} = 32$, $KC_{irms} = 20$ and $KC_{irms} = 0.11$. a) Linear and nonlinear results for $D = 1m$. $KC_{rms} = \infty$ added for comparison. b)Nonlinear results for $D = 0.5\,m$, $D = 0.75\,m$ and $D = 1\,m$.

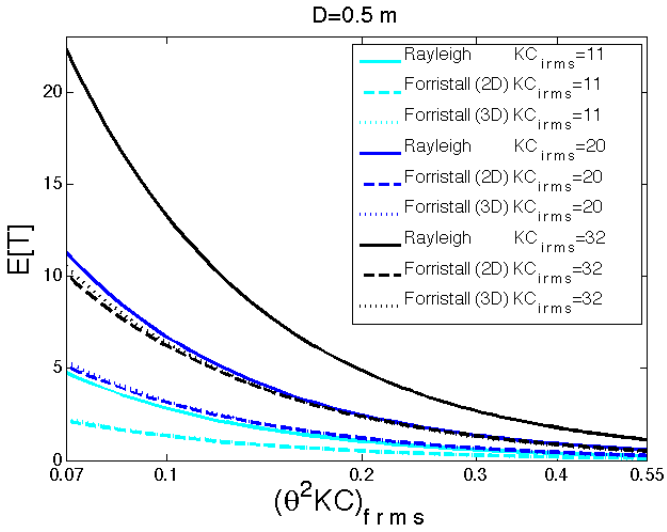

(a)

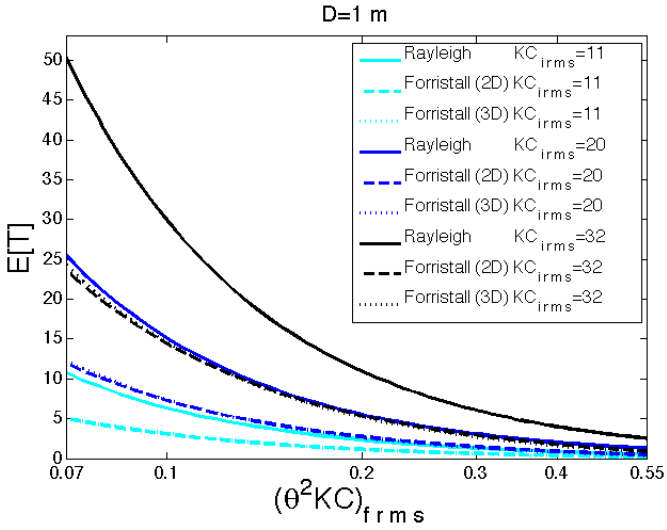

(b)

Figure 8.12: The expected value T (min) of backfilling around a slender vertical pile when the initial hole was generated by $KC_{irms} = 32$, $KC_{irms} = 20$ and $KC_{irms} = 0.11$. a) $D = 0.5\,m$. b) $D = 1\,m$.

8.2.3 Backfilling around a slender pile by waves and current when initial hole was generated by a current (CASE 5)

Fig. 8.13 displays the time scale T^* of backfilling by waves and current around a slender vertical pile where the initial hole was generated by a current, described in Eq. (78) and calculated with the stochastic method proposed in Ch. 6.2. When the value of Eq. (78) exceeds the value for backfilling by waves alone given by Eq. (70), T^* takes the values from waves alone. This is because when the current becomes more dominant, the intensity increases and therefore backfilling by waves alone should give the smallest time scale. When evaluating U_{cwrms} from Eq. (21) for a given KC_{rms} and θ_{rms}, U_{rms} remains constant such that U_c is the only parameter increasing when U_{cwrms} increases in each of the 3 examples. More details are found in Ch. 7.4 and in Appendix A. 5.

Fig. 8.13 shows that the linear solution decreases at a higher rate than the nonlinear solution when the current increases. The isocurves for this case is not plotted but this behaviour should corresponds to an increase in R_1. This is consistent with the results from Fig. 4 in Ong et al. (2013) where R_1 represents the ratio between the nonlinear and linear S/D, which decreases for increased U_{cwrms}. As earlier mentioned, it is expected that R_1 and R_2 representing S/D should behave the opposite way compared to R_1 and R_2 for the time scale because increased intensity decreases the time scale, but increases S/D.

Fig. 8.13 is plotted for 3 different combinations of KC_{rms} and θ_{rms}. When comparing the plots of $(KC_{rms1}, \theta_{rms1})$ and $(KC_{rms2}, \theta_{rms2})$, where θ_{rms} is fixed, the effect of varying KC_{rms} can be evaluated. It can be observed in Fig. 8.13b that R_1 should decrease when KC_{rms} increases; $R_1(KC_{rms1}) \approx 6.5/13.15 = 0.48$ while $R_1(KC_{rms2}) \approx 2.3/6 = 0.38$. This is consistent with the results in Fig. 4 from Ong et al. (2013). It shows that R_1 for S/D increases with higher KC_{rms}, which appears as a reduction of R_1 for the time scale.

Fig. 8.14 displays the time scale T given in minutes for backfilling by waves and current, for $KC_{rms} = 4$ and $KC_{rms} = 7$. It can be observed that the increase in KC_{rms} results in a shorter time of backfilling because the initial and final depth are closer. In the following, the variation of R_2 with KC_{rms} will be evaluated:

When $D = 0.5\,m$ and $KC_{rms} = 4$ (Fig. 8.14a), the $2D$ solution is lower than the $3D$, which should result in a positive value of R_2. This is due to the low value of U_r (see App. A. 5, Tab. A.12, example 1). When $D = 0.5\,m$ and $KC_{rms} = 7$ (Fig. 8.14b) it can be seen that R_2 has decreased (going closer to 1). The reduction in R_2 also appears in the other diameters when KC_{rms} increases. This is consistent with the results from Ong et al. (2013), Fig. 4 where R_2 for S/D increases for higher KC_{rms}.

It should be noted that there is some inconsistency with the present results calculated by the stochastic method, compared to Fig. 5.6 from Sumer et al. (2012). In Fig. 5.6, the point where T^* calculated by waves and current equals the value for waves alone (horizontal line), appears at higher values of U_{cw} for lower values of KC. The present results show the opposite; this point moves to the right for increased KC_{rms}. The reason for this behaviour is not known.

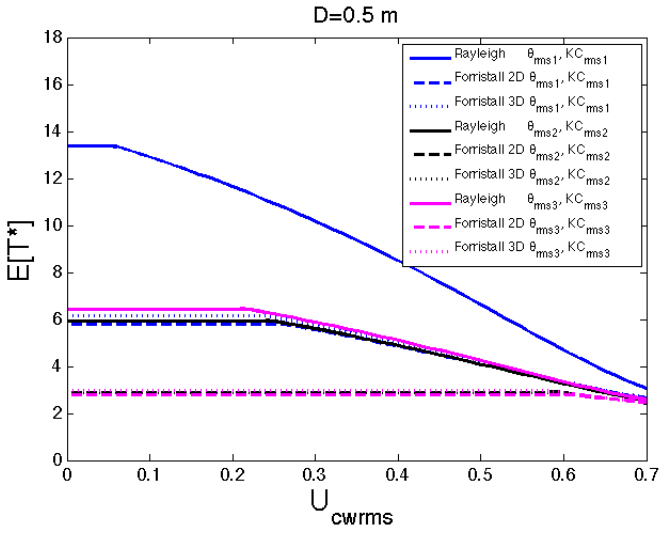

(a)

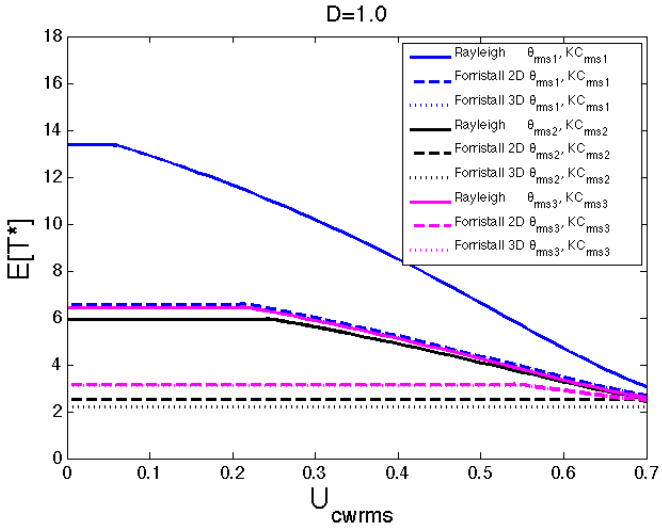

(b)

Figure 8.13: The expected value of the time scale T^* of backfilling around a slender pile in waves and current combined when the initial hole was generated by a current. (KC_{rms1}, θ_{rms1})=(4, 0.07), (KC_{rms2}, θ_{rms2})=(7, 0.07) and (KC_{rms3}, θ_{rms3})=(4, 0.09). a)$D = 0.5\,m$. b) $D = 1.0\,m$.

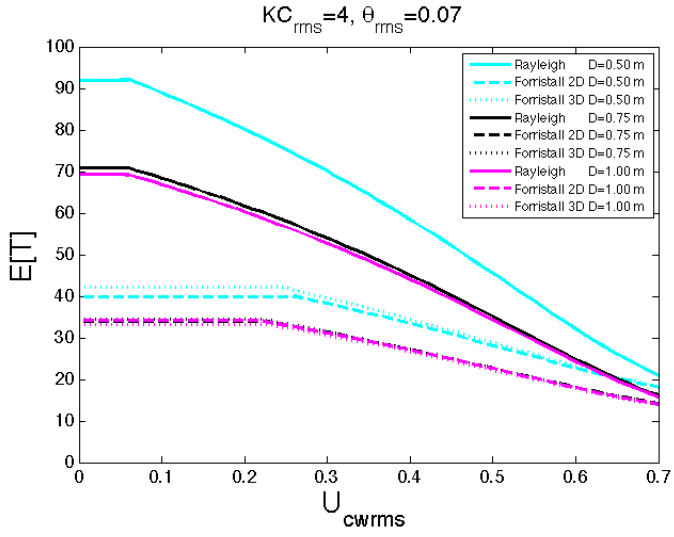

(a)

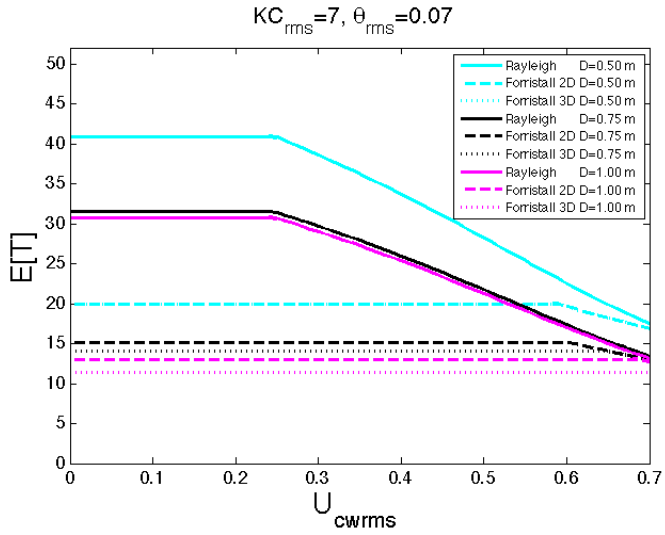

(b)

Figure 8.14: The expected value of the time scale T (min) for backfilling around a slender pile in waves and current combined when the initial hole was generated by a current for $D = 0.5\,m$, $D = 0.75\,m$ and $D = 1.0\,m$.
a) (KC_{rms1}, θ_{rms1})=(4, 0.07). b) (KC_{rms2}, θ_{rms2})=(7, 0.07).

8.2.4 Backfilling around a large pile by waves and current when initial hole was generated by current (CASE 6)

Figs. 8.15 and 8.16 display the time scale of backfilling by waves and current around a large vertical pile where the initial hole was generated by a current, described in Eq. (80) and calculated with the stochastic method proposed in Ch. 6.2. Fig. 8.15 shows the dimensionless time scale T^* given for $D = 3\,m$ and $D = 5\,m$, where it can be observed that the time scale decreases when KC_{rms} increases, similar to CASE 5. Fig. 8.16 shows that the time scale T given in minutes is significantly larger than for the slender pile. This can be explained by the large diameter, which appears in second potential in the conversion from T^* to T in Eq. (43). This results in extremely low vortex shedding frequency, which can be seen in Appendix A. 6, Tabs. A.16- A.18. When $D = 3\,m$ and $KC_{rms} = 0.7$, the time scale for $2D$ waves is lower compared to $3D$ waves due to the low value of U_r, which can be seen in Tab. A.16. In the remaining plots, the short-crested waves gives the lowest time scale.

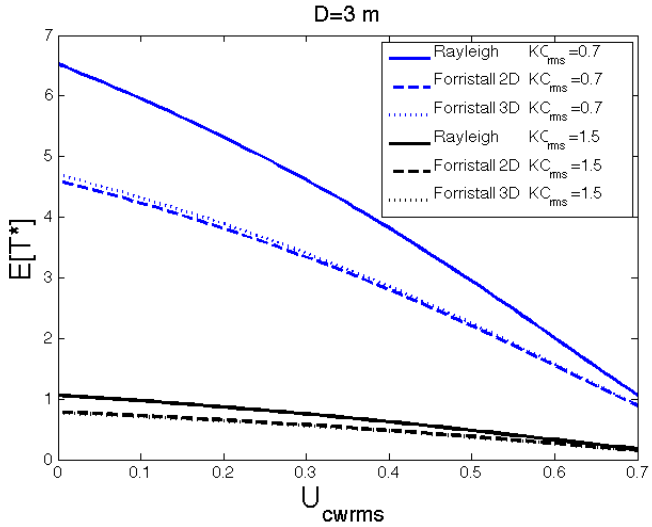

(a)

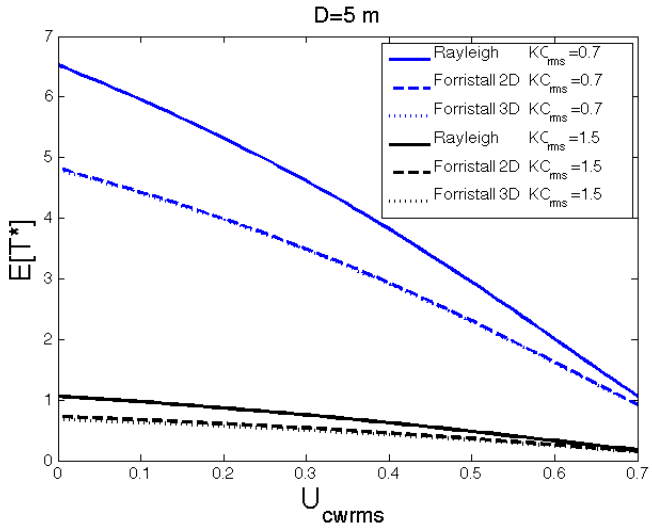

(b)

Figure 8.15: The expected value of the time scale T^* of backfilling around a large pile in waves and current combined when the initial hole is generated by a current. a) $D = 3\,m$. b) $D = 5\,m$.

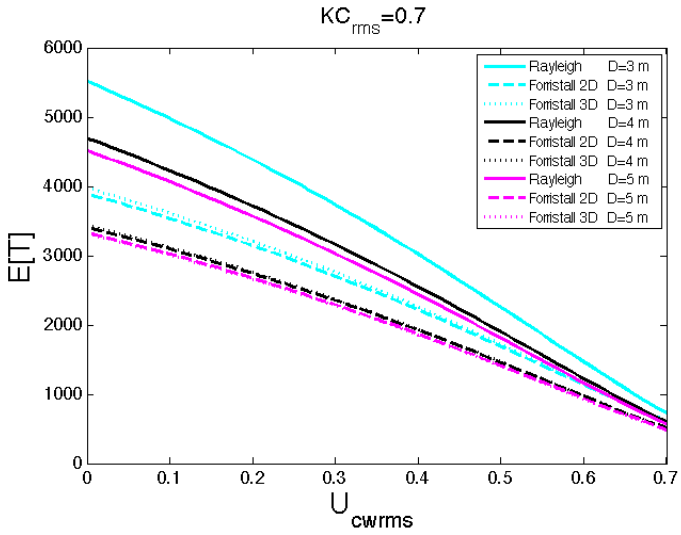

(a)

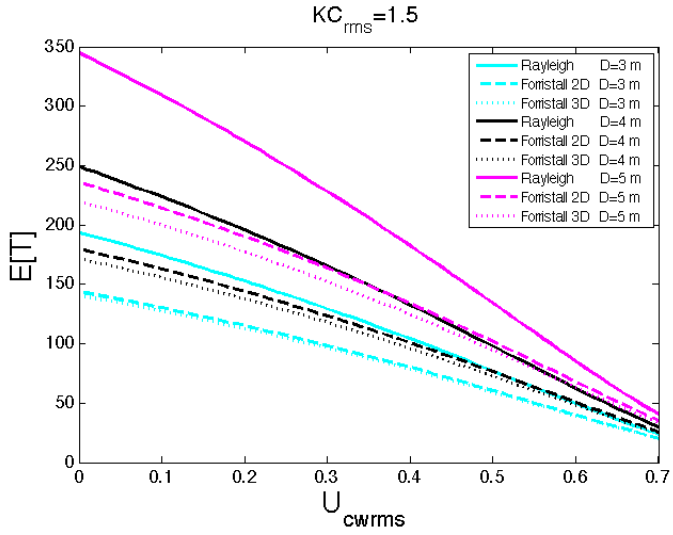

(b)

Figure 8.16: The expected value of the time scale T (min) of backfilling around a large pile in waves and current combined when the initial hole is generated by a current. a) $KC_{rms} = 0.7$. b) $KC_{rms} = 1.5$.

9 Conclusions and Further Work

9.1 Conclusion

The time scale of scour is highly dependent on the strength of incoming flow near the seabed. Overall, the time scale of scour and backfilling becomes smaller in second-order long-crested and second-order short-crested waves compared to linear sinusoidal waves. This is due to the presence of nonlinear effects that indicate higher and sharper waves and thereby higher nearbed velocities. Most of the results lie within finite water depth where the set-down effects causes the short-crested waves to be higher and sharper than the long-crested waves. The time scale of the short-crested waves becomes even smaller relative to the long-crested waves when KC_{rms} increases. However, when the nonlinear effects become small corresponding to deeper water waves (long waves relative to the depth), the long-crested waves might appear as slightly larger than the short-crested waves resulting in a smaller time scale for long-crested waves. The effects become most significant for small numbers of KC_{rms}. This is because Forristall (2000) neglects the set-down effects in deep water and includes only the sum-frequency, which is larger for long-crested than for short-crested nonlinear waves.

The method proposed in this thesis should be applied as a first approximation to find the time scale of scour and backfilling in random waves below pipelines and around vertical piles, and for backfilling around vertical piles in random waves plus current. Comparisons with data are required to validate the results.

9.2 Further work

Petersen (2015) performed experiments presented in Fig. 9.1 for scour around vertical piles in waves and current combined, and derived the empirical formula $T^* = 0.0028\theta^{-3}$, which is valid within $0.3 < U_{cw} < 0.5$. In the present thesis, the formula $T^* = 0.0028\,\theta^{-3} 10^{(-1.88\,\theta^{-0.51}\,(U_{cw}-0.5))}$ has been fitted to the result for $0.5 < U_{cw} < 0.7$. It is of interest to apply the stochastic method, but an improvement of the formula is necessary. In the experiments, the lowest value of T^* is 0.17 and occurs at $U_{cw} \approx 0.73$. The formula should be modified such that values below this are invalid. This is necessary because the stochastic method with $n = 10$ decreases the time scale.

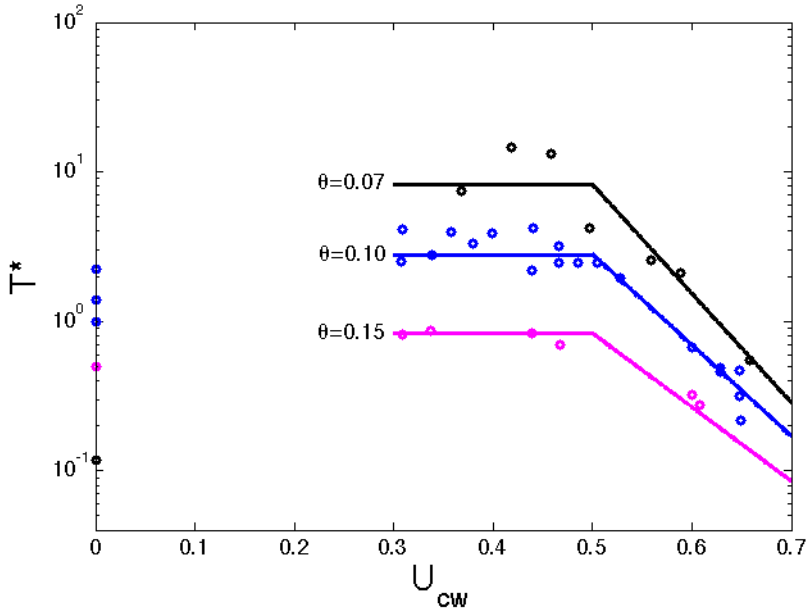

Figure 9.1: The time scale T^* of scour around a vertical slender pile in current and waves combined for $\theta = 0.07$, $\theta = 0.10$ and $\theta = 0.15$.

In addition efforts should be made to understand the origin of the discrepancy found between our results and Sumer et al. (2012) (see Figs. 5.6, 8.13 and 8.14).

References

Cataño-Lopera, Y. A. and García, M. H. (2007). Geometry of scour hole around, and the influence of the angle of attack on the burial of finite cylinders under combined flows, *Ocean Engineering* **34**(5): 856–869.

Dean, R. G. and Dalrymple, R. A. (1984). Water wave mechanics for engineers and scientists, *Englewood Cliffs, New jersey* .

Faltinsen, O. (1993). *Sea loads on ships and offshore structures*, Vol. 1, Cambridge university press.

Forristall, G. Z. (2000). Wave crest distributions: Observations and second-order theory, *Journal of Physical Oceanography* **30**(8): 1931–1943.

Fredsøe, J., Sumer, B., Arnskov, M. et al. (1992). Time scale for wave/current scour below pipelines, *The First International Offshore and Polar Engineering Conference*, International Society of Offshore and Polar Engineers.

Hesten, P. (2011). *Scour around wind turbine foundations, marine pipelines and short cylinders due to long-crested and short-crested nonlinear random waves plus currents*, Master's thesis, Department of Marine Technology, Faculty of Engineering Science and Technology, NTNU.

Isaacson, M. (1979). Wave-induced forces in the diffraction regime, *Mechanics of wave-induced forces on cylinders* pp. 68–89.

Kjeldsen, S. P., Gjorsvik, O., Bringaker, K. and Jacobsen, J. (1973). Local scour near offshore pipelines, *Paper available only as part of the complete Proceedings of the Second International Conference on Port and Ocean Engineering Under Arctic Conditions (POAC), August 27-30.*

Longuet-Higgins, M. S. (1952). On the statistical distributions of sea waves, *J. mar. Res.* **11**(3): 245–265.

Mao, Y. (1986). The interaction between a pipeline and an erodible bed, *SERIES PAPER TECHNICAL UNIVERSITY OF DENMARK* **1**(39).

Myrhaug, D. (2004). *Marin dynamikk - Uregelmessig sjø*, Marine Technology centre, Trondheim, Norway.

Myrhaug, D., Holmedal, L. E., Simons, R. R. and MacIver, R. D. (2001). Bottom friction in random waves plus current flow, *Coastal engineering* **43**(2): 75–92.

Myrhaug, D. and Ong, M. (2012). Random wave-induced scour around marine structures using a stochastic method, *Marine Technology and Engineering, CENTEC Anniversary Book, CRC Press* .

Myrhaug, D. and Ong, M. C. (2011). Random wave-induced onshore scour characteristics around submerged breakwaters using a stochastic method, *Ocean Engineering* **37**(13): 1233–1238.

Myrhaug, D. and Ong, M. C. (2014). Burial and scour of truncated cones due to long-crested and short-crested nonlinear random waves, *Ocean Systems Engineering* **4**(1): 21–37.

Myrhaug, D., Ong, M. C., Føien, H., Gjengedal, C. and Leira, B. J. (2009). Scour below pipelines and around vertical piles due to second-order random waves plus a current, *Ocean Engineering* **36**(8): 605–616.

Ong, M. C., Myrhaug, D. and Hesten, P. (2013). Scour around vertical piles due to long-crested and short-crested nonlinear random waves plus a current, *Coastal Engineering* **73**: 106–114.

Petersen, T. U. (2015). Private communication.

Pettersen, B. (2004). *TMR4247 Marin teknikk 3 - Hydrodynamikk*, Marine Technology centre, Trondheim, Norway.

Sharma, J., Dean, R. et al. (1981). Second-order directional seas and associated wave forces, *Society of Petroleum Engineers Journal* **21**(1): 129–140.

Soulsby, R. (1997). *Dynamics of marine sands: a manual for practical applications*, Thomas Telford.

Sumer, B., Christiansen, N., Fredsoe, J. et al. (1992). Time scale of scour around a vertical pile, *The Second International Offshore and Polar Engineering Conference*, International Society of Offshore and Polar Engineers.

Sumer, B. M., Christiansen, N. and Fredsøe, J. (1997). The horseshoe vortex and vortex shedding around a vertical wall-mounted cylinder exposed to waves, *Journal of Fluid Mechanics* **332**: 41–70.

Sumer, B. M. and Fredsøe, J. (1990). Scour below pipelines in waves, *Journal of waterway, port, coastal, and ocean engineering* **116**(3): 307–323.

Sumer, B. M. and Fredsøe, J. (2001a). Scour around pile in combined waves and current, *Journal of Hydraulic Engineering* **127**(5): 403–411.

Sumer, B. M. and Fredsøe, J. (2001b). Wave scour around a large vertical circular cylinder, *Journal of waterway, port, coastal, and ocean engineering* **127**(3): 125–134.

Sumer, B. M. and Fredsøe, J. (2002). *The mechanics of scour in the marine environment*, World Scientific Publishing Co Pte Ltd.

Sumer, B. M., Petersen, T. U., Locatelli, L., Fredsøe, J., Musumeci, R. E. and Foti, E. (2012). Backfilling of a scour hole around a pile in waves and current, *Journal of Waterway, Port, Coastal, and Ocean Engineering* **139**(1): 9–23.

Wist, H. T. (2003). *Statistical properties of successive ocean wave parameters*, PhD thesis, Department of Marine Technology, Faculty of Engineering Science and Technology, NTNU.

Appendix A

A. 1 - CASE 1

Given parameters	
Water depth (h)	$10\,m$
Significant wave height (H_s)	$3\,m$
Diameter (D)	-
Shields parameter (θ_{rms})	Col. 1
Ratio quartz sand/fluid density (s)	2.65
Median grain diameter (d_{50})	$0.001\,m$
Constant from friction formula (c)	1.39
Constant from friction formula (d)	0.52
rms value of wave amplitude (a_{rms})	$1.06\,m$
Bed roughness (z_0)	$0.0000833\,m$

Table A.1: Given parameters CASE 1

θ_{rms} [−]	k_p $[\frac{rad}{m}]$	ω_p $[\frac{rad}{s}]$	U_{rms} $[\frac{m}{s}]$	A_{rms} $[m]$	h/L_p [-]	S_1 [-]	U_r [-]	A_{rms}/z_0 [-]
0.05	0.27	1.61	0.24	0.15	0.42	0.13	0.04	1783
0.06	0.25	1.55	0.27	0.18	0.40	0.12	0.05	2113
0.07	0.24	1.50	0.31	0.20	0.37	0.11	0.05	2449
0.08	0.22	1.46	0.34	0.23	0.35	0.10	0.06	2795
0.09	0.21	1.42	0.37	0.26	0.33	0.10	0.07	3153
0.10	0.12	1.37	0.40	0.29	0.32	0.09	0.08	3525
0.11	0.19	1.33	0.43	0.33	0.30	0.09	0.08	3915
0.12	0.18	1.29	0.47	0.36	0.29	0.08	0.09	4327
0.13	0.17	1.25	0.50	0.40	0.27	0.08	0.10	4765
0.14	0.16	1.21	0.53	0.44	0.26	0.07	0.11	5236
0.15	0.15	1.17	0.56	0.48	0.24	0.07	0.13	5746
0.16	0.15	1.13	0.59	0.53	0.23	0.06	0.14	6308
0.17	0.14	1.09	0.63	0.58	0.22	0.06	0.16	6938
0.18	0.13	1.04	0.66	0.64	0.20	0.05	0.18	7660
0.19	0.12	0.99	0.70	0.71	0.19	0.05	0.21	8517

Table A.2: Resulting values CASE 1

A. 2 - CASE 2

Given parameters	
Water depth (h)	$10\,m$
Significant wave height (H_s)	$3\,m$
Diameter (D)	Col. 1
Shields parameter (θ_{rms})	Tab. A.5, Row 1
Keulegan-Carpenter number (KC_{rms})	Col. 2
Ratio quartz sand/fluid density (s)	2.65
Median grain diameter (d_{50})	-
Constant from friction formula (c)	1.39
Constant from friction formula (d)	0.52
rms value of wave amplitude (a_{rms})	$1.06\,m$
Bed roughness (z_0)	Tab. A.5, Col. 3,5,7

Table A.3: Given parameters CASE 2

D $[m]$	KC_{rms} [-]	k_p $[\frac{rad}{m}]$	ω_p $[\frac{rad}{s}]$	U_{rms} $[\frac{m}{s}]$	A_{rms} $[m]$	h/L_p [-]	D/L_p [-]	f_v $[\frac{1}{s}]$	S_1 [-]	U_r [-]
0.50	7	0.14	1.10	0.61	0.56	0.22	0.011	0.25	0.06	0.15
	8	0.13	1.04	0.66	0.64	0.20	0.010	0.27	0.05	0.18
	9	0.12	0.98	0.70	0.72	0.19	0.009	0.28	0.05	0.21
	10	0.11	0.93	0.74	0.80	0.17	0.009	0.30	0.04	0.25
	11	0.10	0.88	0.77	0.88	0.16	0.008	0.31	0.04	0.29
	12	0.10	0.84	0.80	0.96	0.15	0.008	0.32	0.03	0.33
0.75	7	0.11	0.90	0.76	0.84	0.17	0.013	0.20	0.04	0.27
	8	0.10	0.84	0.80	0.96	0.15	0.011	0.21	0.03	0.33
	9	0.09	0.78	0.83	1.07	0.14	0.010	0.22	0.03	0.39
	10	0.08	0.72	0.86	1.19	0.13	0.010	0.23	0.03	0.47
	11	0.07	0.68	0.89	1.31	0.12	0.009	0.24	0.02	0.55
	12	0.07	0.63	0.91	1.43	0.11	0.008	0.24	0.02	0.64
1.00	7	0.09	0.76	0.84	1.11	0.13	0.010	0.17	0.03	0.42
	8	0.08	0.69	0.88	1.27	0.12	0.009	0.18	0.02	0.52
	9	0.07	0.63	0.91	1.43	0.11	0.008	0.18	0.02	0.64
	10	0.06	0.58	0.93	1.59	0.10	0.007	0.19	0.02	0.77
	11	0.06	0.54	0.95	1.75	0.09	0.007	0.19	0.01	0.91
	12	0.05	0.50	0.96	1.91	0.08	0.006	0.19	0.01	1.07

Table A.4: Resulting values CASE 2

D	KC_{rms}	$\theta_{rms} = 0.07$		$\theta_{rms} = 0.13$		$\theta_{rms} = 0.18$	
		z_0	A_{rms}/z_o	z_0	A_{rms}/z_0	z_0	A_{rms}/z_0
$[m]$	[-]	$[m]$	[-]	$[m]$	[-]	$[m]$	[-]
0.50	7	0.00050	1104	0.00014	4010	0.00007	7900
	8	0.00059	1071	0.00016	3890	0.00008	7662
	9	0.00067	1064	0.00019	3864	0.00009	7611
	10	0.00074	1076	0.00020	3907	0.00010	7696
	11	0.00079	1102	0.00022	4004	0.00011	7887
	12	0.00084	1141	0.00023	4145	0.00012	8165
0.75	7	0.00077	1087	0.00021	3949	0.00012	7779
	8	0.00084	1141	0.00023	4145	0.00012	8165
	9	0.00088	1219	0.00024	4426	0.00012	8719
	10	0.00091	1316	0.00025	4780	0.00013	9417
	11	0.00092	1432	0.00025	5199	0.00013	10241
	12	0.00092	1563	0.00025	5677	0.00013	11182
1.00	7	0.00089	1249	0.00025	4537	0.00012	8937
	8	0.00092	1391	0.00025	5052	0.00013	9953
	9	0.00092	1563	0.00025	5677	0.00013	11182
	10	0.00090	1763	0.00025	6401	0.00013	12609
	11	0.00090	1989	0.00024	7222	0.00012	14226
	12	0.00085	2240	0.00023	8136	0.00012	16027

Table A.5: Resulting values CASE 2

A. 3 - CASE 3

Given parameters	
Water depth (h)	$10\,m$
Significant wave height (H_s)	$3\,m$
Diameter (D)	Col. 1
Shields parameter (θ_{rms})	Tab. A.8, Row 1
Keulegan-Carpenter number (KC_{rms})	Col. 2
Ratio quartz sand/fluid density (s)	2.65
Median grain diameter (d_{50})	-
Constant from friction formula (c)	1.39
Constant from friction formula (d)	0.52
rms value of wave amplitude (a_{rms})	$1.06\,m$
Bed roughness (z_0)	Tab. A.8, Col. 3,5,7

Table A.6: Given parameters CASE 3

D $[m]$	KC_{rms} [-]	k_p $[\frac{rad}{m}]$	ω_p $[\frac{rad}{s}]$	U_{rms} $[\frac{m}{s}]$	A_{rms} $[m]$	h/L_p [-]	D/L_p [-]	f_v $[\frac{1}{s}]$	S_1 [-]	U_r [-]
0.50	5	0.17	1.25	0.50	0.40	0.27	0.014	0.20	0.08	0.10
	6	0.15	1.17	0.56	0.48	0.24	0.012	0.22	0.07	0.13
	7	0.14	1.10	0.61	0.56	0.22	0.011	0.25	0.06	0.15
	8	0.13	1.04	0.66	0.64	0.20	0.010	0.26	0.05	0.18
	9	0.12	0.98	0.70	0.72	0.19	0.009	0.28	0.05	0.21
	10	0.11	0.93	0.74	0.8	0.17	0.009	0.3	0.04	0.25
	11	0.10	0.88	0.77	0.88	0.16	0.008	0.31	0.04	0.29
	12	0.10	0.84	0.80	0.95	0.15	0.008	0.32	0.03	0.33
0.75	5	0.13	1.07	0.64	0.60	0.21	0.016	0.17	0.06	0.17
	6	0.12	0.98	0.70	0.72	0.19	0.014	0.19	0.05	0.21
	7	0.11	0.90	0.76	0.84	0.17	0.013	0.20	0.04	0.27
	8	0.10	0.84	0.80	0.95	0.15	0.011	0.21	0.03	0.33
	9	0.09	0.78	0.83	1.07	0.14	0.010	0.22	0.03	0.39
	10	0.08	0.72	0.86	1.19	0.13	0.010	0.23	0.03	0.47
	11	0.07	0.67	0.89	1.31	0.12	0.009	0.24	0.02	0.55
	12	0.07	0.63	0.91	1.43	0.11	0.008	0.24	0.02	0.64
1.00	5	0.11	0.93	0.74	0.80	0.17	0.017	0.15	0.04	0.25
	6	0.10	0.84	0.80	0.95	0.15	0.015	0.16	0.03	0.33
	7	0.08	0.76	0.84	1.11	0.13	0.013	0.17	0.03	0.42
	8	0.08	0.69	0.88	1.27	0.12	0.012	0.18	0.02	0.52
	9	0.07	0.63	0.91	1.43	0.11	0.011	0.18	0.02	0.64
	10	0.06	0.58	0.93	1.59	0.10	0.010	0.19	0.02	0.77
	11	0.06	0.54	0.95	1.75	0.09	0.009	0.19	0.01	0.91
	12	0.05	0.50	0.96	1.91	0.08	0.008	0.19	0.01	1.07

Table A.7: Resulting values CASE 3

D	KC_{rms}	$\theta_{rms} = 0.07$		$\theta_{rms} = 0.10$		$\theta_{rms} = 0.15$	
		z_0	A_{rms}/z_o	z_0	A_{rms}/z_0	z_0	A_{rms}/z_0
$[m]$	[-]	$[m]$	[-]	$[m]$	[-]	$[m]$	[-]
0.50	5	0.00030	1310	0.00014	2755	0.00006	6412
	6	0.00041	1176	0.00019	2473	0.00008	5754
	7	0.00050	1104	0.00024	2322	0.00010	5403
	8	0.00059	1071	0.00028	2252	0.00012	5241
	9	0.00067	1063	0.00032	2237	0.00014	5206
	10	0.00074	1076	0.00035	2262	0.00015	5264
	11	0.00079	1102	0.00038	2318	0.00016	5394
	12	0.00084	1141	0.00040	2400	0.00017	5584
0.75	5	0.00055	1084	0.0026	2279	0.00011	5303
	6	0.00067	1064	0.00032	2237	0.00014	5205
	7	0.00077	1087	0.00037	2286	0.00016	5321
	8	0.00084	1141	0.00040	2400	0.00017	5584
	9	0.00088	1219	0.00042	2563	0.00018	5964
	10	0.00091	1316	0.00043	2767	0.00019	6441
	11	0.00092	1432	0.00044	3010	0.00019	7004
	12	0.00092	1563	0.00044	3286	0.00019	7648
1.00	5	0.00074	1076	0.00035	2262	0.00015	5264
	6	0.00084	1141	0.00040	2400	0.00017	5584
	7	0.00089	1249	0.00042	2626	0.00018	6113
	8	0.00092	1391	0.00044	2925	0.00019	6807
	9	0.00092	1563	0.00044	3286	0.00019	7648
	10	0.00090	1763	0.00043	3706	0.00018	8625
	11	0.00088	1989	0.00042	4181	0.00018	9730
	12	0.00085	2240	0.00041	4710	0.00017	10962

Table A.8: Resulting values CASE 3

A. 4 - CASE 4

Given parameters	
Water depth (h)	$10\,m$
Significant wave height (H_s)	$3\,m$
Diameter (D)	Col. 1
Shields parameter (θ_{rms})	Col. 6
Keulegan-Carpenter number (KC_{rms})	Col. 2
Ratio quartz sand/fluid density (s)	2.65
Median grain diameter (d_{50})	0.001
Constant from friction formula (c)	1.39
Constant from friction formula (d)	0.52
rms value of wave amplitude (a_{rms})	$1.06\,m$
Bed roughness (z_0)	0.0000833

Table A.9: Given parameters CASE 4

D [m]	KC_{rms} [-]	k_p [$\frac{rad}{m}$]	ω_p [$\frac{rad}{s}$]	U_{rms} [$\frac{m}{s}$]	θ_{rms} [-]	$\theta^2_{rms}*$ KC_{rms}	h/L_p [-]	D/L_p [-]	f_v [$\frac{1}{s}$]	S_1 [-]	U_r [-]	A_{rms}/z_0 [-]
	4	0.19	1.43	0.43	0.108	0.046	0.31	0.015	0.17	0.09	0.08	3820
	5	0.17	1.25	0.50	0.130	0.09	0.27	0.014	0.20	0.08	0.10	4775
	6	0.15	1.17	0.56	0.150	0.13	0.24	0.012	0.22	0.07	0.13	5730
	7	0.14	1.10	0.61	0.166	0.19	0.22	0.011	0.25	0.06	0.15	6685
0.5	8	0.13	1.04	0.66	0.180	0.26	0.20	0.010	0.27	0.05	0.18	7639
	9	0.12	0.98	0.70	0.191	0.33	0.19	0.009	0.28	0.05	0.21	85944
	10	0.11	0.93	0.74	0.200	0.40	0.17	0.009	0.30	0.04	0.25	9549
	11	0.10	0.88	0.77	0.207	0.47	0.16	0.008	0.31	0.04	0.29	10504
	12	0.10	0.84	0.80	0.212	0.54	0.15	0.008	0.32	0.03	0.33	11459
	13	0.09	0.80	0.82	0.216	0.61	0.14	0.007	0.33	0.03	0.37	12414
	3	0.18	1.29	0.46	0.119	0.043	0.29	0.022	0.12	0.08	0.09	4297
	4	0.15	1.17	0.56	0.150	0.09	0.24	0.018	0.15	0.07	0.13	5730
	5	0.13	1.07	0.64	0.173	0.15	0.21	0.016	0.17	0.06	0.17	7162
	6	0.12	0.98	0.70	0.191	0.22	0.19	0.014	0.19	0.05	0.21	8594
0.75	7	0.11	0.90	0.76	0.203	0.29	0.17	0.013	0.20	0.04	0.27	10027
	8	0.10	0.84	0.80	0.212	0.36	0.15	0.011	0.21	0.03	0.33	11459
	9	0.09	0.76	0.83	0.217	0.42	0.14	0.010	0.22	0.03	0.39	12892
	10	0.08	0.72	0.86	0.220	0.49	0.13	0.010	0.23	0.03	0.47	14324
	11	0.07	0.68	0.89	0.221	0.54	0.12	0.009	0.24	0.02	0.55	15756
	12	0.07	0.63	0.91	0.221	0.59	0.11	0.008	0.24	0.02	0.64	17189
	3	0.15	1.17	0.56	0.150	0.07	0.24	0.024	0.11	0.07	0.13	5730
	4	0.13	1.04	0.66	0.180	0.13	0.20	0.020	0.13	0.05	0.18	7639
	5	0.11	0.93	0.74	0.200	0.20	0.17	0.017	0.15	0.04	0.25	9549
	6	0.10	0.84	0.80	0.212	0.27	0.15	0.015	0.16	0.03	0.33	11459
1	7	0.09	0.76	0.84	0.218	0.33	0.13	0.013	0.17	0.03	0.42	13369
	8	0.08	0.69	0.88	0.221	0.39	0.12	0.012	0.18	0.02	0.52	15279
	9	0.07	0.63	0.91	0.221	0.44	0.11	0.011	0.18	0.02	0.64	17189
	10	0.06	0.58	0.93	0.220	0.48	0.10	0.010	0.19	0.02	0.77	19099
	11	0.06	0.54	0.95	0.217	0.52	0.09	0.009	0.19	0.01	0.91	21008
	12	0.05	0.50	0.96	0.214	0.55	0.08	0.008	0.19	0.01	1.07	22918

Table A.10: Resulting values CASE 4

A. 5 - CASE 5

Given parameters	
Water depth (h)	$10\,m$
Significant wave height (H_s)	$3\,m$
Diameter (D)	Row 1
Keulegan-Carpenter number (KC_{rms})	Row. 2
Ratio quartz sand/fluid density (s)	2.65
Median grain diameter (d_{50})	-
Constant from friction formula (c)	1.39
Constant from friction formula (d)	0.52
r.m.s. value of wave amplitude (a_{rms})	$1.06\,m$
Bed roughness (z_0)	Row 19

Table A.11: Given parameters CASE 5

$D = 0.5\,m$													
	Example 1 $KC_{rms} = 4$, $\theta_{rms} = 0.07$				Example 2 $KC_{rms} = 7$, $\theta_{rms} = 0.07$				Example 3 $KC_{rms} = 4$, $\theta_{rms} = 0.09$			
	k_p $[rad/m]$		0.1919		k_p $[rad/m]$		0.1400		k_p $[rad/m]$		0.1919	
	ω_r $[rad/s]$		1.3426		ω_r $[rad/s]$		1.1026		ω_r $[rad/s]$		1.3426	
	U_{rms} $[m/s]$		0.4274		U_{rms} $[m/s]$		0.6142		U_{rms} $[m/s]$		0.4274	
U_{cwrms} $[\frac{m}{s}]$	U_c $[\frac{m}{s}]$	ω_p $[\frac{rad}{s}]$	f_v $[\frac{1}{s}]$	S_1 [-]	U_c $[\frac{m}{s}]$	ω_p $[\frac{rad}{s}]$	f_v $[\frac{1}{s}]$	S_1 [-]	U_c $[\frac{m}{s}]$	ω_p $[\frac{rad}{s}]$	f_v $[\frac{1}{s}]$	S_1 [-]
0.0	0.00	1.34	0.17	0.09	0.00	1.10	0.25	0.06	0.00	1.34	0.17	0.09
0.1	0.05	1.35	0.17	0.09	0.07	1.11	0.25	0.06	0.05	1.35	0.17	0.09
0.2	0.11	1.36	0.17	0.09	0.15	1.12	0.25	0.06	0.11	1.36	0.17	0.09
0.3	0.18	1.38	0.18	0.09	0.26	1.14	0.25	0.06	0.18	1.38	0.18	0.09
0.4	0.29	1.40	0.18	0.10	0.41	1.16	0.26	0.07	0.29	1.40	0.18	0.10
0.5	0.43	1.42	0.18	0.10	0.61	1.19	0.26	0.07	0.43	1.42	0.18	0.10
0.6	0.64	1.47	0.19	0.10	0.92	1.23	0.27	0.07	0.64	1.47	0.19	0.10
0.7	1.00	1.53	0.20	0.11	1.43	1.30	0.29	0.08	1.00	1.53	0.20	0.11
	h/L_p [-]		0.3053		h/L_p [-]		0.2228		h/L_p [-]		0.3053	
	D/L_p [-]		0.0153		D/L_p [-]		0.0111		D/L_p [-]		0.0153	
	U_r [-]		0.0815		U_r [-]		0.1531		U_r [-]		0.0815	
	A_{rms} $[m]$		0.3183		A_{rms} $[m]$		0.5570		A_{rms} $[m]$		0.3183	
	z_0 $[m]$		0.0002		z_0 $[m]$		0.0004		z_0 $[m]$		0.00012	
	A_{rms}/z_0 [-]		1560		A_{rms}/z_0 [-]		1459		A_{rms}/z_0 [-]		2633	

Table A.12: Resulting values CASE 5, $D = 0.5\,m$

$D = 0.75\,m$												
	Example 1 $KC_{rms} = 4$, $\theta_{rms} = 0.07$				Example 2 $KC_{rms} = 7$, $\theta_{rms} = 0.07$				Example 3 $KC_{rms} = 4$, $\theta_{rms} = 0.09$			
	k_p $[rad/m]$		0.1538		k_p $[rad/m]$		0.1060		k_p $[rad/m]$		0.1538	
	ω_r $[rad/s]$		1.1731		ω_r $[rad/s]$		0.9036		ω_r $[rad/s]$		1.1731	
	U_{rms} $[m/s]$		0.5601		U_{rms} $[m/s]$		0.7551		U_{rms} $[m/s]$		0.5601	
U_{cwrms} $[\frac{m}{s}]$	U_c $[\frac{m}{s}]$	ω_p $[\frac{rad}{s}]$	f_v $[\frac{1}{s}]$	S_1 [-]	U_c $[\frac{m}{s}]$	ω_p $[\frac{rad}{s}]$	f_v $[\frac{1}{s}]$	S_1 [-]	U_c $[\frac{m}{s}]$	ω_p $[\frac{rad}{s}]$	f_v $[\frac{1}{s}]$	S_1 [-]
0.0	0.00	1.17	0.15	0.07	0.00	0.90	0.20	0.04	0.00	1.17	0.15	0.07
0.1	0.06	1.18	0.15	0.07	0.09	0.91	0.20	0.04	0.06	1.18	0.15	0.07
0.2	0.14	1.19	0.15	0.07	0.19	0.92	0.21	0.04	0.14	1.19	0.15	0.07
0.3	0.24	1.21	0.15	0.07	0.32	0.93	0.21	0.04	0.24	1.21	0.15	0.07
0.4	0.37	1.23	0.16	0.07	0.50	0.96	0.21	0.04	0.37	1.23	0.16	0.07
0.5	0.56	1.26	0.16	0.08	0.76	0.98	0.22	0.05	0.56	1.26	0.16	0.08
0.6	0.84	1.30	0.17	0.08	1.13	1.02	0.23	0.05	0.84	1.30	0.17	0.08
0.7	1.31	1.37	0.18	0.09	1.76	1.09	0.24	0.06	1.31	1.37	0.18	0.09
	h/L_p [-]		0.2449		h/L_p [-]		0.1686		h/L_p [-]		0.2449	
	D/L_p [-]		0.0184		D/L_p [-]		0.0126		D/L_p [-]		0.0184	
	U_r [-]		0.1267		U_r [-]		0.2672		U_r [-]		0.1267	
	A_{rms} $[m]$		0.4775		A_{rms} $[m]$		0.8356		A_{rms} $[m]$		0.4775	
	z_0 $[m]$		0.0004		z_0 $[m]$		0.0008		z_0 $[m]$		0.0002	
	A_{rms}/z_0 [-]		1176		A_{rms}/z_0 [-]		1087		A_{rms}/z_0 [-]		1985	

Table A.13: Resulting values CASE 5, $D = 0.75\,m$

$D = 1\,m$												
	Example 1 $KC_{rms} = 4$, $\theta_{rms} = 0.07$				Example 2 $KC_{rms} = 7$, $\theta_{rms} = 0.07$				Example 3 $KC_{rms} = 4$, $\theta_{rms} = 0.09$			
	k_p $[rad/m]$		0.1283		k_p $[rad/m]$		0.0847		k_p $[rad/m]$		0.1283	
	ω_r $[rad/s]$		1.0390		ω_r $[rad/s]$		0.7569		ω_r $[rad/s]$		1.0390	
	U_{rms} $[m/s]$		0.6615		U_{rms} $[m/s]$		0.8433		U_{rms} $[m/s]$		0.6615	
U_{cwrms} $[\frac{m}{s}]$	U_c $[\frac{m}{s}]$	ω_p $[\frac{rad}{s}]$	f_v $[\frac{1}{s}]$	S_1 [-]	U_c $[\frac{m}{s}]$	ω_p $[\frac{rad}{s}]$	f_v $[\frac{1}{s}]$	S_1 [-]	U_c $[\frac{m}{s}]$	ω_p $[\frac{rad}{s}]$	f_v $[\frac{1}{s}]$	S_1 [-]
0.0	0.00	1.04	0.13	0.05	0.00	0.76	0.17	0.03	0.00	1.04	0.13	0.05
0.1	0.07	1.05	0.13	0.05	0.09	0.76	0.17	0.03	0.07	1.05	0.13	0.05
0.2	0.17	1.06	0.13	0.05	0.21	0.77	0.17	0.03	0.17	1.06	0.13	0.05
0.3	0.28	1.08	0.14	0.06	0.36	0.79	0.18	0.03	0.28	1.08	0.14	0.06
0.4	0.44	1.10	0.14	0.06	0.56	0.80	0.18	0.03	0.44	1.10	0.14	0.06
0.5	0.66	1.12	0.14	0.06	0.84	0.83	0.18	0.03	0.66	1.12	0.14	0.06
0.6	0.99	1.17	0.15	0.07	1.27	0.86	0.29	0.04	0.99	1.17	0.15	0.07
0.7	1.54	1.24	0.16	0.07	1.97	0.92	0.21	0.04	1.54	1.24	0.16	0.07
	h/L_p [-]		0.2043		h/L_p [-]		0.1348		h/L_p [-]		0.2043	
	D/L_p [-]		0.0204		D/L_p [-]		0.0135		D/L_p [-]		0.0204	
	U_r [-]		0.1821		U_r [-]		0.4181		U_r [-]		0.1821	
	A_{rms} $[m]$		0.6366		A_{rms} $[m]$		1.1141		A_{rms} $[m]$		0.6366	
	z_0 $[m]$		0.0006		z_0 $[m]$		0.0009		z_0 $[m]$		0.0004	
	A_{rms}/z_0 [-]		1071		A_{rms}/z_0 [-]		1249		A_{rms}/z_0 [-]		1808	

Table A.14: Resulting values CASE 5, $D = 1\,m$

A. 6 - CASE 6

Given parameters	
Water depth (h)	$10\,m$
Significant wave height (H_s)	$3\,m$
Diameter (D)	Row 1
Keulegan-Carpenter number (KC_{rms})	Row. 2
Ratio quartz sand/fluid density (s)	2.65
Median grain diameter (d_{50})	-
Constant from friction formula (c)	1.39
Constant from friction formula (d)	0.52
r.m.s. value of wave amplitude (a_{rms})	$1.06\,m$
Bed roughness (z_0)	Row 19

Table A.15: Given parameters CASE 6

$D = 3\,m$								
	Example 1 $KC_{rms} = 0.7$, $\theta_{rms} = 0.101$				Example 2 $KC_{rms} = 1.5$, $\theta_{rms} = 0.105$			
	k_p $[rad/m]$		0.1872		k_p $[rad/m]$		0.1184	
	ω_r $[rad/s]$		1.3234		ω_r $[rad/s]$		0.9812	
	U_{rms} $[m/s]$		0.4423		U_{rms} $[m/s]$		0.7027	
U_{cwrms} $[\frac{m}{s}]$	U_c $[\frac{m}{s}]$	ω_p $[\frac{rad}{s}]$	f_v $[\frac{1}{s}]$	S_1 [-]	U_c $[\frac{m}{s}]$	ω_p $[\frac{rad}{s}]$	f_v $[\frac{1}{s}]$	S_1 [-]
0.0	0.00	1.32	0.030	0.09	0.00	0.98	0.047	0.05
0.1	0.05	1.33	0.030	0.09	0.08	0.99	0.047	0.05
0.2	0.11	1.34	0.030	0.09	0.18	1.00	0.048	0.05
0.3	0.18	1.36	0.030	0.09	0.30	1.02	0.049	0.05
0.4	0.29	1.38	0.031	0.09	0.47	1.04	0.049	0.05
0.5	0.44	1.41	0.031	0.10	0.70	1.06	0.051	0.06
0.6	0.66	1.45	0.032	0.10	1.05	1.11	0.053	0.06
0.7	1.03	1.52	0.034	0.11	1.64	1.18	0.056	0.07
	h/L_p [-]		0.2980		h/L_p [-]		0.1885	
	D/L_p [-]		0.0894		D/L_p [-]		0.0565	
	U_r [-]		0.0856		U_r [-]		0.2139	
	A_{rms} $[m]$		0.3342		A_{rms} $[m]$		0.7162	
	z_0 $[m]$		0.0001		z_0 $[m]$		0.0003	
	A_{rms}/z_0 [-]		3212		A_{rms}/z_0 [-]		2476	

Table A.16: Resulting values CASE 6, $D = 3\,m$

$D = 4\,m$								
	Example 1 $KC_{rms} = 0.7$, $\theta_{rms} = 0.101$				Example 2 $KC_{rms} = 1.5$, $\theta_{rms} = 0.105$			
	k_p $[rad/m]$		0.1602		k_p $[rad/m]$		0.0958	
	ω_r $[rad/s]$		1.2036		ω_r $[rad/s]$		0.8355	
	U_{rms} $[m/s]$		0.5364		U_{rms} $[m/s]$		0.7979	
U_{cwrms} $[\frac{m}{s}]$	U_c $[\frac{m}{s}]$	ω_p $[\frac{rad}{s}]$	f_v $[\frac{1}{s}]$	S_1 [-]	U_c $[\frac{m}{s}]$	ω_p $[\frac{rad}{s}]$	f_v $[\frac{1}{s}]$	S_1 [-]
0.0	0.00	1.20	0.027	0.07	0.00	0.84	0.040	0.03
0.1	0.06	1.21	0.027	0.07	0.09	0.84	0.040	0.03
0.2	0.13	1.23	0.027	0.07	0.20	0.85	0.041	0.04
0.3	0.23	1.24	0.028	0.07	0.34	0.87	0.041	0.04
0.4	0.36	1.26	0.028	0.08	0.53	0.89	0.042	0.04
0.5	0.54	1.29	0.029	0.08	0.80	0.91	0.044	0.04
0.6	0.80	1.33	0.030	0.09	1.20	0.95	0.045	0.04
0.7	1.25	1.40	0.031	0.10	1.86	1.01	0.048	0.05
	h/L_p [-]		0.2549		h/L_p [-]		0.1524	
	D/L_p [-]		0.1020		D/L_p [-]		0.0610	
	U_r [-]		0.1169		U_r [-]		0.3272	
	A_{rms} $[m]$		0.4456		A_{rms} $[m]$		0.9549	
	z_0 $[m]$		0.0002		z_0 $[m]$		0.0004	
	A_{rms}/z_0 [-]		2619		A_{rms}/z_0 [-]		2656	

Table A.17: Resulting values CASE 6, $D = 4\,m$

$D = 5\,m$								
	Example 1 $KC_{rms} = 0.7$, $\theta_{rms} = 0.101$				Example 2 $KC_{rms} = 1.5$, $\theta_{rms} = 0.105$			
	k_p $[rad/m]$		0.1400		k_p $[rad/m]$		0.0800	
	ω_r $[rad/s]$		1.1026		ω_r $[rad/s]$		0.7222	
	U_{rms} $[m/s]$		0.6142		U_{rms} $[m/s]$		0.8620	
U_{cwrms} $[\frac{m}{s}]$	U_c $[\frac{m}{s}]$	ω_p $[\frac{rad}{s}]$	f_v $[\frac{1}{s}]$	S_1 [-]	U_c $[\frac{m}{s}]$	ω_p $[\frac{rad}{s}]$	f_v $[\frac{1}{s}]$	S_1 [-]
0.0	0.00	1.10	0.025	0.06	0.00	0.72	0.034	0.03
0.1	0.07	1.11	0.025	0.06	0.10	0.73	0.034	0.03
0.2	0.15	1.12	0.025	0.06	0.22	0.74	0.035	0.03
0.3	0.26	1.14	0.025	0.06	0.37	0.75	0.036	0.03
0.4	0.41	1.16	0.026	0.07	0.57	0.77	0.037	0.03
0.5	0.61	1.19	0.027	0.07	0.86	0.79	0.038	0.03
0.6	0.92	1.23	0.027	0.07	1.29	0.83	0.039	0.03
0.7	1.43	1.30	0.029	0.08	2.01	0.88	0.042	0.04
	h/L_p [-]		0.2228		h/L_p [-]		0.1274	
	D/L_p [-]		0.0111		D/L_p [-]		0.0637	
	U_r [-]		0.1531		U_r [-]		0.4683	
	A_{rms} $[m]$		0.5570		A_{rms} $[m]$		1.1937	
	z_0 $[m]$		0.0002		z_0 $[m]$		0.0004	
	A_{rms}/z_0 [-]		2370		A_{rms}/z_0 [-]		3064	

Table A.18: Resulting values CASE 6, $D = 5\,m$

Appendix B

Parameters

```
function [n Hs h g s d50 arms c d]=Parameters()
%THIS FUNCTION GIVES THE GLOBAL PARAMETERS TO ALL THE FUNCTIONS
%USED IN THIS PROJECT. THESE VALUES ARE THE SAME IN ALL THE CASES
%EXCEPT d50, WHICH IS CONSTANT IN CASE 1 AND 4. THE GLOBAL
%PARAMETERS WILL NOT BE REPEATED IN THE OTHER FUNCTIONS.

n=10; %wave fraction [m]
Hs=3; %significant wave heigh [m]
h=10; %water depth [m]
g=9.806; %aceleration of gravity [m/s^2]
s=2.65; %specific gravity [-]
d50=0.001; %diameter sand grains [m]
arms=Hs/(2*sqrt(2)); %the rms value of the wave amplitude [m]
c=1.39; %constant from the friction formula [-]
d=0.52; %constant from the friction formula [-]

end
```

B. 1 - CASE 1

Rayleigh

```
function [R R1 R2 R3]=Rayleigh(x)
%CASE 1: THIS FUNCTION USES THE RAYLEIGH DISTRIBUTION TO CALCULATE
%THE EXPECTED VALUE OF THE TIME SCALE FOR SCOUR BELOW A PIPELINE,
%FOR DIFFERENT VALUES OF THE SHIELDS PARAMETER (trms).

%DESCRIPTION OF SYMBOLS
%x: the normalized linear wave amplitude
%R:  The expeced value of the time scale T* for all D.
%R1: D=0.50 m - The expeced value of the time scale T (min).
%R2: D=0.75 m - The expeced value of the time scale T (min).
%R3: D=1.00 m - The expeced value of the time scale T (min).

%Et: The expected value of t  [-].
%ET: The expected value of T* [-].

syms x;
```

```
[n Hs h g s d50 arms c d]=Parameters();

s1=5/3;
r1=1/50;
v=s1*(2-d);

i=0;
for trms=0.05:0.001:0.19
    i=i+1;

    xmin=sqrt(log(n));
    x=(xmin:0.01:5);

    Et=trapz(x,2*n*(x).^(1-v).*exp(-(x).^2));
    ET=Et*r1*trms^(-s1);

    %RESULTING DATA OF T*
    R(i,1)=trms;
    R(i,2)=ET;
end

%RESULTING DATA OF T FOR D=0.50 m, D=0.75 m and D=1.00 m.
R1(:,1)=R(:,1);
R1(:,2)=R(:,2)*0.5^2/(sqrt(g*(s-1)*(d50)^3))/60;
R2(:,1)=R(:,1);
R2(:,2)=R(:,2)*0.75^2/(sqrt(g*(s-1)*(d50)^3))/60;
R3(:,1)=R(:,1);
R3(:,2)=R(:,2)*1^2/(sqrt(g*(s-1)*(d50)^3))/60;

end
```

Forristall

```
function [F F1 F2 F3]=Forristall(x)
%CASE 1: THIS FUNCTION USES THE FORRISTALL DISTRIBUTION TO
%CALCULATE THE EXPECTED VALUE OF THE TIME SCALE FOR SCOUR BELOW
%A PIPELINE, FOR DIFFERENT VALUES OF THE SHIELDS PARAMETER (trms).

%kp is solved by iteration such that wp also can be found (to find
%Ur and S1). The requirement is that Urms from Eq. (103) equals
%Urms=wp*arms/sin(kp*h). In the equation Urms=Urms, wp are replaced
%by wp=sqrt(g*kp*tanh(kp*h) and the equation are reorganized such
%that all the kps appears inn ledd 2. The only unknown value for
%a given trms is then kp, which is solved in the "while" loop by
%iteration: kp changes until the criterion ledd1=ledd2 is fulfilled.
```

```
%DESCRIPTION OF SYMBOLS
%x:  The normalized second order wave crest.
%F:  The expeced value of the time scale T* for all D.
%F1: D=0.50 m - The expeced value of the time scale T (min).
%F2: D=0.75 m - The expeced value of the time scale T (min).
%F3: D=1.00 m - The expeced value of the time scale T (min).

%Et_2D: The expected value of t  [-] for 2D waves.
%Et_3D: The expected value of t  [-] for 3D waves.
%ET_2D: The expected value of T* [-] for 2D waves.
%ET_3D: The expected value of T* [-] for 3D waves.

%nu: desired numbers behind comma. The computation time will be
%very long if not shortening the numbers, due to the requirement
%ledd1=ledd2.

syms x;

[n Hs h g s d50 arms c d]=Parameters();

s1=5/3;
r1=1/50;
v=s1*(2-d);
nu=4;

i=0;
for trms=0.05:0.001:0.19
    i=i+1;

    kp=0.05; %start value
    ledd1=0;
    ledd2=1/arms*((2*12^(d)*trms*g*(s-1)*d50^(1-d))/c)^(1/(2-d));
    ledd2= round(ledd2*(10^nu))/(10^nu);

    while ledd1~=ledd2
          ledd1=(sqrt(g*kp*tanh(kp*h)))^(1+d/(2-d))/(sinh(kp*h));
          ledd1= round(ledd1*(10^nu))/(10^nu);
          kp=kp+10^(-(nu+2));
    end

    kp=kp-10^(-(nu+2));
    wp=sqrt(g*kp*tanh(kp*h));
    Tp=2*pi/wp;

    S1=2*pi*Hs/(g*Tp^2);
    Ur=Hs/(kp^2*h^3);

    %parameters 2D model
    alpha2=0.3536+0.2892*S1+0.1060*Ur;
```

```
    beta2=2-2.1597*S1+0.0968*Ur^2;
    xmin_2D=sqrt(8)*alpha2*(log(n))^(1/(beta2));
    x2D=(xmin_2D:0.01:5);

    %parameters 3D model
    alpha3=0.3536+0.2568*S1+0.0800*Ur;
    beta3=2-1.7912*S1-0.5302*Ur+0.284*Ur^2;
    xmin_3D=sqrt(8)*alpha3*(log(n))^(1/(beta3));
    x3D=(xmin_3D:0.01:5);

    Et_2D=trapz(x2D,n*beta2*(x2D).^(beta2-1-v)/((sqrt(8)*alpha2)^...
        (beta2)).*exp(-((x2D)./(sqrt(8)*alpha2)).^(beta2)));
    Et_3D=trapz(x3D,n*beta3*(x3D).^(beta3-1-v)/((sqrt(8)*alpha3)^...
        (beta3)).*exp(-((x3D)./(sqrt(8)*alpha3)).^(beta3)));

    ET_2D=Et_2D*r1*trms^(-s1);
    ET_3D=Et_3D*r1*trms^(-s1);

    %RESULTING DATA OF T*
    F(i,1)=trms;
    F(i,2)=ET_2D;
    F(i,3)=ET_3D;
end

%RESULTING DATA OF T FOR D=0.5 m, D=0.75 m and D=1 m
F1(:,1)=F(:,1);
F1(:,2)=F(:,2)*0.5^2/(sqrt(g*(s-1)*(d50)^3))/60;
F1(:,3)=F(:,3)*0.5^2/(sqrt(g*(s-1)*(d50)^3))/60;
F2(:,1)=F(:,1);
F2(:,2)=F(:,2)*0.75^2/(sqrt(g*(s-1)*(d50)^3))/60;
F2(:,3)=F(:,3)*0.75^2/(sqrt(g*(s-1)*(d50)^3))/60;
F3(:,1)=F(:,1);
F3(:,2)=F(:,2)*1^2/(sqrt(g*(s-1)*(d50)^3))/60;
F3(:,3)=F(:,3)*1^2/(sqrt(g*(s-1)*(d50)^3))/60;

end
```

Plot

```
function P=Plot(x)
%CASE 1: THIS FUNCTION PLOTS THE TIME SCALE FOR SCOUR BELOW A
%PIPELINE, FOR DIFFERENT VALUES OF THE SHIELDS PARAMETER (trms).

%Retrieving data from the Rayleigh distibution
[R R1 R2 R3]=Rayleigh();
%R:  Data for E[T*].
%R1: D=0.50 m - Data for E[T] (min).
```

```
%R2: D=0.75 m - Data for E[T] (min).
%R3: D=1.00 m - Data for E[T] (min).

%Retrieving data from the Forristall distribution
[F F1 F2 F3]=Forristall();
%F:  Data for E[T*].
%F1: D=0.50 m - Data for E[T] (min).
%F2: D=0.75 m - Data for E[T] (min).
%F3: D=1.00 m - Data for E[T] (min).

%T*
h1=figure;
set(h1, 'Position', [5 5 700 500],'Visible','off')
h=semilogx(R(:,1),R(:,2),'b',F(:,1), F(:,2),'c--',...
                             F(:,1), F(:,3),'k:');
hleg=legend('Rayleigh','Forristall (2D)','Forristall (3D)',...
    'Location','northeast');
set(hleg,'Fontsize',13)
set (h, 'LineWidth', 2.5)
axis([0.05 0.19 0 0.8]);
u=[0.05 0.07 0.09 0.11 0.13 0.15 0.17 0.19];
set(gca,'XTick',u,'Fontsize',14);
xlabel('\theta_{r m s}','Fontsize',24);
ylabel('E[T*]','Fontsize',22);
hgexport(gcf, '../../Figures/CASE1/CASE1.png',...
    hgexport('factorystyle'), 'Format', 'png')


%T for D=0.5 m, D=0.75 m and D=1 m
h1=figure;
set(h1, 'Position', [5 5 700 500],'Visible','off')
h=semilogx(R1(:,1),R1(:,2),'c',F1(:,1),F1(:,2),'c--',...
                               F1(:,1),F1(:,3),'c:',...
           R2(:,1),R2(:,2),'k',F2(:,1),F2(:,2),'k--',...
                               F2(:,1),F2(:,3),'k:',...
           R3(:,1),R3(:,2),'m',F3(:,1),F3(:,2),'m--',...
                               F3(:,1),F3(:,3),'m:');
hleg=legend('Rayleigh          D=0.50 m','Forristall (2D) D=0.50 m',...
                                         'Forristall (3D) D=0.50 m',...
            'Rayleigh          D=0.75 m','Forristall (2D) D=0.75 m',...
                                         'Forristall (3D) D=0.75 m',...
            'Rayleigh          D=1.00 m','Forristall (2D) D=1.00 m',...
                                         'Forristall (3D) D=1.00 m',...
       'Location','northeast');
set(hleg,'Fontsize',13)
set (h, 'LineWidth', 2.5)
axis([0.05 0.19 0 100 ]);
u=[0.05 0.07 0.09 0.11 0.13 0.15 0.17 0.19];
set(gca,'XTick',u,'Fontsize',14);
```

```
xlabel('\theta_{r m s}','Fontsize',24);
ylabel('E[T]','Fontsize',22);
hgexport(gcf, '../../Figures/CASE1/CASE1_T.png',...
    hgexport('factorystyle'), 'Format', 'png')

end
```

Iso

```
function i=iso()
%CASE 1: THIS FUNCTION USES THE RAYLEIGH AND THE FORRISTALL
%DISTRIBUTION TO FIND THE RATIO BETWEEN THE NONLINEAR AND
%LINEAR SOLUTION (R1) AND THE RATIO BETWEEN THE 3D AND 2D
%SOLUTION (R2), FOR THE TIME SCALE OF SCOUR BELOW PIPELINES.
%R1 AND R2 ARE PLOTTED AS ISOCURVES VERSUS URSELLS NUMBER
%(Ur) AND THE STEEPNESS (S1).

%DESCRIPTION OF SYMBOLS
%x_R:  The normalized linar wave amplitude.
%x_2D: The normalized second-order wave crest for 2D waves.
%x_3D: The normalized second-order wave crest for 3D waves.

syms x_R x_2D x_3D;

[n Hs h g s d50 arms c d]=Parameters();

s1=5/3;
v=s1*(2-d);

o=zeros(101,101);
h=zeros(101,101);

    Ur=-0.01;
for i=1:101

    Ur=Ur+0.01;
    h(:,i)=Ur;

        S1=-0.0015;
    for j=1:101

        S1=S1+0.0015;
        o(j,:)=S1;

        alpha2=0.3536+0.2892*S1+0.1060*Ur;
        beta2=2-2.1597*S1+0.0968*Ur^2;
        alpha3=0.3536+0.2568*S1+0.0800*Ur;
```

```
        beta3=2-1.7912*S1-0.5302*Ur+0.284*Ur^2;

        xmin_R=sqrt(log(n));
        xmin_2D=sqrt(8)*alpha2*(log(n))^(1/(beta2));
        xmin_3D=sqrt(8)*alpha3*(log(n))^(1/(beta3));

        x_R=(xmin_R:0.01:5);
        x_2D=(xmin_2D:0.01:5);
        x_3D=(xmin_3D:0.01:5);

        %The expected value of t
        e_R=2*n*(x_R).^(1-v).*exp(-((x_R).^2));
        e_2D=n*beta2*(x_2D).^(beta2-1-v)/((sqrt(8)*alpha2).^beta2)...
            .*exp(-((x_2D)./(sqrt(8).*alpha2)).^beta2);
        e_3D=n*beta3*(x_3D).^(beta3-1-v)/((sqrt(8)*alpha3).^beta3)...
            .*exp(-((x_3D)./(sqrt(8).*alpha3)).^beta3);

        %The expected value of T*
        E_R=trapz(x_R,e_R);
        E_2D=trapz(x_2D,e_2D);
        E_3D=trapz(x_3D,e_3D);

        %R1
        R1_2D=(E_2D)/(E_R);
        R1_3D=(E_3D)/(E_R);

        %R2
        R2=E_3D/E_2D;

        %data for plot
        k1(j,i)=R1_2D;
        k2(j,i)=R1_3D;
        k3(j,i)=R2;
    end
end

%PLOT
%R1_2D
h1=figure;
set(h1, 'Position', [5 5 700 500],'Visible','off')
c1=contour(h,o,k1,'b','LineWidth',2.5);
clabel(c1,'Fontsize',18);
u=[0 0.1 0.2 0.3 0.4 0.5 0.6 0.7 0.8 0.9 1];
set(gca,'XTick',u,'Fontsize',18);
u=[0 0.02 0.04 0.06 0.08 0.10 0.12 0.14];
set(gca,'YTick',u,'Fontsize',18);
xlabel('U_{R}','Fontsize',22);
ylabel('S_{1}','Fontsize',22);
title('R_{1,2D}', 'Fontsize',22)
```

```
hgexport(gcf, '../../Figures/CASE1/CASE1_R1_2D.png',...
       hgexport('factorystyle'), 'Format', 'png');


%R1_3D
h1=figure;
set(h1, 'Position', [5 5 700 500],'Visible','off')
c1=contour(h,o,k2,'b','LineWidth',2.5);
clabel(c1,'Fontsize',18);
u=[0 0.1 0.2 0.3 0.4 0.5 0.6 0.7 0.8 0.9 1];
set(gca,'XTick',u,'Fontsize',18);
u=[0 0.02 0.04 0.06 0.08 0.10 0.12 0.14];
set(gca,'YTick',u,'Fontsize',18);
xlabel('U_{R}','Fontsize',22);
ylabel('S_{1}','Fontsize',22');
title('R_{1,3D}', 'Fontsize',22)
hgexport(gcf, '../../Figures/CASE1/CASE1_R1_3D.png',...
       hgexport('factorystyle'), 'Format', 'png');


%R2
h1=figure;
set(h1, 'Position', [5 5 700 500],'Visible','off')
c1=contour(h,o,k3,'b','LineWidth',2.5);
clabel(c1,'Fontsize',18);
u=[0 0.1 0.2 0.3 0.4 0.5 0.6 0.7 0.8 0.9 1];
set(gca,'XTick',u,'Fontsize',18);
u=[0 0.02 0.04 0.06 0.08 0.10 0.12 0.14];
set(gca,'YTick',u,'Fontsize',18);
xlabel('U_{R}','Fontsize',22);
ylabel('S_{1}','Fontsize',22);
title('R_{2}', 'Fontsize',22)
hgexport(gcf, '../../Figures/CASE1/CASE1_R2.png',...
       hgexport('factorystyle'), 'Format', 'png');
end
```

B. 2 - CASE 2

Rayleigh

```
function [R R1 R2 R3]=Rayleigh(x)
%CASE 2: THIS FUNCTION USES THE RAYLEIGH DISTRIBUTION TO CALCULATE
%THE EXPECTED VALUE OF THE TIME SCALE OF SCOUR AROUND A VERTICAL
%SLENDER PILE FOR DIFFERENT VALUES OF THE SHIELDS PARAMETER (trms)
%AND KEULEGAN-CARPENTER NUMBERS (KCrms).
```

```
%The expected value of the time scale is shown for 3 different
%values of the trms. T* is independent of D for Rayleigh
%because trms is given. Since trms is given, the grain size
%(z0,d50) will change for each value of KCrms. To find T by
%knowing T*, z0 must be calulated.

%DESCRIPTION OF SYMBOLS
%x: the normalized linear wave amplitude
%R: The expected value of the time scale T* for all D.
%R1: D=0.50 m - The expeced value of the time scale T (min).
%R2: D=0.75 m - The expeced value of the time scale T (min).
%R3: D=1.00 m - The expeced value of the time scale T (min).

%Et: The expected value of t  [-].
%ET: The expected value of T* [-].

syms x;

[n Hs h g s d50 arms c d]=Parameters();

trms1=0.07;
trms2=0.13;
trms3=0.18;

s1=3;
r1=10^(-6);
v=s1*(1-d);

for j=1:3

    if j==1
        D=0.5;
    elseif j==2
        D=0.75;
    else
        D=1;
    end

        i=0;
    for KCrms=7:0.01:12
        i=i+1;

        kp=1/h*asinh(2*pi*arms/(D*KCrms));
        wp=sqrt(kp*g*tanh(kp*h));
        Urms=wp*arms/(sinh(kp*h));

        z0_1=(24/(wp^d)*trms1*g*(s-1)/(c*Urms^(2-d)))^(1/(d-1));
        z0_2=(24/(wp^d)*trms2*g*(s-1)/(c*Urms^(2-d)))^(1/(d-1));
        z0_3=(24/(wp^d)*trms3*g*(s-1)/(c*Urms^(2-d)))^(1/(d-1));
```

```
        xmin=sqrt(log(n));
        x=(xmin:0.01:5);
        Et=trapz(x,2*n*(x).^(1-v).*exp(-(x).^2));

        ET_1=Et*r1*KCrms.^(s1)*trms1^(-s1);
        ET_2=Et*r1*KCrms.^(s1)*trms2^(-s1);
        ET_3=Et*r1*KCrms.^(s1)*trms3^(-s1);

        %RESULTING DATA OF T*
        R(i,1)=KCrms;
        R(i,2)=ET_1;
        R(i,3)=ET_2;
        R(i,4)=ET_3;

        %RESULTING DATA OF T
        if D==0.5
            R1(i,1)=KCrms;
            R1(i,2)=ET_1*D^2/(sqrt(g*(s-1)*(12*z0_1)^3))/60;
            R1(i,3)=ET_2*D^2/(sqrt(g*(s-1)*(12*z0_2)^3))/60;
            R1(i,4)=ET_3*D^2/(sqrt(g*(s-1)*(12*z0_3)^3))/60;
        elseif D==0.75
            R2(i,1)=KCrms;
            R2(i,2)=ET_1*D^2/(sqrt(g*(s-1)*(12*z0_1)^3))/60;
            R2(i,3)=ET_2*D^2/(sqrt(g*(s-1)*(12*z0_2)^3))/60;
            R2(i,4)=ET_3*D^2/(sqrt(g*(s-1)*(12*z0_3)^3))/60;
        else
            R3(i,1)=KCrms;
            R3(i,2)=ET_1*D^2/(sqrt(g*(s-1)*(12*z0_1)^3))/60;
            R3(i,3)=ET_2*D^2/(sqrt(g*(s-1)*(12*z0_2)^3))/60;
            R3(i,4)=ET_3*D^2/(sqrt(g*(s-1)*(12*z0_3)^3))/60;
        end
    end
end
end
```

Forristall

```
function [F1, F2, F3]=Forristall(x)
%CASE 2: THIS FUNCTION USES THE FORRISTALL DISTRIBUTION TO
%CALCULATE THE EXPECTED VALUE OF THE TIME SCALE FOR SCOUR
%AROUND A VERTICAL SLENDER PILE FOR DIFFERENT VALUES OF
%THE SHIELDS PARAMETER (trms) AND KC NUMBER (KCrms).

%The expected value of the time scale is shown for 3 different
%values of the trms. Since trms is given, the grain size
%(z0,d50) will change for each value of KCrms, affecting T.
```

```
%DESCRIPTION OF SYMBOLS
%x: The normalized second order wave crest.
%F1: D=0.50 m - The expected value of the time scale T*
%(col 1-7) and T(min) (col 8-13).
%F2: D=0.75 m - The expected value of the time scale T*
%(col 1-7) and T in minutes (col 8-13).
%F3: D=1.00 m - The expected value of the time scale T*
%(col 1-7) and T(min) (col 8-13).

%Et_2D: The expected value of t  [-] for 2D waves.
%Et_3D: The expected value of t  [-] for 3D waves.
%ET_2D: The expected value of T* [-] for 2D waves.
%ET_3D: The expected value of T* [-] for 3D waves.

syms x;

[n Hs h g s d50 arms c d]=Parameters();

s1=3;
r1=10^(-6);
v=s1*(1-d);

trms1=0.07;
trms2=0.13;
trms3=0.18;


for j=1:3
    if j==1
        D=0.5;
    elseif j==2
        D=0.75;
    else
        D=1;
    end

        i=0;
    for KCrms=7:0.01:12
        i=i+1;

        kp=(1/h*asinh(2*pi*arms/(D*KCrms)));
        wp=sqrt(kp*g*tanh(kp*h));
        Tp=2*pi/wp;
        Urms=wp*arms/(sinh(kp*h));

        z0_1=(24/(wp^d)*trms1*g*(s-1)/(c*Urms^(2-d)...
        ))^(1/(d-1));
        z0_2=(24/(wp^d)*trms2*g*(s-1)/(c*Urms^(2-d)...
```

```
))^(1/(d-1));
z0_3=(24/(wp^d)*trms3*g*(s-1)/(c*Urms^(2-d)...
))^(1/(d-1));

S1=2*pi*Hs/(g*Tp^2);
Ur=Hs/(kp^2*h^3);

%parameters for 2D model
alpha2=0.3536+0.2892*S1+0.1060*Ur;
beta2=2-2.1597*S1+0.0968*Ur^2;
xmin_2D=sqrt(8)*alpha2*(log(n))^(1/(beta2));
x2D=(xmin_2D:0.01:5);

%parameters for 3D model
alpha3=0.3536+0.2568*S1+0.0800*Ur;
beta3=2-1.7912*S1-0.5302*Ur+0.284*Ur^2;
xmin_3D=sqrt(8)*alpha3*(log(n))^(1/(beta3));
x3D=(xmin_3D:0.01:5);


Et_2D=trapz(x2D,n*beta2*(x2D).^(beta2-1-v)/((sqrt(8)*...
alpha2)^(beta2)).*exp(-((x2D)./(sqrt(8)*alpha2)).^(beta2)));
Et_3D=trapz(x3D,n*beta3*(x3D).^(beta3-1-v)/((sqrt(8)*...
alpha3)^(beta3)).*exp(-((x3D)./(sqrt(8)*alpha3)).^(beta3)));

ET_2D_1=Et_2D*r1*KCrms.^(s1)*trms1^(-s1);
ET_3D_1=Et_3D*r1*KCrms.^(s1)*trms1^(-s1);

ET_2D_2=Et_2D*r1*KCrms.^(s1)*trms2^(-s1);
ET_3D_2=Et_3D*r1*KCrms.^(s1)*trms2^(-s1);

ET_2D_3=Et_2D*r1*KCrms.^(s1)*trms3^(-s1);
ET_3D_3=Et_3D*r1*KCrms.^(s1)*trms3^(-s1);

%RESULTING DATA
if D==0.5
   %T*
   F1(i,1)=KCrms;
   F1(i,2)=ET_2D_1;
   F1(i,3)=ET_3D_1;
   F1(i,4)=ET_2D_2;
   F1(i,5)=ET_3D_2;
   F1(i,6)=ET_2D_3;
   F1(i,7)=ET_3D_3;
   %T
   F1(i,8)= ET_2D_1*D^2/(sqrt(g*(s-1)*(12*z0_1)^3))/60;
   F1(i,9)= ET_3D_1*D^2/(sqrt(g*(s-1)*(12*z0_1)^3))/60;
   F1(i,10)=ET_2D_2*D^2/(sqrt(g*(s-1)*(12*z0_2)^3))/60;
   F1(i,11)=ET_3D_2*D^2/(sqrt(g*(s-1)*(12*z0_2)^3))/60;
```

```
            F1(i,12)=ET_2D_3*D^2/(sqrt(g*(s-1)*(12*z0_3)^3))/60;
            F1(i,13)=ET_3D_3*D^2/(sqrt(g*(s-1)*(12*z0_3)^3))/60;

         elseif D==0.75
            %T*
            F2(i,1)=KCrms;
            F2(i,2)=ET_2D_1;
            F2(i,3)=ET_3D_1;
            F2(i,4)=ET_2D_2;
            F2(i,5)=ET_3D_2;
            F2(i,6)=ET_2D_3;
            F2(i,7)=ET_3D_3;
            %T
            F2(i,8)= ET_2D_1*D^2/(sqrt(g*(s-1)*(12*z0_1)^3))/60;
            F2(i,9)= ET_3D_1*D^2/(sqrt(g*(s-1)*(12*z0_1)^3))/60;
            F2(i,10)=ET_2D_2*D^2/(sqrt(g*(s-1)*(12*z0_2)^3))/60;
            F2(i,11)=ET_3D_2*D^2/(sqrt(g*(s-1)*(12*z0_2)^3))/60;
            F2(i,12)=ET_2D_3*D^2/(sqrt(g*(s-1)*(12*z0_3)^3))/60;
            F2(i,13)=ET_3D_3*D^2/(sqrt(g*(s-1)*(12*z0_3)^3))/60;

         else
            %T*
            F3(i,1)=KCrms;
            F3(i,2)=ET_2D_1;
            F3(i,3)=ET_3D_1;
            F3(i,4)=ET_2D_2;
            F3(i,5)=ET_3D_2;
            F3(i,6)=ET_2D_3;
            F3(i,7)=ET_3D_3;
            %T
            F3(i,8)= ET_2D_1*D^2/(sqrt(g*(s-1)*(12*z0_1)^3))/60;
            F3(i,9)= ET_3D_1*D^2/(sqrt(g*(s-1)*(12*z0_1)^3))/60;
            F3(i,10)=ET_2D_2*D^2/(sqrt(g*(s-1)*(12*z0_2)^3))/60;
            F3(i,11)=ET_3D_2*D^2/(sqrt(g*(s-1)*(12*z0_2)^3))/60;
            F3(i,12)=ET_2D_3*D^2/(sqrt(g*(s-1)*(12*z0_3)^3))/60;
            F3(i,13)=ET_3D_3*D^2/(sqrt(g*(s-1)*(12*z0_3)^3))/60;

         end
    end
end
end
```

Plot

```
function P=Plot(x)
%CASE 2: THIS FUNCTION PLOTS THE EXPECTED VALUE OF THE TIME
%SCALE OF SCOUR AROUND A VERTICAL SLENDER PILE FOR DIFFERENT
```

```
%VALUES OF THE SHIELDS PARAMETERS AND KC NUMBERS.

%Retrieving data from the Rayleigh distibution
[R R1 R2 R3]=Rayleigh();
% R:  Data for of E[T*].
% R1: D=0.50 m - Data for E[T].
% R2: D=0.75 m - Data for E[T].
% R3: D=1.00 m - Data for E[T].

%Retrieving data from the Forristall distribution
[F1 F2 F3]=Forristall();
% F1: D=0.50 m - Data for E[T*] (Col 1-7) and E[T] (Col 8-13).
% F2: D=0.75 m - Data for E[T*] (Col 1-7) and E[T] (Col 8-13).
% F3: D=1.00 m - Data for E[T*] (Col 1-7) and E[T] (Col 8-13).

%T* for D=0.5 m, D=0.75 m and D=1 m for trms=0.07
h1=figure;
set(h1, 'Position', [5 5 700 500],'Visible','off')
h=semilogx(R(:,1),R(:,2),'b',F1(:,1), F1(:,2),'c--',...
                             F1(:,1), F1(:,3),'c:',...
                             F2(:,1), F2(:,2),'k--',...
                             F2(:,1), F2(:,3),'k:',...
                             F3(:,1), F3(:,2),'m--',...
                             F3(:,1), F3(:,3),'m:');
hleg=legend('Rayleigh','Forristall (2D) D=0.50 m',...
                       'Forristall (3D) D=0.50 m',...
                       'Forristall (2D) D=0.75 m',...
                       'Forristall (3D) D=0.75 m',...
                       'Forristall (2D) D=1.00 m',...
                       'Forristall (3D) D=1.00 m',...
                       'Location','northwest');
set(hleg,'Fontsize',13)
set (h, 'LineWidth', 2.5)
u=[7 8 9 10 11 12];
set(gca,'XTick',u,'Fontsize',14);
axis([7 12 0 2.5]);
xlabel('KC_{r m s}','Fontsize',22);
ylabel('E[T*]','Fontsize',22);
hgexport(gcf, '../../Figures/CASE2/CASE21.png',...
    hgexport('factorystyle'), 'Format', 'png');


%T* for D=0.5 m, D=0.75 m and D=1 m for trms=0.13 and trms=0.18
h1=figure;
set(h1, 'Position', [5 5 700 500],'Visible','off')
h=semilogx(R(:,1),R(:,3),'b',F1(:,1), F1(:,4),'c--',...
                             F1(:,1), F1(:,5),'c:',...
                             F2(:,1), F2(:,4),'k--',...
                             F2(:,1), F2(:,5),'k:',...
```

```
                              F3(:,1), F3(:,4),'m--',...
                              F3(:,1), F3(:,5),'m:',...
           R(:,1),R(:,4),'b',F1(:,1), F1(:,6),'c--',...
                              F1(:,1), F1(:,7),'c:',...
                              F2(:,1), F2(:,6),'k--',...
                              F2(:,1), F2(:,7),'k:',...
                              F3(:,1), F3(:,6),'m--',...
                              F3(:,1), F3(:,7),'m:');
hleg=legend('Rayleigh','Forristall (2D) D=0.50 m',...
                       'Forristall (3D) D=0.50 m',...
                       'Forristall (2D) D=0.75 m',...
                       'Forristall (3D) D=0.75 m',...
                       'Forristall (2D) D=1.00 m',...
                       'Forristall (3D) D=1.00 m',...
                       'Location','northwest');
set(hleg,'Fontsize',13)
set (h, 'LineWidth', 2.5)
u=[7 8 9 10 11 12];
set(gca,'XTick',u,'Fontsize',14);
axis([7 12 0 0.35 ]);
xlabel('KC_{r m s}','Fontsize',22);
ylabel('E[T*]','Fontsize',22);
hgexport(gcf, '../../Figures/CASE2/CASE22.png',...
    hgexport('factorystyle'), 'Format', 'png');


%T for D=0.5 m, D=0.75 m and D=1 m for trms=0.07
h1=figure;
set(h1, 'Position', [5 5 700 500],'Visible','off')
h=semilogx(R1(:,1),R1(:,2),'c',F1(:,1), F1(:,8),'c--',...
                               F1(:,1), F1(:,9),'c:',...
           R2(:,1),R2(:,2),'k',F2(:,1), F2(:,8),'k--',...
                               F2(:,1), F2(:,9),'k:',...
           R3(:,1),R3(:,2),'m',F3(:,1), F3(:,8),'m--',...
                               F3(:,1), F3(:,9),'m:');
hleg=legend('Rayleigh          D=0.50 m',...
                              'Forristall (2D) D=0.50 m',...
                              'Forristall (3D) D=0.50 m',...
            'Rayleigh          D=0.75 m',...
                              'Forristall (2D) D=0.75 m',...
                              'Forristall (3D) D=0.75 m',...
            'Rayleigh          D=1.00 m',...
                              'Forristall (2D) D=1.00 m',...
                               'Forristall (3D) D=1.00 m',...
            'Location','northwest');
set(hleg,'Fontsize',13)
set (h, 'LineWidth', 2.5)
u=[7 8 9 10 11 12];
set(gca,'XTick',u,'Fontsize',14);
```

```
axis([7 12 0 10 ]);
xlabel('KC_{r m s}','Fontsize',22);
ylabel('E[T]','Fontsize',22);
title('\theta_{r m s}=0.07','Fontsize',17)
hgexport(gcf, '../../Figures/CASE2/CASE2T1.png',...
    hgexport('factorystyle'), 'Format', 'png');


%T for D=0.5 m, D=0.75 m and D=1 m for trms=0.18
h1=figure;
set(h1, 'Position', [5 5 700 500],'Visible','off')
h=semilogx(R1(:,1),R1(:,4),'c',F1(:,1), F1(:,12),'c--',...
                               F1(:,1), F1(:,13),'c:',...
           R2(:,1),R2(:,4),'k',F2(:,1), F2(:,12),'k--',...
                               F2(:,1), F2(:,13),'k:',...
           R3(:,1),R3(:,4),'m',F3(:,1), F3(:,12),'m--',...
                               F3(:,1), F3(:,13),'m:');
hleg=legend('Rayleigh          D=0.50 m',...
            'Forristall (2D) D=0.50 m',...
            'Forristall (3D) D=0.50 m',...
            'Rayleigh          D=0.75 m',...
            'Forristall (2D) D=0.75 m',...
            'Forristall (3D) D=0.75 m',...
            'Rayleigh          D=1.00 m',...
            'Forristall (2D) D=1.00 m',...
            'Forristall (3D) D=1.00 m',...
            'Location','northwest');
set(hleg,'Fontsize',13)
set (h, 'LineWidth', 2.5)
u=[7 8 9 10 11 12];
set(gca,'XTick',u,'Fontsize',14);
axis([7 12 0 10]);
xlabel('KC_{r m s}','Fontsize',22);
ylabel('E[T]','Fontsize',22);
title('\theta_{r m s}=0.18','Fontsize',17)
hgexport(gcf, '../../Figures/CASE2/CASE2T3.png',...
    hgexport('factorystyle'), 'Format', 'png');
end
```

Iso

```
function i=iso()
%CASE 2: THIS FUNCTION USES THE RAYLEIGH AND THE FORRISTALL
%DISTRIBUTION TO FIND THE RATIO OF THE NONLINEAR AND LINEAR
%SOLUTION (R1) AND THE RATIO OF THE 3D AND 2D SOLUTION (R2),
%FOR THE TIME SCALE OF SCOUR AROUND VERTICAL SLENDER PILES.
%%R1 AND R2 ARE PLOTTED AS ISOCURVES VERSUS URSELLS NUMBER
```

```
%(Ur) AND THE STEEPNESS (S1).

%DESCRIPTION OF SYMBOLS
%x_R:  The normalized linar wave amplitude.
%x_2D: The normalized second-order wave crest for 2D waves.
%x_3D: The normalized second-order wave crest for 3D waves.

syms x_R x_2D x_3D;

[n Hs h g s d50 arms c d]=Parameters();

s1=3;
v=s1*(1-d);

o=zeros(101,101);
h=zeros(101,101);

    Ur=-0.01;
for i=1:101

    Ur=Ur+0.01;
    h(:,i)=Ur;

        S1=-0.0015;
    for j=1:101

        S1=S1+0.0015;
        o(j,:)=S1;

        alpha2=0.3536+0.2892*S1+0.1060*Ur;
        beta2=2-2.1597*S1+0.0968*Ur^2;
        alpha3=0.3536+0.2568*S1+0.0800*Ur;
        beta3=2-1.7912*S1-0.5302*Ur+0.284*Ur^2;

        xmin_R=sqrt(log(n));
        xmin_2D=sqrt(8)*alpha2*(log(n))^(1/(beta2));
        xmin_3D=sqrt(8)*alpha3*(log(n))^(1/(beta3));

        x_R=(xmin_R:0.01:5);
        x_2D=(xmin_2D:0.01:5);
        x_3D=(xmin_3D:0.01:5);

        %THE EXPECTED VALUE t
        e_R=2*n*(x_R).^(1-v).*exp(-((x_R).^2));
        e_2D=n*beta2*(x_2D).^(beta2-1-v)/((sqrt(8)*alpha2).^beta2...
        ).*exp(-((x_2D)./(sqrt(8).*alpha2)).^beta2);
        e_3D=n*beta3*(x_3D).^(beta3-1-v)/((sqrt(8)*alpha3).^beta3...
        ).*exp(-((x_3D)./(sqrt(8).*alpha3)).^beta3);
```

```
        E_R=trapz(x_R,e_R);
        E_2D=trapz(x_2D,e_2D);
        E_3D=trapz(x_3D,e_3D);

        %R1
        R1_2D=(E_2D)/(E_R);
        R1_3D=(E_3D)/(E_R);

        %R2
        R2=E_3D/E_2D;

        %data for plot
        k1(j,i)=R1_2D;
        k2(j,i)=R1_3D;
        k3(j,i)=R2;
   end
end

%PLOT
%R1_2D
h1=figure;
set(h1, 'Position', [5 5 700 500],'Visible','off')
c1=contour(h,o,k1,'b','LineWidth',2.5);
clabel(c1,'Fontsize',18);
u=[0 0.1 0.2 0.3 0.4 0.5 0.6 0.7 0.8 0.9 1];
set(gca,'XTick',u,'Fontsize',18);
u=[0 0.02 0.04 0.06 0.08 0.10 0.12 0.14];
set(gca,'YTick',u,'Fontsize',18);
xlabel('U_{R}','Fontsize',22);
ylabel('S_{1}','Fontsize',22);
title('R_{1,2D}', 'Fontsize',22)
hgexport(gcf, '../../Figures/CASE2/CASE2_R1_2D.png',...
       hgexport('factorystyle'), 'Format', 'png');

%R1_3D
h1=figure;
set(h1, 'Position', [5 5 700 500],'Visible','off')
c1=contour(h,o,k2,'b','LineWidth',2.5);
clabel(c1,'Fontsize',18);
u=[0 0.1 0.2 0.3 0.4 0.5 0.6 0.7 0.8 0.9 1];
set(gca,'XTick',u,'Fontsize',18);
u=[0 0.02 0.04 0.06 0.08 0.10 0.12 0.14];
set(gca,'YTick',u,'Fontsize',18);
xlabel('U_{R}','Fontsize',22);
ylabel('S_{1}','Fontsize',22');
title('R_{1,3D}', 'Fontsize',22)
hgexport(gcf, '../../Figures/CASE2/CASE2_R1_3D.png',...
       hgexport('factorystyle'), 'Format', 'png');
```

```
%R2
h1=figure;
set(h1, 'Position', [5 5 700 500],'Visible','off')
c1=contour(h,o,k3,'b','LineWidth',2.5);
clabel(c1,'Fontsize',18);
u=[0 0.1 0.2 0.3 0.4 0.5 0.6 0.7 0.8 0.9 1];
set(gca,'XTick',u,'Fontsize',18);
u=[0 0.02 0.04 0.06 0.08 0.10 0.12 0.14];
set(gca,'YTick',u,'Fontsize',18);
xlabel('U_{R}','Fontsize',22);
ylabel('S_{1}','Fontsize',22);
title('R_{2}', 'Fontsize',22)
hgexport(gcf, '../../Figures/CASE2/CASE2_R2.png',...
       hgexport('factorystyle'), 'Format', 'png');
end
```

B. 3 - CASE 3

Rayleigh

```
function [R, R1, R2, R3]=Rayleigh(x)
%CASE 3: THIS FUNCTION USES THE RAYLEIGH DISTRIBUTION TO CALCULATE
%THE EXPECTED VALUE OF THE TIME SCALE OF BACKFILLING BY WAVES ALONE
%AROUND A PILE WHEN THE INITIAL HOLE WAS GENERATED BY A CURRENT.

%The expected value of the time scale is shown for 3 different
%values of the trms. T* is independent of D for Rayleigh
%because trms is given. Since trms is given, the grain size
%(z0,d50) will change for each value of KCrms. To find T by
%knowing T*, z0 must be calulated.

%Et: The expected value of t  [-].
%ET: The expected value of T* [-].

%Rayleigh because trms is given.
%R1: D=0.50 m - The expeced value of the time scale T (min).
%R2: D=0.75 m - The expeced value of the time scale T (min).
%R3: D=1.00 m - The expeced value of the time scale T (min).

syms x;

[n Hs h g s d50 arms c d]=Parameters();

s1=2;
s2=1.45;
```

```
v=s2*(s1*(2-d)+1);

trms1=0.07;
trms2=0.10;
trms3=0.15;

for j=1:3
    if j==1
       D=0.5;
    elseif j==2
       D=0.75;
    else
       D=1;
    end

    i=0;
    for KCrms=5:0.01:12
        i=i+1;

        kp=1/h*asinh(2*pi*arms/(D*KCrms));
        wp=sqrt(g*kp*tanh(kp*h));
        Urms=wp*arms/(sinh(kp*h));

        z0_1=(24/(wp^d)*trms1*g*(s-1)/(c*Urms^(2-d)))^(1/(d-1));
        z0_2=(24/(wp^d)*trms2*g*(s-1)/(c*Urms^(2-d)))^(1/(d-1));
        z0_3=(24/(wp^d)*trms3*g*(s-1)/(c*Urms^(2-d)))^(1/(d-1));

        xmin=sqrt(log(n));
        x=(xmin:0.01:5);
        Et=trapz(x,2*n*(x).^(1-v).*exp(-(x).^2));

        ET_1=Et*trms1^(-s1*s2)*KCrms.^(-s2);
        ET_2=Et*trms2^(-s1*s2)*KCrms.^(-s2);
        ET_3=Et*trms3^(-s1*s2)*KCrms.^(-s2);

        %RESULTING DATA of T*
        R(i,1)=KCrms;
        R(i,2)=ET_1;
        R(i,3)=ET_2;
        R(i,4)=ET_3;

        %RESULTING DATA OF T
        if D==0.50
            R1(i,1)=KCrms;
            R1(i,2)=ET_1*D^2/(sqrt(g*(s-1)*(12*z0_1)^3))/60;
            R1(i,3)=ET_2*D^2/(sqrt(g*(s-1)*(12*z0_2)^3))/60;
            R1(i,4)=ET_3*D^2/(sqrt(g*(s-1)*(12*z0_3)^3))/60;
        elseif D==0.75
            R2(i,1)=KCrms;
```

```
            R2(i,2)=ET_1*D^2/(sqrt(g*(s-1)*(12*z0_1)^3))/60;
            R2(i,3)=ET_2*D^2/(sqrt(g*(s-1)*(12*z0_2)^3))/60;
            R2(i,4)=ET_3*D^2/(sqrt(g*(s-1)*(12*z0_3)^3))/60;
        else
            R3(i,1)=KCrms;
            R3(i,2)=ET_1*D^2/(sqrt(g*(s-1)*(12*z0_1)^3))/60;
            R3(i,3)=ET_2*D^2/(sqrt(g*(s-1)*(12*z0_2)^3))/60;
            R3(i,4)=ET_3*D^2/(sqrt(g*(s-1)*(12*z0_3)^3))/60;
        end
    end
end
end
```

Forristall

```
function [F1 F2 F3]=Forristall(x)
%CASE 3: THIS FUNCTION USES THE FORRISTALL DISTRIBUTION TO CALCULATE
%THE EXPECTED VALUE OF THE TIME SCALE OF BACKFILLING BY WAVES ALONE
%AROUND A PILE WHEN THE INITIAL HOLE WAS GENERATED BY A CURRENT.

%The expected value of the time scale is shown for 3 different
%values of the trms. Since trms is given, the grain size
%(z0,d50) will change for each value of KCrms, affecting T.

%DESCRIPTION OF SYMBOLS
%x: The normalized second-order wave crest.
%F1: D=0.50 m - The expected values of the time scale T*
%(col 1-7) and T(min) (col 8-13).
%F2: D=0.75 m - The expected value of the time scale T*
%(col 1-7) and T in minutes (col 8-13).
%F3: D=1.00 m - The expected value of the time scale T*
%(col 1-7) and T(min) (col 8-13).

%Et_2D: The expected value of t  [-] for 2D waves.
%Et_3D: The expected value of t  [-] for 3D waves.
%ET_2D: The expected value of T* [-] for 2D waves.
%ET_3D: The expected value of T* [-] for 3D waves.

syms x;

[n Hs h g s d50 arms c d]=Parameters();

s1=2;
s2=1.45;
v=s2*(s1*(2-d)+1);

trms1=0.07;
```

```
trms2=0.10;
trms3=0.15;

for j=1:3

    if j==1
       D=0.5;
    elseif j==2
       D=0.75;
    else
       D=1;
    end

        i=0;
    for KCrms=5:0.01:12
        i=i+1;
        kp=1/h*asinh(2*pi*arms/(D*KCrms));
        wp=sqrt(g*kp*tanh(kp*h));
        Tp=2*pi/wp;
        Urms=wp*arms/(sinh(kp*h));

        z0_1=(24/(wp^d)*trms1*g*(s-1)/(c*Urms^(2-d)...
        ))^(1/(d-1));
        z0_2=(24/(wp^d)*trms2*g*(s-1)/(c*Urms^(2-d)...
        ))^(1/(d-1));
        z0_3=(24/(wp^d)*trms3*g*(s-1)/(c*Urms^(2-d)...
        ))^(1/(d-1));

        S1=2*pi*Hs/(g*Tp^2);
        Ur=Hs/(kp^2*h^3);

        %parameters for 2D model
        alpha2=0.3536+0.2892*S1+0.1060*Ur;
        beta2=2-2.1597*S1+0.0968*Ur^2;
        xmin_2D=sqrt(8)*alpha2*(log(n))^(1/(beta2));
        x2D=(xmin_2D:0.01:5);

        %parameters for 3D model
        alpha3=0.3536+0.2568*S1+0.0800*Ur;
        beta3=2-1.7912*S1-0.5302*Ur+0.284*Ur^2;
        xmin_3D=sqrt(8)*alpha3*(log(n))^(1/(beta3));
        x3D=(xmin_3D:0.01:5);


       Et_2D=trapz(x2D,n*beta2*(x2D).^(beta2-1-v)/((sqrt(8)*...
     alpha2)^(beta2)).*exp(-((x2D)./(sqrt(8)*alpha2)).^(beta2)));
       Et_3D=trapz(x3D,n*beta3*(x3D).^(beta3-1-v)/((sqrt(8)*...
     alpha3)^(beta3)).*exp(-((x3D)./(sqrt(8)*alpha3)).^(beta3)));
```

```
ET_2D_1=Et_2D*trms1^(-s1*s2)*KCrms.^(-s2);
ET_3D_1=Et_3D*trms1^(-s1*s2)*KCrms.^(-s2);

ET_2D_2=Et_2D*trms2^(-s1*s2)*KCrms.^(-s2);
ET_3D_2=Et_3D*trms2^(-s1*s2)*KCrms.^(-s2);

ET_2D_3=Et_2D*trms3^(-s1*s2)*KCrms.^(-s2);
ET_3D_3=Et_3D*trms3^(-s1*s2)*KCrms.^(-s2);

%RESULTING DATA
if D==0.5
   %T*
   F1(i,1)=KCrms;
   F1(i,2)=ET_2D_1;
   F1(i,3)=ET_3D_1;
   F1(i,4)=ET_2D_2;
   F1(i,5)=ET_3D_2;
   F1(i,6)=ET_2D_3;
   F1(i,7)=ET_3D_3;
   %T
   F1(i,8)=ET_2D_1*D^2/(sqrt(g*(s-1)*(12*z0_1)^3))/60;
   F1(i,9)=ET_3D_1*D^2/(sqrt(g*(s-1)*(12*z0_1)^3))/60;
   F1(i,10)=ET_2D_2*D^2/(sqrt(g*(s-1)*(12*z0_2)^3))/60;
   F1(i,11)=ET_3D_2*D^2/(sqrt(g*(s-1)*(12*z0_2)^3))/60;
   F1(i,12)=ET_2D_3*D^2/(sqrt(g*(s-1)*(12*z0_3)^3))/60;
   F1(i,13)=ET_3D_3*D^2/(sqrt(g*(s-1)*(12*z0_3)^3))/60;

 elseif D==0.75
   %T*
   F2(i,1)=KCrms;
   F2(i,2)=ET_2D_1;
   F2(i,3)=ET_3D_1;
   F2(i,4)=ET_2D_2;
   F2(i,5)=ET_3D_2;
   F2(i,6)=ET_2D_3;
   F2(i,7)=ET_3D_3;
   %T
   F2(i,8)=ET_2D_1*D^2/(sqrt(g*(s-1)*(12*z0_1)^3))/60;
   F2(i,9)=ET_3D_1*D^2/(sqrt(g*(s-1)*(12*z0_1)^3))/60;
   F2(i,10)=ET_2D_2*D^2/(sqrt(g*(s-1)*(12*z0_2)^3))/60;
   F2(i,11)=ET_3D_2*D^2/(sqrt(g*(s-1)*(12*z0_2)^3))/60;
   F2(i,12)=ET_2D_3*D^2/(sqrt(g*(s-1)*(12*z0_3)^3))/60;
   F2(i,13)=ET_3D_3*D^2/(sqrt(g*(s-1)*(12*z0_3)^3))/60;

else
   %T*
   F3(i,1)=KCrms;
   F3(i,2)=ET_2D_1;
   F3(i,3)=ET_3D_1;
```

```
            F3(i,4)=ET_2D_2;
            F3(i,5)=ET_3D_2;
            F3(i,6)=ET_2D_3;
            F3(i,7)=ET_3D_3;
            %T
            F3(i,8)=ET_2D_1*D^2/(sqrt(g*(s-1)*(12*z0_1)^3))/60;
            F3(i,9)=ET_3D_1*D^2/(sqrt(g*(s-1)*(12*z0_1)^3))/60;
            F3(i,10)=ET_2D_2*D^2/(sqrt(g*(s-1)*(12*z0_2)^3))/60;
            F3(i,11)=ET_3D_2*D^2/(sqrt(g*(s-1)*(12*z0_2)^3))/60;
            F3(i,12)=ET_2D_3*D^2/(sqrt(g*(s-1)*(12*z0_3)^3))/60;
            F3(i,13)=ET_3D_3*D^2/(sqrt(g*(s-1)*(12*z0_3)^3))/60;
        end
    end
end
end
```

Plot

```
function P=Plot(x)
%CASE 3: THIS FUNCTION PLOTS THE EXPECTED VALUE OF THE TIME SCALE
%OF BACKFILLING BY WAVES ALONE AROUND A PILE WHEN THE INITIAL HOLE
%WAS GENERATED BY A CURRENT.

%Retrieving data from the Rayleigh distibution
[R R1 R2 R3]=Rayleigh();
% R:  Data for of E[T*].
% R1: D=0.50 m - Data for E[T].
% R2: D=0.75 m - Data for E[T].
% R3: D=1.00 m - Data for E[T].

%Retrieving data from the Forristall distribution
[F1, F2, F3]=Forristall();
% F1: D=0.50 m - Data for E[T*] (Col 1-7) and E[T] (Col 8-13).
% F2: D=0.75 m - Data for E[T*] (Col 1-7) and E[T] (Col 8-13).
% F3: D=1.00 m - Data for E[T*] (Col 1-7) and E[T] (Col 8-13).

%T* with trms=0.07 and D=0.5 m, D=0.75 m and D=1 m
h1=figure;
set(h1, 'Position', [5 5 700 500],'Visible','off')
h=semilogx(R(:,1),R(:,2),'b',F1(:,1), F1(:,2),'c--',...
                             F1(:,1), F1(:,3),'c:',...
                             F2(:,1), F2(:,2),'k--',...
                             F2(:,1), F2(:,3),'k:',...
                             F3(:,1), F3(:,2),'m--', ...
                             F3(:,1), F3(:,3),'m:');
hleg=legend('Rayleigh','Forristall (2D) D=0.50 m',...
                       'Forristall (3D) D=0.50 m',...
```

```
                        'Forristall (2D) D=0.75 m',...
                        'Forristall (3D) D=0.75 m',...
                        'Forristall (2D) D=1.00 m',...
                        'Forristall (3D) D=1.00 m',...
                        'Location','northeast');
set(hleg,'Fontsize',13)
set (h, 'LineWidth', 2.5)
u=[5 6 7 8 9 10 12];
set(gca,'XTick',u,'Fontsize',14);
axis([5 12 0 10]);
xlabel('KC_{f r m s}','Fontsize',22);
ylabel('E[T*]','Fontsize',22);
title('\theta_{f r m s}=0.07','Fontsize',17)
hgexport(gcf, '../../Figures/CASE3/CASE31.png',...
    hgexport('factorystyle'), 'Format', 'png');


%T* with trms=0.15 and D=0.5 m, D=0.75 m and D=1 m
h1=figure;
set(h1, 'Position', [5 5 700 500],'Visible','off')
h=semilogx(R(:,1),R(:,4),'b',F1(:,1), F1(:,6),'c--',...
                             F1(:,1), F1(:,7),'c:',...
                             F2(:,1), F2(:,6),'k--',...
                             F2(:,1), F2(:,7),'k:',...
                             F3(:,1), F3(:,6),'m--',...
                             F3(:,1), F3(:,7),'m:');
hleg=legend('Rayleigh','Forristall (2D) D=0.50 m',...
                        'Forristall (3D) D=0.50 m',...
                        'Forristall (2D) D=0.75 m',...
                        'Forristall (3D) D=0.75 m',...
                        'Forristall (2D) D=1.00 m',...
                        'Forristall (3D) D=1.00 m',...
                        'Location','northeast');
set(hleg,'Fontsize',13);
set (h, 'LineWidth', 2.5)
u=[5 6 7 8 9 10 11 12];
set(gca,'XTick',u,'Fontsize',14);
axis([5 11 0 1.1]);
xlabel('KC_{f r m s}','Fontsize',22);
ylabel('E[T*]','Fontsize',22);
title('\theta_{f r m s}=0.15','Fontsize',17)
hgexport(gcf, '../../Figures/CASE3/CASE33.png',...
    hgexport('factorystyle'), 'Format', 'png');


%T* for D=0.5 m - All theta
h1=figure;
set(h1, 'Position', [5 5 700 500],'Visible','off')
h=semilogx(R(:,1),R(:,2),'c',F1(:,1), F1(:,2),'c--',...
```

```
                              F1(:,1), F1(:,3),'c:',...
          R(:,1),R(:,3),'k',F1(:,1), F1(:,4),'k--',...
                              F1(:,1), F1(:,5),'k:',...
          R(:,1),R(:,4),'m',F1(:,1), F1(:,6),'m--',...
                              F1(:,1), F1(:,7),'m:');
hleg=legend('Rayleigh          \theta_{frms}=0.07',...
            'Forristall (2D) \theta_{frms}=0.07',...
            'Forristall (3D) \theta_{frms}=0.07',...
            'Rayleigh          \theta_{frms}=0.10',...
            'Forristall (2D) \theta_{frms}=0.10',...
            'Forristall (3D) \theta_{frms}=0.10',...
            'Rayleigh          \theta_{frms}=0.15',...
            'Forristall (2D) \theta_{frms}=0.15',...
            'Forristall (3D) \theta_{frms}=0.15',...
            'Location','northeast');
set(hleg,'Fontsize',10)
set (h, 'LineWidth', 2.5)
u=[5 6 7 8 9 10 12];
set(gca,'XTick',u,'Fontsize',14);
axis([5 12 0 10]);
xlabel('KC_{f r m s}','Fontsize',22);
ylabel('E[T*]','Fontsize',22);
title('D=0.5 m','Fontsize',17)
hgexport(gcf, '../../Figures/CASE3/CASE3_D05.png',...
    hgexport('factorystyle'), 'Format', 'png');


%T* for D=1.0 - All theta
h1=figure;
set(h1, 'Position', [5 5 700 500],'Visible','off')
h=semilogx(R(:,1),R(:,2),'c',F3(:,1), F3(:,2),'c--',...
                              F3(:,1), F3(:,3),'c:',...
          R(:,1),R(:,3),'k',F3(:,1), F3(:,4),'k--',...
                              F3(:,1), F3(:,5),'k:',...
          R(:,1),R(:,4),'m',F3(:,1), F3(:,6),'m--',...
                              F3(:,1), F3(:,7),'m:');
hleg=legend('Rayleigh          \theta_{rms}=0.07',...
            'Forristall (2D) \theta_{rms}=0.07',....
            'Forristall (3D) \theta_{rms}=0.07',...
            'Rayleigh          \theta_{rms}=0.10',...
            'Forristall (2D) \theta_{rms}=0.10',...
            'Forristall (3D) \theta_{rms}=0.10',...
            'Rayleigh          \theta_{rms}=0.15',...
            'Forristall (2D) \theta_{rms}=0.15',...
            'Forristall (3D) \theta_{rms}=0.15',...
            'Location','northeast');
set (h, 'LineWidth', 2.5)
set(hleg,'Fontsize',10)
u=[5 6 7 8 9 10 12];
```

```
set(gca,'XTick',u,'Fontsize',14);
axis([5 12 0 10]);
xlabel('KC_{f r m s}','Fontsize',22);
ylabel('E[T*]','Fontsize',22);
title('D=1 m','Fontsize',17)
hgexport(gcf, '../../Figures/CASE3/CASE3_D10.png',...
    hgexport('factorystyle'), 'Format', 'png');


%T for all D and trms=0.07
h1=figure;
set(h1, 'Position', [5 5 700 500],'Visible','off')
h=semilogx(R1(:,1),R1(:,2),'c',F1(:,1), F1(:,8),'c--',...
                               F1(:,1), F1(:,9),'c:',...
           R2(:,1),R2(:,2),'k',F2(:,1), F2(:,8),'k--',...
                               F2(:,1), F2(:,9),'k:',...
           R3(:,1),R3(:,2),'m',F3(:,1), F3(:,8),'m--',...
                               F3(:,1), F3(:,9),'m:');
hleg=legend('Rayleigh          D=0.50 m','Forristall (2D) D=0.50 m',...
                                         'Forristall (3D) D=0.50 m',...
            'Rayleigh          D=0.75 m','Forristall (2D) D=0.75 m',...
                                         'Forristall (3D) D=0.75 m',...
            'Rayleigh          D=1.00 m','Forristall (2D) D=1.00 m',...
                                         'Forristall (3D) D=1.00 m',...
            'Location','northeast');
set(hleg,'Fontsize',13)
set (h, 'LineWidth', 2.5)
u=[5 6 7 8 9 10 12];
set(gca,'XTick',u,'Fontsize',14);
axis([5 12 0 50]);
xlabel('KC_{f r m s}','Fontsize',22);
ylabel('E[T]','Fontsize',22);
title('\theta_{f r m s}=0.07','Fontsize',17)
hgexport(gcf, '../../Figures/CASE3/CASE3T1.png',...
    hgexport('factorystyle'), 'Format', 'png');


%T all D and trms=0.15
h1=figure;
set(h1, 'Position', [5 5 700 500],'Visible','off')
h=semilogx(R1(:,1),R1(:,4),'c',F1(:,1), F1(:,12),'c--',...
                               F1(:,1), F1(:,13),'c:',...
           R2(:,1),R2(:,4),'k',F2(:,1), F2(:,12),'k--',...
                               F2(:,1), F2(:,13),'k:',...
           R3(:,1),R3(:,4),'m',F3(:,1), F3(:,12),'m--',...
                               F3(:,1), F3(:,13),'m:');
hleg=legend('Rayleigh          D=0.50 m','Forristall (2D) D=0.50 m',...
                                         'Forristall (3D) D=0.50 m',...
            'Rayleigh          D=0.75 m','Forristall (2D) D=0.75 m',...
```

```
                                        'Forristall (3D) D=0.75 m',...
            'Rayleigh          D=1.00 m','Forristall (2D) D=1.00 m',...
                                        'Forristall (3D) D=1.00 m',...
            'Location','northeast');
set(hleg,'Fontsize',13)
set (h, 'LineWidth', 2.5)
u=[5 6 7 8 9 10 12];
set(gca,'XTick',u,'Fontsize',14);
axis([5 12 0 60]);
xlabel('KC_{f r m s}','Fontsize',22);
ylabel('E[T]','Fontsize',22);
title('\theta_{f r m s}=0.15','Fontsize',17)
hgexport(gcf, '../../Figures/CASE3/CASE3T2.png',...
    hgexport('factorystyle'), 'Format', 'png');

end
```

Iso

```
function i=iso()
%CASE 3: THIS FUNCTION USES THE RAYLEIGH AND THE FORRISTALL
%DISTRIBUTION TO FIND THE RATIO OF THE NONLINEAR AND LINEAR
%SOLUTION (R1) AND THE RATIO OF THE 3D AND 2D SOLUTION (R2),
%FOR THE TIME SCALE OF BACKFILLING AROUND VERTICAL SLENDER PILES.
%%R1 AND R2 ARE PLOTTED AS ISOCURVES VERSUS URSELLS NUMBER
%(Ur) AND THE STEEPNESS (S1).

%DESCRIPTION OF SYMBOLS
%x_R:  The normalized linar wave amplitude.
%x_2D: The normalized second-order wave crest for 2D waves.
%x_3D: The normalized second-order wave crest for 3D waves.

syms x_R x_2D x_3D;

[n Hs h g s d50 arms c d]=Parameters();

s1=2;
s2=1.45;
v=s2*(s1*(2-d)+1);

o=zeros(101,101);
h=zeros(101,101);

    Ur=0.01;
for i=1:101

    Ur=Ur+0.01;
```

```
    h(:,i)=Ur;

        S1=0.0015;
    for j=1:101

        S1=S1+0.0015;
        o(j,:)=S1;

        alpha2=0.3536+0.2892*S1+0.1060*Ur;
        beta2=2-2.1597*S1+0.0968*Ur^2;
        alpha3=0.3536+0.2568*S1+0.0800*Ur;
        beta3=2-1.7912*S1-0.5302*Ur+0.284*Ur^2;

        xmin_R=sqrt(log(n));
        xmin_2D=sqrt(8)*alpha2*(log(n))^(1/(beta2));
        xmin_3D=sqrt(8)*alpha3*(log(n))^(1/(beta3));

        x_R=(xmin_R:0.01:5);
        x_2D=(xmin_2D:0.01:5);
        x_3D=(xmin_3D:0.01:5);

        %THE EXPECTED VALUE t
        e_R=2*n*(x_R).^(1-v).*exp(-((x_R).^2));
        e_2D=n*beta2*(x_2D).^(beta2-1-v)/((sqrt(8)*alpha2).^...
          beta2).*exp(-((x_2D)./(sqrt(8).*alpha2)).^beta2);
        e_3D=n*beta3*(x_3D).^(beta3-1-v)/((sqrt(8)*alpha3).^...
          beta3).*exp(-((x_3D)./(sqrt(8).*alpha3)).^beta3);

        E_R=trapz(x_R,e_R);
        E_2D=trapz(x_2D,e_2D);
        E_3D=trapz(x_3D,e_3D);

        %R1
        R1_2D=(E_2D)/(E_R);
        R1_3D=(E_3D)/(E_R);

        %R2
        R2=E_3D/E_2D;

        %data for plot
        k1(j,i)=R1_2D;
        k2(j,i)=R1_3D;
        k3(j,i)=R2;
    end
end

%PLOT
%R1_2D
h1=figure;
```

```
set(h1, 'Position', [5 5 700 500],'Visible','off')
c1=contour(h,o,k1,'b','LineWidth',2.5);
clabel(c1,'Fontsize',18);
u=[0 0.1 0.2 0.3 0.4 0.5 0.6 0.7 0.8 0.9 1];
set(gca,'XTick',u,'Fontsize',18);
u=[0 0.02 0.04 0.06 0.08 0.10 0.12 0.14];
set(gca,'YTick',u,'Fontsize',18);
xlabel('U_{R}','Fontsize',22);
ylabel('S_{1}','Fontsize',22);
title('R_{1,2D}', 'Fontsize',22)
hgexport(gcf, '../../Figures/CASE3/CASE3_R1_2D.png',...
       hgexport('factorystyle'), 'Format', 'png');


%R1_3D
h1=figure;
set(h1, 'Position', [5 5 700 500],'Visible','off')
c1=contour(h,o,k2,'b','LineWidth',2.5);
clabel(c1,'Fontsize',18);
u=[0 0.1 0.2 0.3 0.4 0.5 0.6 0.7 0.8 0.9 1];
set(gca,'XTick',u,'Fontsize',18);
u=[0 0.02 0.04 0.06 0.08 0.10 0.12 0.14];
set(gca,'YTick',u,'Fontsize',18);
xlabel('U_{R}','Fontsize',22);
ylabel('S_{1}','Fontsize',22');
title('R_{1,3D}', 'Fontsize',22)
hgexport(gcf, '../../Figures/CASE3/CASE3_R1_3D.png',...
       hgexport('factorystyle'), 'Format', 'png');


%R2
h1=figure;
set(h1, 'Position', [5 5 700 500],'Visible','off')
c1=contour(h,o,k3,'b','LineWidth',2.5);
clabel(c1,'Fontsize',18);
u=[0 0.1 0.2 0.3 0.4 0.5 0.6 0.7 0.8 0.9 1];
set(gca,'XTick',u,'Fontsize',18);
u=[0 0.02 0.04 0.06 0.08 0.10 0.12 0.14];
set(gca,'YTick',u,'Fontsize',18);
xlabel('U_{R}','Fontsize',22);
ylabel('S_{1}','Fontsize',22);
title('R_{2}', 'Fontsize',22)
hgexport(gcf, '../../Figures/CASE3/CASE3_R2.png',...
       hgexport('factorystyle'), 'Format', 'png');
end
```

B. 4 - CASE 4

Rayleigh

```
function [R1 R2 R3]=Rayleigh(x)
%CASE 4: THIS FUNCTION USES THE RAYLEIGH DISTRIBUTION TO CALCULATE
%THE  EXPECTED VALUE OF THE TIME SCALE FOR BACKFILLING AROUND A PILE
%WHEN THE INITIAL HOLE WAS GENERATED BY WAVES. THE TIME SCALE WHEN
%THE INITIAL HOLE WAS GENERATED BY A CURRENT (CASE 3) IS OF INTEREST FOR
%COMPARISON.

%The time is calculated for 3 different initial values of KC (KCirms),
%and plotted versus KCfrms*tfrms^2 where tfrms is calculated for the
%given KCfrms.

%DESCRIPTION OF SYMBOLS
%x: the normalized linear wave amplitude
%R1:D=0.50 m - The expected values of the time scale T*
%(col 1-5) and T(min) (col 6-9).
%R2: D=0.75 m - The expected values of the time scale T*
%(col 1-5) and T(min9) (col 6-9).
%R3 D=1.00 m - The expected values of the time scale T*
%(col 1-5) and T(min) (col 6-9).

%Et: The expected value of t  [-].
%ET: The expected value of T* [-] (CASE 3)
%ET_1, ET_2 and ET_3: The expected value of T* [-] (CASE 4)

syms x;

[n Hs h g s d50 arms c d]=Parameters();

KCirms1=11;
KCirms2=20;
KCirms3=32;

s1=2;
s2=1.45;
r1=70;
v=s2*(s1*(2-d)+1);

for j=1:3
    if j==1
        D=0.5;
    elseif j==2
        D=0.75;
```

```
else
    D=1;
end

    i=0;
for KCrms=2:0.1:13
    i=i+1;

    kp=1/h*asinh(2*pi*arms/(D*KCrms));
    wp=sqrt(g*kp*tanh(kp*h));
    Arms=arms/(sinh(kp*h));
    Urms=wp*Arms;
    trms=0.5*c*(wp*d50/12)^d*Urms^(2-d)/(g*(s-1)*d50);

    %The expected value of T*
    xmin=sqrt(log(n));
    x=(xmin:0.01:5);
    Et=trapz(x,2*n*(x).^(1-v).*exp(-(x).^2));

    %CASE 3
    ET=Et*trms^(-s1*s2)*KCrms^(-s2);

    %CASE 4
    ET_1=Et*(r1*KCrms.*(trms).^(s1)/KCirms1).^(-s2);
    ET_2=Et*(r1*KCrms.*(trms).^(s1)/KCirms2).^(-s2);
    ET_3=Et*(r1*KCrms.*(trms).^(s1)/KCirms3).^(-s2);

        %RESULTING DATA
        if D==0.5
            %T*
            R1(i,1)=KCrms*trms^2;
            R1(i,2)=ET_1;
            R1(i,3)=ET_2;
            R1(i,4)=ET_3;
            R1(i,5)=ET;
            %T
            R1(i,6)=ET_1*D^2/sqrt(g*(s-1)*d50^3)/60;
            R1(i,7)=ET_2*D^2/sqrt(g*(s-1)*d50^3)/60;
            R1(i,8)=ET_3*D^2/sqrt(g*(s-1)*d50^3)/60;
            R1(i,9)=ET*D^2/sqrt(g*(s-1)*d50^3)/60;

        elseif D==0.75
            %T*
            R2(i,1)=KCrms*trms^2;
            R2(i,2)=ET_1;
            R2(i,3)=ET_2;
            R2(i,4)=ET_3;
            R2(i,5)=ET;
            %T
```

```
                R2(i,6)=ET_1*D^2/sqrt(g*(s-1)*d50^3)/60;
                R2(i,7)=ET_2*D^2/sqrt(g*(s-1)*d50^3)/60;
                R2(i,8)=ET_3*D^2/sqrt(g*(s-1)*d50^3)/60;
                R2(i,9)=ET*D^2/sqrt(g*(s-1)*d50^3)/60;

            else
                %T*
                R3(i,1)=KCrms*trms^2;
                R3(i,2)=ET_1;
                R3(i,3)=ET_2;
                R3(i,4)=ET_3;
                R3(i,5)=ET;
                %T
                R3(i,6)=ET_1*D^2/sqrt(g*(s-1)*d50^3)/60;
                R3(i,7)=ET_2*D^2/sqrt(g*(s-1)*d50^3)/60;
                R3(i,8)=ET_3*D^2/sqrt(g*(s-1)*d50^3)/60;
                R3(i,9)=ET*D^2/sqrt(g*(s-1)*d50^3)/60;
            end
    end
end
end
```

Forristall

```
function [F1 F2 F3]=Forristall(x)
%CASE 4: THIS FUNCTION USES THE FORRISTALL DISTRIBUTION TO CALCULATE
%THE  EXPECTED VALUE OF THE TIME SCALE FOR BACKFILLING AROUND A PILE
%WHEN THE INITIAL HOLE WAS GENERATED BY WAVES. THE TIME SCALE WHEN
%THE INITIAL HOLE WAS GENERATED BY A CURRENT (CASE 3) IS OF INTEREST
%FOR COMPARISON.

%The time is calculated for 3 different initial values of KC (KCirms),
%and plotted versus KCfrms*tfrms^2 where tfrms is calculated for the
%given KCfrms.

%DESCRIPTION OF SYMBOLS
%x: the normalized nonlinear wave amplitude
%F1: D=0.50 m - The expected values of the time scale T*
%(col 1-9) and T(min) (col 10-17).
%F2: D=0.75 m - The expected values of the time scale T*
%(col 1-9) and T(min) (col 10-17).
%F3: D=1.00 m - The expected values of the time scale T*
%(col 1-9) and T in minutes (col 10-17).

%ET_2D and ET_3D: The expected value of T* [-] (CASE 3)
%ET_1_2D, ET_1_3D - ET_2_2D, ET_2_3D - ET_3_2D, ET_3_3D:
%The expected value of T* [-] (CASE 4) for each case of
```

```
%different KCirms

syms x;

[n Hs h g s d50 arms c d]=Parameters();

KCirms1=11;
KCirms2=20;
KCirms3=32;

s1=2;
s2=1.45;
r1=70;
v=s2*(s1*(2-d)+1);

for j=1:3
    if j==1
        D=0.5;
    elseif j==2
        D=0.75;
    else
        D=1;
    end

        i=0;
    for KCrms=2:0.1:13
        i=i+1;

        kp=1/h*asinh(2*pi*arms/(D*KCrms));
        wp=sqrt(g*kp*tanh(kp*h));
        Tp=2*pi/wp;
        Arms=arms/(sinh(kp*h));
        Urms=wp*Arms;
        trms=0.5*c*(wp*d50/12)^d*Urms^(2-d)/(g*(s-1)*d50);

        S1=2*pi*Hs/(g*Tp^2);
        Ur=Hs/(kp^2*h^3);

        %parameters for 2D model
        alpha2=0.3536+0.2892*S1+0.1060*Ur;
        beta2=2-2.1597*S1+0.0968*Ur^2;
        xmin_2D=sqrt(8)*alpha2*(log(n))^(1/(beta2));
        x2D=[xmin_2D:0.01:5];

        %parameters for 3D model
        alpha3=0.3536+0.2568*S1+0.0800*Ur;
        beta3=2-1.7912*S1-0.5302*Ur+0.284*Ur^2;
        xmin_3D=sqrt(8)*alpha3*(log(n))^(1/(beta3));
        x3D=[xmin_3D:0.01:5];
```

```
    %THE EXPECTED VALUE OF THE TIME SCALE T*
    Et_2D=trapz(x2D,n*beta2*(x2D).^(beta2-1-v)/((sqrt(8)*...
alpha2)^(beta2)).*exp(-((x2D)./(sqrt(8)*alpha2)).^(beta2)));
    Et_3D=trapz(x3D,n*beta3*(x3D).^(beta3-1-v)/((sqrt(8)*...
alpha3)^(beta3)).*exp(-((x3D)./(sqrt(8)*alpha3)).^(beta3)));

    %CASE 3
    ET_2D=Et_2D*trms^(-s2*s1)*KCrms^(-s2);
    ET_3D=Et_3D*trms^(-s2*s1)*KCrms^(-s2);

    %CASE 4
    ET_2D_1=Et_2D*(r1*KCrms*trms^2/KCirms1)^(-s2);
    ET_3D_1=Et_3D*(r1*KCrms*trms^2/KCirms1)^(-s2);

    ET_2D_2=Et_2D*(r1*KCrms*trms^2/KCirms2)^(-s2);
    ET_3D_2=Et_3D*(r1*KCrms*trms^2/KCirms2)^(-s2);

    ET_2D_3=Et_2D*(r1*KCrms*trms^2/KCirms3)^(-s2);
    ET_3D_3=Et_3D*(r1*KCrms*trms^2/KCirms3)^(-s2);

    %RESULTING DATA

        if D==0.5
            %T*
            F1(i,1)=KCrms*trms^2;
            F1(i,2)=ET_2D_1;
            F1(i,3)=ET_3D_1;
            F1(i,4)=ET_2D_2;
            F1(i,5)=ET_3D_2;
            F1(i,6)=ET_2D_3;
            F1(i,7)=ET_3D_3;
            F1(i,8)=ET_2D;
            F1(i,9)=ET_3D;
            %T
            F1(i,10)=ET_2D_1*D^2/sqrt(g*(s-1)*d50^3)/60;
            F1(i,11)=ET_3D_1*D^2/sqrt(g*(s-1)*d50^3)/60;
            F1(i,12)=ET_2D_2*D^2/sqrt(g*(s-1)*d50^3)/60;
            F1(i,13)=ET_3D_2*D^2/sqrt(g*(s-1)*d50^3)/60;
            F1(i,14)=ET_2D_3*D^2/sqrt(g*(s-1)*d50^3)/60;
            F1(i,15)=ET_3D_3*D^2/sqrt(g*(s-1)*d50^3)/60;
            F1(i,16)=ET_2D*D^2/sqrt(g*(s-1)*d50^3)/60;
            F1(i,17)=ET_3D*D^2/sqrt(g*(s-1)*d50^3)/60;

        elseif D==0.75
            %T*
            F2(i,1)=KCrms*trms^2;
            F2(i,2)=ET_2D_1;
            F2(i,3)=ET_3D_1;
```

```
                F2(i,4)=ET_2D_2;
                F2(i,5)=ET_3D_2;
                F2(i,6)=ET_2D_3;
                F2(i,7)=ET_3D_3;
                F2(i,8)=ET_2D;
                F2(i,9)=ET_3D;
                %T
                F2(i,10)=ET_2D_1*D^2/sqrt(g*(s-1)*d50^3)/60;
                F2(i,11)=ET_3D_1*D^2/sqrt(g*(s-1)*d50^3)/60;
                F2(i,12)=ET_2D_2*D^2/sqrt(g*(s-1)*d50^3)/60;
                F2(i,13)=ET_3D_2*D^2/sqrt(g*(s-1)*d50^3)/60;
                F2(i,14)=ET_2D_3*D^2/sqrt(g*(s-1)*d50^3)/60;
                F2(i,15)=ET_3D_3*D^2/sqrt(g*(s-1)*d50^3)/60;
                F2(i,16)=ET_2D*D^2/sqrt(g*(s-1)*d50^3)/60;
                F2(i,17)=ET_3D*D^2/sqrt(g*(s-1)*d50^3)/60;

            else
                %T*
                F3(i,1)=KCrms*trms^2;
                F3(i,2)=ET_2D_1;
                F3(i,3)=ET_3D_1;
                F3(i,4)=ET_2D_2;
                F3(i,5)=ET_3D_2;
                F3(i,6)=ET_2D_3;
                F3(i,7)=ET_3D_3;
                F3(i,8)=ET_2D;
                F3(i,9)=ET_3D;
                %T
                F3(i,10)=ET_2D_1*D^2/sqrt(g*(s-1)*d50^3)/60;
                F3(i,11)=ET_3D_1*D^2/sqrt(g*(s-1)*d50^3)/60;
                F3(i,12)=ET_2D_2*D^2/sqrt(g*(s-1)*d50^3)/60;
                F3(i,13)=ET_3D_2*D^2/sqrt(g*(s-1)*d50^3)/60;
                F3(i,14)=ET_2D_3*D^2/sqrt(g*(s-1)*d50^3)/60;
                F3(i,15)=ET_3D_3*D^2/sqrt(g*(s-1)*d50^3)/60;
                F3(i,16)=ET_2D*D^2/sqrt(g*(s-1)*d50^3)/60;
                F3(i,17)=ET_3D*D^2/sqrt(g*(s-1)*d50^3)/60;
            end
    end
end
end
```

Plot

```
function P=Plot(x)
%CASE 4: THIS FUNCTION PLOTS THE EXPECTED VALUE OF THE TIME SCALE FOR
%BACKFILLING AROUND A PILE WHEN THE INITIAL HOLE WAS GENERATED BY WAVES.
%THE TIME SCALE WHEN
```

```
%Retrieving data from the Rayleigh distibution
[R1 R2 R3]=Rayleigh();
% R1: D=0.50 m - Data for E[T*] (Col 1-5) and E[T] (Col 6-9)
% R2: D=0.75 m - Data for E[T*] (Col 1-5) and E[T] (Col 6-9)
% R3: D=1.00 m - Data for E[T*] (Col 1-5) and E[T] (Col 6-9)

%Retrieving data from the Forristall distribution
[F1 F2 F3]=Forristall();
% F1: D=0.50 m - Data for E[T*] (Col 1-9) and E[T] (Col 10-17)
% F2: D=0.75 m - Data for E[T*] (Col 1-9) and E[T] (Col 10-17)
% F3: D=1.00 m - Data for E[T*] (Col 1-9) and E[T] (Col 10-17)

%T* for D=1 m; All cases of KCi
h1=figure;
set(h1, 'Position', [5 5 700 500],'Visible','off')
h=semilogx(R3(:,1),R3(:,2),'c',F3(:,1),F3(:,2),'c--',...
                               F3(:,1),F3(:,3),'c:',...
           R3(:,1),R3(:,3),'b',F3(:,1),F3(:,4),'b--',...
                               F3(:,1),F3(:,5),'b:',...
           R3(:,1),R3(:,4),'k',F3(:,1),F3(:,6),'k--',...
                               F3(:,1),F3(:,7),'k:',...
           R3(:,1),R3(:,5),'m',F3(:,1),F3(:,8),'m--',...
                               F3(:,1),F3(:,9),'m:');
hleg=legend('Rayleigh       KC_{i r m s}=11',...
            'Forristall (2D) KC_{i r m s}=11',...
            'Forristall (3D) KC_{i r m s}=11',...
            'Rayleigh       KC_{i r m s}=20',...
            'Forristall (2D) KC_{i r m s}=20',...
            'Forristall (3D) KC_{i r m s}=20',...
            'Rayleigh       KC_{i r m s}=32',...
            'Forristall (2D) KC_{i r m s}=32',...
            'Forristall (3D) KC_{i r m s}=32',...
            'Rayleigh       KC_{i r m s}=\infty',...
            'Forristall (2D) KC_{i r m s}=\infty',...
            'Forristall (3D) KC_{i r m s}=\infty');
set (h, 'LineWidth', 2.5)
set(hleg,'Fontsize',11)
axis([0.07 0.55 0 2.2 ]);
u = [0.07 0.1 0.2 0.3 0.4 0.55];
set(gca,'XTick',u,'Fontsize',14);
xlabel('(\theta^2KC)_{f r m s}','Fontsize',22)
ylabel('E[T*]','Fontsize',22)
title('D=1 m','Fontsize',17)
hgexport(gcf,'../../Figures/CASE4/CASE41.png',...
    hgexport('factorystyle'),'Format','png')


%T* for all D and all KCi (except current)
```

```
h1=figure;
set(h1, 'Position', [5 5 700 500],'Visible','off')
h=semilogx(F1(:,1),F1(:,2),'c--',F1(:,1),F1(:,3),'c:',...
           F1(:,1),F1(:,4),'c--',F1(:,1),F1(:,5),'c:',...
           F1(:,1),F1(:,6),'c--',F1(:,1),F1(:,7),'c:',...
           F2(:,1),F2(:,2),'k--',F2(:,1),F2(:,3),'k:',...
           F2(:,1),F2(:,4),'k--',F2(:,1),F2(:,5),'k:',...
           F2(:,1),F2(:,6),'k--',F2(:,1),F2(:,7),'k:',...
           F3(:,1),F3(:,2),'m--',F3(:,1),F3(:,3),'m:',...
           F3(:,1),F3(:,4),'m--',F3(:,1),F3(:,5),'m:',...
           F3(:,1),F3(:,6),'m--',F3(:,1),F3(:,7),'m:');
hleg=legend(h([1 2 7 8 13 14]),'Forristall (2D) D=0.50 m',...
                               'Forristall (3D) D=0.50 m',...
                               'Forristall (2D) D=0.75 m',...
                               'Forristall (3D) D=0.75 m',...
                               'Forristall (2D) D=1.00 m',...
                               'Forristall (3D) D=1.00 m');
set (h, 'LineWidth', 2.5)
set(hleg,'Fontsize',13)
axis([0.07 0.55 0.01 0.35]);
u = [0.07 0.2 0.3 0.4 0.55];
set(gca,'XTick',u,'Fontsize',14);
xlabel('(\theta^2KC)_{f r m s}','Fontsize',22)
ylabel('E[T*]','Fontsize',22)
hgexport(gcf,'../../Figures/CASE4/CASE42.png',...
    hgexport('factorystyle'),'Format','png')


%T for D=0.5 m
h1=figure;
set(h1, 'Position', [5 5 700 500],'Visible','off')
h=semilogx(R1(:,1),R1(:,6),'c',F1(:,1),F1(:,10),'c--',...
                           F1(:,1),F1(:,11),'c:',...
           R1(:,1),R1(:,7),'b',F1(:,1),F1(:,12),'b--',...
                           F1(:,1),F1(:,13),'b:',...
           R1(:,1),R1(:,8),'k',F1(:,1),F1(:,14),'k--',...
                           F1(:,1),F1(:,15),'k:');
hleg=legend('Rayleigh          KC_{i r m s}=11',...
            'Forristall (2D) KC_{i r m s}=11',...
            'Forristall (3D) KC_{i r m s}=11',...
            'Rayleigh          KC_{i r m s}=20',...
            'Forristall (2D) KC_{i r m s}=20',...
            'Forristall (3D) KC_{i r m s}=20',...
            'Rayleigh          KC_{i r m s}=32',...
            'Forristall (2D) KC_{i r m s}=32',...
            'Forristall (3D) KC_{i r m s}=32');
set(hleg,'Fontsize',13)
      set (h, 'LineWidth', 2.5)
axis([0.07 0.55 0 23]);
```

```
u = [0.07 0.1 0.2 0.3 0.4 0.55];
set(gca,'XTick',u,'Fontsize',14);
xlabel('(\theta^2KC)_{f r m s}','Fontsize',22)
ylabel('E[T]','Fontsize',22)
title('D=0.5 m','Fontsize',17)
hgexport(gcf,'../../Figures/CASE4/CASE4T1.png',...
    hgexport('factorystyle'),'Format','png')


%T for D=1 m
h1=figure;
set(h1, 'Position', [5 5 700 500],'Visible','off')
h=semilogx(R2(:,1),R2(:,6),'c',F2(:,1),F2(:,10),'c--',...
                               F2(:,1),F2(:,11),'c:',...
           R2(:,1),R2(:,7),'b',F2(:,1),F2(:,12),'b--',...
                               F2(:,1),F2(:,13),'b:',...
           R2(:,1),R2(:,8),'k',F2(:,1),F2(:,14),'k--',...
                               F2(:,1),F2(:,15),'k:');
hleg=legend('Rayleigh          KC_{i r m s}=11',...
            'Forristall (2D) KC_{i r m s}=11',...
            'Forristall (3D) KC_{i r m s}=11',...
            'Rayleigh          KC_{i r m s}=20',...
            'Forristall (2D) KC_{i r m s}=20',...
            'Forristall (3D) KC_{i r m s}=20',...
            'Rayleigh          KC_{i r m s}=32',...
            'Forristall (2D) KC_{i r m s}=32',...
            'Forristall (3D) KC_{i r m s}=32');
set(hleg,'Fontsize',13)
     set (h, 'LineWidth', 2.5)
axis([0.07 0.55 0 53 ]);
u = [0.07 0.1 0.2 0.3 0.4 0.55];
set(gca,'XTick',u,'Fontsize',14);
xlabel('(\theta^2KC)_{f r m s}','Fontsize',22)
ylabel('E[T]','Fontsize',22)
title('D=1 m','Fontsize',17)
hgexport(gcf,'../../Figures/CASE4/CASE4T3.png',...
    hgexport('factorystyle'),'Format','png')
end
```

B. 5 - CASE 5

wc1

```
function x1=wc1()
%CASE 5: THIS FUNCTION FINDS THE LOWER VALUE OF wc FOR EACH
%VALUE OF Ucwrms.
```

```
%The highest value of wcmin is 1 and will appear when
%Ucwrms=0.7. When Ucwrms decreases, the denominator can
%be higher before "ledd" equals 0.7. This means that
%wcmin will decrease for decreases value of Ucrwms.

    l=0;
for Ucwrms=0:0.01:0.7
    j=0;
    l=l+1;
    for x=1:-0.001:0
        ledd=Ucwrms./(x.*(1-Ucwrms)+Ucwrms);
        if ledd>=0.7
            j=j+1;
            x=x-0.001;

            if j==1;
                x=x+0.002;
               x1(l,1)=x;
            end
        end
    end
end
end
```

Rayleigh

```
function [R R1 R2 R3]=Rayleigh(x)
%CASE 5: THIS FUNCTION USES THE RAYLEIGH DISTRIBUTION TO CALCULATE
%THE EXPECTED VALUE OF THE TIME SCALE FOR BACKFILLING IN WAVES +
%CURRENT AROUND A SLENDER VERTICAL PILE WHEN THE INITAL HOLE WAS
%GENERATED BY A CURRENT. THE TIME SCALE IS CALCULATED FOR DIFFERENT
%VALUES OF THE CURRENT WAVE VELOCITY (Ucwrms).

%When the time scale exceeds the value of waves alone (CASE 3),
%the time scale takes this value. The time scale is shown for 3
%different values of (KCrms, trms). T* is independent of D for
%Rayleigh because trms is given. %Since trms is given, the grain
%size (z0,d50) will change for each value of KCrms. To find T when
%knowing T*, z0 must be calulated.

%DESCRIPTION OF SYMBOLS
%x: the normalized linear wave amplitude
%R: The expected value of the time scale T* is
%R1: D=0.50 m - The expeced value of the time scale T (min).
%R2: D=0.75 m - The expeced value of the time scale T (min).
%R3: D=1.00 m - The expeced value of the time scale T (min).
```

```
%Et: The expected value of t  [-].
%ET1: The expected value of T* [-] (CASE 3).
%ET2: The expected value of T* [-] (CASE 5).

syms x;

[n Hs h g s d50 arms c d]=Parameters();
[x1]=wc1();

KCrms1=4;
KCrms2=7;
KCrms3=4;

trms1=0.07;
trms2=0.07;
trms3=0.09;

%CASE 3
s1=2;
s2=1.45;
v=s2*(s1*(2-d)+1);

xmin=sqrt(log(n));
x=(xmin:0.01:5);
Et=trapz(x,2*n*(x).^(1-v).*exp(-(x).^2));

ET11=Et*trms1^(-s1*s2)*KCrms1^(-s2);
ET12=Et*trms2^(-s1*s2)*KCrms2^(-s2);
ET13=Et*trms3^(-s1*s2)*KCrms3^(-s2);

%CASE 5
s1=2;

for l=1:3
    if l==1
        D=0.5;
    elseif l==2
        D=0.75;
    else
        D=1;
    end

    for i=1:3
        if i==1;
           KCrms=KCrms1;
           trms=trms1;
        elseif i==2
            KCrms=KCrms2;
```

```
        trms=trms2;
    else
        KCrms=KCrms3;
        trms=trms3;
    end

    kp=1/h*asinh(2*pi*arms/(D*KCrms));
    wr=sqrt(g*kp*tanh(kp*h));
    Urms=wr*arms/(sinh(kp*h));

        j=0;
    for Ucwrms=0:0.01:0.7
        j=j+1;

        Uc=Ucwrms*Urms/(1-Ucwrms);
        wp=Uc*kp+sqrt(g*kp*tanh(kp*h));

        z0_1=(24/(wp^d)*trms1*g*(s-1)/(c*Urms^(2-d)))^(1/(d-1));
        z0_2=(24/(wp^d)*trms2*g*(s-1)/(c*Urms^(2-d)))^(1/(d-1));
        z0_3=(24/(wp^d)*trms3*g*(s-1)/(c*Urms^(2-d)))^(1/(d-1));

        x1n=sqrt(log(n)+(x1(j))^2);
        x=[x1n:0.001:5];
        pd=2*n.*x.*exp((x1(j)).^2-(x).^2);
        ET=trapz(x,pd.*(1.9-(0.65./(nthroot((trms.^(s1).*...
        KCrms.*x.^(s1*(2-d)+1)-0.01).^(42),25))+2).*...
        (Ucwrms./(x.*(1-Ucwrms)+Ucwrms)-0.7)));

        if i==1;
           ET2(j,1)=ET;
        elseif i==2;
           ET2(j,2)=ET;
        else
           ET2(j,3)=ET;
        end
    end
end


%COMPARING VALUES
for i=1:71 %if the value from CASE 5 exceeds the value from
%CASE 3, T* takes the value of CASE 3.

    if ET2(i,1)>ET11;
       ET_1(i,1)=ET11;
    else
       ET_1(i,1)=ET2(i,1);
    end
```

```
        if ET2(i,2)>ET12;
           ET_2(i,1)=ET12;
        else
           ET_2(i,1)=ET2(i,2);
        end

        if ET2(i,3)>ET13;
           ET_3(i,1)=ET13;
        else
           ET_3(i,1)=ET2(i,3);
        end
    end

    %RESULTING DATA OF T*
    R(:,1)=(0:0.01:0.7);
    R(:,2)=ET_1;
    R(:,3)=ET_2;
    R(:,4)=ET_3;

    %RESULTING DATA OF T
    if D==0.5
       R1(:,1)=(0:0.01:0.7);
       R1(:,2)=ET_1*0.5^2/(sqrt(g*(s-1)*(12*z0_1)^3))/60;
       R1(:,3)=ET_2*0.5^2/(sqrt(g*(s-1)*(12*z0_2)^3))/60;
       R1(:,4)=ET_3*0.5^2/(sqrt(g*(s-1)*(12*z0_3)^3))/60;

    elseif D==0.75
       R2(:,1)=(0:0.01:0.7);
       R2(:,2)=ET_1*0.75^2/(sqrt(g*(s-1)*(12*z0_1)^3))/60;
       R2(:,3)=ET_2*0.75^2/(sqrt(g*(s-1)*(12*z0_2)^3))/60;
       R2(:,4)=ET_3*0.75^2/(sqrt(g*(s-1)*(12*z0_3)^3))/60;

    else
       R3(:,1)=(0:0.01:0.7);
       R3(:,2)=ET_1*1^2/(sqrt(g*(s-1)*(12*z0_1)^3))/60;
       R3(:,3)=ET_2*1^2/(sqrt(g*(s-1)*(12*z0_2)^3))/60;
       R3(:,4)=ET_3*1^2/(sqrt(g*(s-1)*(12*z0_3)^3))/60;
    end
end
end
```

Forristall

```
function [F1 F2 F3]=Forristall(x)
%CASE 5: THIS FUNCTION USES THE FORRISTALL DISTRIBUTION TO CALCULATE
%THE EXPECTED VALUE OF THE TIME SCALE FOR BACKFILLING IN WAVES +
%CURRENT AROUND A SLENDER VERTICAL PILE WHEN THE INITAL HOLE WAS
```

```
%GENERATED BY A CURRENT. THE TIME SCALE IS CALCULATED FOR DIFFERENT
%VALUES OF THE CURRENT WAVE VELOCITY (Ucwrms).

%When the time scale exceeds the value of waves alone (CASE 3),
%the time scale takes this value. The time scale is shown for 3
%different values of (KCrms, trms). Since trms is given, the grain
%size (z0,d50) will change for each value of KCrms. To find T when
%knowing T*, z0 must be calulated.

%DESCRIPTION OF SYMBOLS
%x: The normalized second-order wave crest.
%F1: D=0.50 m - The expected values of the time scale T*
%(col 1-7) and T(min) (col 8-13).
%F2: D=0.75 m - The expected value of the time scale T*
%(col 1-7) and T in minutes (col 8-13).
%F3: D=1.00 m - The expected value of the time scale T*
%(col 1-7) and T(min) (col 8-13).

%Et: The expected value of t  [-].
%ET1: The expected value of T* [-] (CASE 3).
%ET2: The expected value of T* [-] (CASE 5).
syms x;

[n Hs h g s d50 arms c d]=Parameters();
[x1]=wc1();

KCrms1=4;
KCrms2=7;
KCrms3=4;

trms1=0.07;
trms2=0.07;
trms3=0.09;

for l=1:3
    if l==1
       D=0.5;
    elseif l==2
       D=0.75;
    else
       D=1;
    end

    for i=1:3
        if i==1;
           KCrms=KCrms1;
           trms=trms1;
        elseif i==2;
            KCrms=KCrms2;
```

```
    trms=trms2;
else
    KCrms=KCrms3;
    trms=trms3;
end

kp=1/h*asinh(2*pi*arms/(D*KCrms));
wr=sqrt(g*kp*tanh(kp*h));
Urms=wr*arms/(sinh(kp*h));

    j=0;
for Ucwrms=0:0.01:0.7
    j=j+1;

    %CASE 3
    S1=2*pi*Hs/(g*(2*pi/wr)^2);
    Ur=Hs/(kp^2*h^3);

    %parameters 2D model
    alpha2=0.3536+0.2892*S1+0.1060*Ur;
    beta2=2-2.1597*S1+0.0968*Ur^2;
    xmin_2D=sqrt(8)*alpha2*(log(n))^(1/(beta2));
    x2D=(xmin_2D:0.001:5);

    %parameters 3D model
    alpha3=0.3536+0.2568*S1+0.0800*Ur;
    beta3=2-1.7912*S1-0.5302*Ur+0.284*Ur^2;
    xmin_3D=sqrt(8)*alpha3*(log(n))^(1/(beta3));
    x3D=(xmin_3D:0.001:5);

    %CASE 3
    s1=2;
    s2=1.45;
    v=s2*(s1*(2-d)+1);

    Et1_2D=trapz(x2D,n*beta2*(x2D).^(beta2-1-v)/...
    ((sqrt(8)*alpha2)^(beta2)).*exp(-((x2D)./...
    (sqrt(8)*alpha2)).^(beta2)));

    Et1_3D=trapz(x3D,n*beta3*(x3D).^(beta3-1-v)/...
    ((sqrt(8)*alpha3)^(beta3)).*exp(-((x3D)./...
    (sqrt(8)*alpha3)).^(beta3)));

    ET1_2D=Et1_2D*trms^(-s1*s2)*KCrms^(-s2);
    ET1_3D=Et1_3D*trms^(-s1*s2)*KCrms^(-s2);

    if i==1
       ET11_2D(1,j)=ET1_2D;
       ET11_3D(1,j)=ET1_3D;
```

```
elseif i==2
   ET12_2D(1,j)=ET1_2D;
   ET12_3D(1,j)=ET1_3D;
else
   ET13_2D(1,j)=ET1_2D;
   ET13_3D(1,j)=ET1_3D;
end

%CASE 5
s1=2;
Uc=Ucwrms*Urms/(1-Ucwrms);
wp=Uc*kp+sqrt(g*kp*tanh(kp*h));
Tp=2*pi/wp;

z0_1=(24/(wp^d)*trms1*g*(s-1)/(c*Urms^(2-d)))^(1/(d-1));
z0_2=(24/(wp^d)*trms2*g*(s-1)/(c*Urms^(2-d)))^(1/(d-1));
z0_3=(24/(wp^d)*trms3*g*(s-1)/(c*Urms^(2-d)))^(1/(d-1));

S1=2*pi*Hs/(g*(2*pi/wp)^2);
Ur=Hs/(kp^2*h^3);

%parameters 2D model
alpha2=0.3536+0.2892*S1+0.1060*Ur;
beta2=2-2.1597*S1+0.0968*Ur^2;
xmin_2D=sqrt(8)*alpha2*(log(n))^(1/(beta2));
x2D=(xmin_2D:0.001:5);

%parameters 3D model
alpha3=0.3536+0.2568*S1+0.0800*Ur;
beta3=2-1.7912*S1-0.5302*Ur+0.284*Ur^2;
xmin_3D=sqrt(8)*alpha3*(log(n))^(1/(beta3));
x3D=(xmin_3D:0.001:5);

for y=1:2
    if y==1
       alpha=alpha2;
       beta=beta2;
    else
       alpha=alpha3;
       beta=beta3;
    end

    x1n=sqrt(8)*alpha*((x1(j)/(sqrt(8)*alpha))...
    ^(beta)+log(n))^(1/beta);
    x=(x1n:0.001:5);
    pd=(n*(1/(sqrt(8)*alpha))^(beta)*beta.*x.^...
    (beta-1).*exp((x1(j)/(sqrt(8)*alpha))^(beta))...
    .*exp(-(x./(sqrt(8)*alpha)).^beta));
```

```
            ET2=trapz(x,pd.*(1.9-(0.65./(nthroot((trms.^...
            (s1).*KCrms.*x.^(s1*(2-d)+1)-0.01).^(42),25))+2).*...
            ((Ucwrms./(x.*(1-Ucwrms)+Ucwrms))-0.7)));

            %Writes data for 2D
            if y==1;
               if i==1
                  ET21_2D(1,j)=ET2;
               elseif i==2
                  ET22_2D(1,j)=ET2;
               else
                  ET23_2D(1,j)=ET2;
               end

            %Writes data for 3D
            else
                if i==1
                   ET21_3D(1,j)=ET2;
                elseif i==2
                   ET22_3D(1,j)=ET2;
                else
                   ET23_3D(1,j)=ET2;
                end
            end
        end
    end
end

%LOOP COMPARING BACKFILLING WAVES/WAVES+CURRENT
for j=1:71
    if ET21_2D(1,j)>ET11_2D(1,j)  %example 1
       ET_2D_1(1,j)=ET11_2D(1,j);
    else
       ET_2D_1(1,j)=ET21_2D(1,j);
    end

    if ET21_3D(1,j)>ET11_3D(1,j);
       ET_3D_1(1,j)=ET11_3D(1,j);
    else
       ET_3D_1(1,j)=ET21_3D(1,j);
    end

    if ET22_2D(1,j)>ET12_2D(1,j)  %example 2
       ET_2D_2(1,j)=ET12_2D(1,j);
    else
       ET_2D_2(1,j)=ET22_2D(1,j);
    end

    if ET22_3D(1,j)>ET12_3D(1,j);
```

```
        ET_3D_2(1,j)=ET12_3D(1,j);
    else
        ET_3D_2(1,j)=ET22_3D(1,j);
    end

    if ET23_2D(1,j)>ET13_2D(1,j)  %example 3
        ET_2D_3(1,j)=ET13_2D(1,j);
    else
        ET_2D_3(1,j)=ET23_2D(1,j);
    end

    if ET23_3D(1,j)>ET13_3D(1,j);
        ET_3D_3(1,j)=ET13_3D(1,j);
    else
        ET_3D_3(1,j)=ET23_3D(1,j);
    end
end

%RESULTING DATA
if D==0.5
   F1(:,1)=(0:0.01:0.7);
   F1(:,2)=ET_2D_1;
   F1(:,3)=ET_3D_1;
   F1(:,4)=ET_2D_2;
   F1(:,5)=ET_3D_2;
   F1(:,6)=ET_2D_3;
   F1(:,7)=ET_3D_3;

   F1(:,8)=ET_2D_1*0.5^2/(sqrt(g*(s-1)*(12*z0_1)^3))/60;
   F1(:,9)=ET_3D_1*0.5^2/(sqrt(g*(s-1)*(12*z0_1)^3))/60;
   F1(:,10)=ET_2D_2*0.5^2/(sqrt(g*(s-1)*(12*z0_2)^3))/60;
   F1(:,11)=ET_3D_2*0.5^2/(sqrt(g*(s-1)*(12*z0_2)^3))/60;
   F1(:,12)=ET_2D_3*0.5^2/(sqrt(g*(s-1)*(12*z0_3)^3))/60;
   F1(:,13)=ET_3D_3*0.5^2/(sqrt(g*(s-1)*(12*z0_3)^3))/60;

elseif D==0.75
   F2(:,1)=(0:0.01:0.7);
   F2(:,2)=ET_2D_1;
   F2(:,3)=ET_3D_1;
   F2(:,4)=ET_2D_2;
   F2(:,5)=ET_3D_2;
   F2(:,6)=ET_2D_3;
   F2(:,7)=ET_3D_3;

   F2(:,8)=ET_2D_1*0.75^2/(sqrt(g*(s-1)*(12*z0_1)^3))/60;
   F2(:,9)=ET_3D_1*0.75^2/(sqrt(g*(s-1)*(12*z0_1)^3))/60;
   F2(:,10)=ET_2D_2*0.75^2/(sqrt(g*(s-1)*(12*z0_2)^3))/60;
   F2(:,11)=ET_3D_2*0.75^2/(sqrt(g*(s-1)*(12*z0_2)^3))/60;
   F2(:,12)=ET_2D_3*0.75^2/(sqrt(g*(s-1)*(12*z0_3)^3))/60;
```

```
        F2(:,13)=ET_3D_3*0.75^2/(sqrt(g*(s-1)*(12*z0_3)^3))/60;

    else
        F3(:,1)=(0:0.01:0.7);
        F3(:,2)=ET_2D_1;
        F3(:,3)=ET_3D_1;
        F3(:,4)=ET_2D_2;
        F3(:,5)=ET_3D_2;
        F3(:,6)=ET_2D_3;
        F3(:,7)=ET_3D_3;

        F3(:,8)=ET_2D_1*1^2/(sqrt(g*(s-1)*(12*z0_1)^3))/60;
        F3(:,9)=ET_3D_1*1^2/(sqrt(g*(s-1)*(12*z0_1)^3))/60;
        F3(:,10)=ET_2D_2*1^2/(sqrt(g*(s-1)*(12*z0_2)^3))/60;
        F3(:,11)=ET_3D_2*1^2/(sqrt(g*(s-1)*(12*z0_2)^3))/60;
        F3(:,12)=ET_2D_3*1^2/(sqrt(g*(s-1)*(12*z0_3)^3))/60;
        F3(:,13)=ET_3D_3*1^2/(sqrt(g*(s-1)*(12*z0_3)^3))/60;
    end
end
end
```

Plot

```
function P=Plot(x)
%CASE 5: THIS FUNCTION USES PLOTS THE TIME SCALE FOR BACKFILLING IN
%WAVES + CURRENT AROUND A SLENDER VERTICAL PILE WHEN THE INITAL HOLE
%WAS GENERATED BY A CURRENT, FOR DIFFERENT VALUES OF Ucwrms.

%Retrieving data from the Rayleigh distibution
[R R1 R2 R3]=Rayleigh();
% R:  Data for of E[T*].
% R1: D=0.50 m - Data for E[T].
% R2: D=0.75 m - Data for E[T].
% R3: D=1.00 m - Data for E[T].

%Retrieving data from the Forristall distibution
[F1 F2 F3]=Forristall();
% F1: D=0.50 m - Data for E[T*] (Col 1-7) and E[T] (Col 8-13).
% F2: D=0.75 m - Data for E[T*] (Col 1-7) and E[T] (Col 8-13).
% F3: D=1.00 m - Data for E[T*] (Col 1-7) and E[T] (Col 8-13).

%T* for D=0.5 m
h1=figure;
set(h1, 'Position', [5 5 700 500],'Visible','off')
h=plot(R(:,1),R(:,2),'b',F1(:,1),F1(:,2),'b--',...
                         F1(:,1),F1(:,3),'b:',...
       R(:,1),R(:,3),'k',F1(:,1),F1(:,4),'k--',...
```

```
                        F1(:,1),F1(:,5),'k:',...
       R(:,1),R(:,4),'m',F1(:,1),F1(:,6),'m--',...
                        F1(:,1),F1(:,7),'m:');
hleg=legend('Rayleigh      \theta_{rms1}, KC_{rms1}',...
            'Forristall 2D \theta_{rms1}, KC_{rms1}', ...
            'Forristall 3D \theta_{rms1}, KC_{rms1}',...
            'Rayleigh      \theta_{rms2}, KC_{rms2}',...
            'Forristall 2D \theta_{rms2}, KC_{rms2}', ...
            'Forristall 3D \theta_{rms2}, KC_{rms2}',...
            'Rayleigh      \theta_{rms3}, KC_{rms3}',...
            'Forristall 2D \theta_{rms3}, KC_{rms3}', ...
            'Forristall 3D \theta_{rms3}, KC_{rms3}');
set(hleg,'Fontsize',10)
set (h, 'LineWidth', 2.5)
axis([0 0.7 0 18])
u = [0 0.1 0.2 0.3 0.4 0.5 0.6 0.7];
set(gca,'XTick',u);
u = [0 2 4 6 8 10 12 14 16 18];
set(gca,'YTick',u,'Fontsize',14);
xlabel('U_{cwrms}','Fontsize',22)
ylabel('E[T*]','Fontsize',22)
title('D=0.5 m','Fontsize',17);
hgexport(gcf,'../../Figures/CASE5/CASE5_D=0.5.png',...
    hgexport('factorystyle'), 'Format', 'png')


%T* for D=1 m
h1=figure;
set(h1, 'Position', [5 5 700 500],'Visible','off')
h=plot(R(:,1),R(:,2),'b',F3(:,1),F3(:,2),'b--',...
                        F3(:,1),F3(:,3),'b:',...
       R(:,1),R(:,3),'k',F3(:,1),F3(:,4),'k--',...
                        F3(:,1),F3(:,5),'k:',...
       R(:,1),R(:,4),'m',F3(:,1),F3(:,6),'m--',...
                        F3(:,1),F3(:,7),'m:');
hleg=legend('Rayleigh      \theta_{rms1}, KC_{rms1}',...
            'Forristall 2D \theta_{rms1}, KC_{rms1}', ...
            'Forristall 3D \theta_{rms1}, KC_{rms1}',...
            'Rayleigh      \theta_{rms2}, KC_{rms2}',...
            'Forristall 2D \theta_{rms2}, KC_{rms2}', ...
            'Forristall 3D \theta_{rms2}, KC_{rms2}',...
            'Rayleigh      \theta_{rms3}, KC_{rms3}',...
            'Forristall 2D \theta_{rms3}, KC_{rms3}',...
            'Forristall 3D \theta_{rms3}, KC_{rms3}');
set(hleg,'Fontsize',10)
set (h, 'LineWidth', 2.5)
axis([0 0.7 0 18])
u = [0 0.1 0.2 0.3 0.4 0.5 0.6 0.7];
set(gca,'XTick',u);
```

```
u = [0 2 4 6 8 10 12 14 16 18];
set(gca,'YTick',u,'Fontsize',14);
xlabel('U_{cwrms}','Fontsize',22)
ylabel('E[T*]','Fontsize',22)
title('D=1.0','Fontsize',17);
hgexport(gcf,'../../Figures/CASE5/CASE5_D=1.png',...
    hgexport('factorystyle'), 'Format', 'png')


%T for ex 1, D=0.5 m, D=0.75 m and D=1 m
h1=figure;
set(h1, 'Position', [5 5 700 500],'Visible','off')
h=plot(R1(:,1),R1(:,2),'c',F1(:,1),F1(:,8),'c--',...
                           F1(:,1),F1(:,9),'c:',...
       R2(:,1),R2(:,2),'k',F2(:,1),F2(:,8),'k--',...
                           F2(:,1),F2(:,9),'k:',...
       R3(:,1),R3(:,2),'m',F3(:,1),F3(:,8),'m--',...
                           F3(:,1),F3(:,9),'m:');
hleg=legend('Rayleigh       D=0.50 m','Forristall 2D D=0.50 m',...
                                      'Forristall 3D D=0.50 m',...
            'Rayleigh       D=0.75 m','Forristall 2D D=0.75 m',...
                                      'Forristall 3D D=0.75 m',...
            'Rayleigh       D=1.00 m','Forristall 2D D=1.00 m',...
                                      'Forristall 3D D=1.00 m');
set(hleg,'Fontsize',10)
set (h, 'LineWidth', 2.5)
axis([0 0.7 0 100])
u = [0 0.1 0.2 0.3 0.4 0.5 0.6 0.7];
set(gca,'XTick',u,'Fontsize',14);
xlabel('U_{cwrms}','Fontsize',22)
ylabel('E[T]','Fontsize',22)
title('KC_{rms}=4, \theta_{rms}=0.07','Fontsize',17);
hgexport(gcf,'../../Figures/CASE5/CASE51_T.png',...
    hgexport('factorystyle'), 'Format', 'png')


%T for ex 2, D=0.5 m, D=0.75 m and D=1 m
h1=figure;
set(h1, 'Position', [5 5 700 500],'Visible','off')
h=plot(R1(:,1),R1(:,3),'c',F1(:,1),F1(:,10),'c--',...
                           F1(:,1),F1(:,11),'c:',...
       R2(:,1),R2(:,3),'k',F2(:,1),F2(:,10),'k--',...
                           F2(:,1),F2(:,11),'k:',...
       R3(:,1),R3(:,3),'m',F3(:,1),F3(:,10),'m--',...
                           F3(:,1),F3(:,11),'m:');
hleg=legend('Rayleigh       D=0.50 m','Forristall 2D D=0.50 m',...
                                      'Forristall 3D D=0.50 m',...
            'Rayleigh       D=0.75 m','Forristall 2D D=0.75 m',...
                                      'Forristall 3D D=0.75 m',...
```

```
            'Rayleigh       D=1.00 m','Forristall 2D D=1.00 m',...
                                       'Forristall 3D D=1.00 m');
set(hleg,'Fontsize',10)
set (h, 'LineWidth', 2.5)
axis([0 0.7 0 52])
u = [0 0.1 0.2 0.3 0.4 0.5 0.6 0.7];
set(gca,'XTick',u,'Fontsize',14);
xlabel('U_{cwrms}','Fontsize',22)
ylabel('E[T]','Fontsize',22)
title('KC_{rms}=7, \theta_{rms}=0.07','Fontsize',17);
hgexport(gcf,'../../Figures/CASE5/CASE52_T.png',...
    hgexport('factorystyle'), 'Format', 'png')


%T for ex 3, D=0.5 m, D=0.75 m and D=1 m
h1=figure;
set(h1, 'Position', [5 5 700 500],'Visible','off')
h=plot(R1(:,1),R1(:,4),'c',F1(:,1),F1(:,12),'c--',...
                           F1(:,1),F1(:,13),'c:',...
       R2(:,1),R2(:,4),'k',F2(:,1),F2(:,12),'k--',...
                           F2(:,1),F2(:,13),'k:',...
       R3(:,1),R3(:,4),'m',F3(:,1),F3(:,12),'m--',...
                           F3(:,1),F3(:,13),'m:');
hleg=legend('Rayleigh       D=0.50 m','Forristall 2D D=0.50 m',...
                                      'Forristall 3D D=0.50 m',...
            'Rayleigh       D=0.75 m','Forristall 2D D=0.75 m',...
                                      'Forristall 3D D=0.75 m',...
            'Rayleigh       D=1.00 m','Forristall 2D D=1.00 m',...
                                      'Forristall 3D D=1.00 m');
set(hleg,'Fontsize',10)
set (h, 'LineWidth', 2.5)
axis([0 0.7 0 110])
u = [0 0.1 0.2 0.3 0.4 0.5 0.6 0.7];
set(gca,'XTick',u,'Fontsize',14);
xlabel('U_{cwrms}','Fontsize',22)
ylabel('E[T]','Fontsize',22)
title('KC_{rms}=4, \theta_{rms}=0.09','Fontsize',17);
hgexport(gcf,'../../Figures/CASE5/CASE53_T.png',...
    hgexport('factorystyle'), 'Format', 'png')
end
```

B. 6 - CASE 6

wc1

```
function x1=wc1()
```

```
%CASE 6: THIS FUNCTION FINDS THE LOWER VALUE OF wc FOR EACH
%VALUE OF Ucwrms.

%The highest value of wcmin is 1 and will appear when
%Ucwrms=0.7. When Ucwrms decreases, the denominator can
%be higher before "ledd" equals 0.7. This means that
%wcmin will decrease for decreases value of Ucrwms.

    l=0;
for Ucwrms=0:0.01:0.7
    j=0;
    l=l+1;
    for x=1:-0.001:0
        ledd=Ucwrms./(x.*(1-Ucwrms)+Ucwrms);
        if ledd>=0.7
            j=j+1;
            x=x-0.001;

            if j==1;
                x=x+0.002;
               x1(l,1)=x;
            end
        end
    end
end
end
```

Rayleigh

```
function [R R1 R2 R3]=Rayleigh(x)
%CASE 6: THIS FUNCTION USES THE RAYLEIGH DISTRIBUTION TO CALCULATE
%THE EXPECTED VALUE OF THE TIME SCALE FOR BACKFILLING IN WAVES +
%CURRENT AROUND A LARGE VERTICAL PILE WHEN THE INITAL HOLE WAS
%GENERATED BY A CURRENT. THE TIME SCALE IS CALCULATED FOR DIFFERENT
%VALUES OF THE CURRENT WAVE VELOCITY (Ucwrms).

%The time scale is shown for 2 different values of (KCrms, trms).
%T* is independent of D for Rayleigh because trms is given.
%Since trms is given, the grain size (z0,d50) will change
%for each value of KCrms. To find T when knowing T*, z0 must be
%calulated.

%DESCRIPTION OF SYMBOLS
%x: the normalized linear wave amplitude
%R: The expected value of the time scale T*
%R1: D=3 m - The expeced value of the time scale T (min).
%R2: D=4 m - The expeced value of the time scale T (min).
```

```
%R3: D=5 m - The expeced value of the time scale T (min).

%ET: The expected value of T* [-].

syms x;

[n Hs h g s d50 arms c d]=Parameters();
[x1]=wc1();

KCrms1=0.7;
trms1=0.101;

KCrms2=1.5;
trms2=0.105;

s1=2.38;

for D=3:5

    for i=1:2

        if i==1;
           KCrms=KCrms1;
        else
           KCrms=KCrms2;
        end

        kp=1/h*asinh(2*pi*arms/(D*KCrms));
        wr=sqrt(g*kp*tanh(kp*h));
        Urms=wr*arms/(sinh(kp*h));

            j=0;
        for Ucwrms=0:0.01:0.7
            j=j+1;

            Uc=Ucwrms*Urms/(1-Ucwrms);
            wp=Uc*kp+sqrt(g*kp*tanh(kp*h));

            z0_1=(24/(wp^d)*trms1*g*(s-1)/(c*Urms^(2-d)))^(1/(d-1));
            z0_2=(24/(wp^d)*trms2*g*(s-1)/(c*Urms^(2-d)))^(1/(d-1));

            x1n=sqrt(log(n)+(x1(j))^2);

            x=(x1n:0.001:5);
            pd=2*n.*x.*exp((x1(j)).^2-(x).^2);

            ET=trapz(x,pd.*(-15.15./((KCrms.*x).^(s1))).*...
            (Ucwrms./(x.*(1-Ucwrms)+Ucwrms)-0.7));
```

```
            %RESULTING DATA

               R(j,1)=Ucwrms;
            if i==1;
               R(j,2)=ET;
            else
               R(j,3)=ET;
            end

            if D==3
               R1(j,1)=Ucwrms;
               if i==1;
               R1(j,2)=ET*D^2/(sqrt(g*(s-1)*(12*z0_1)^3))/60;
               else
               R1(j,3)=ET*D^2/(sqrt(g*(s-1)*(12*z0_2)^3))/60;
               end

            elseif D==4
               R2(j,1)=Ucwrms;
               if i==1;
               R2(j,2)=ET*D^2/(sqrt(g*(s-1)*(12*z0_1)^3))/60;
               else
               R2(j,3)=ET*D^2/(sqrt(g*(s-1)*(12*z0_2)^3))/60;
               end

            else
               R3(j,1)=Ucwrms;
               if i==1;
               R3(j,2)=ET*D^2/(sqrt(g*(s-1)*(12*z0_1)^3))/60;
               else
               R3(j,3)=ET*D^2/(sqrt(g*(s-1)*(12*z0_2)^3))/60;
               end
            end
         end
      end
end
end
```

Forristall

```
function [F1 F2 F3]=Forristall(x)
%CASE 6: THIS FUNCTION USES THE FORRISTALL DISTRIBUTION TO CALCULATE
%THE EXPECTED VALUE OF THE TIME SCALE FOR BACKFILLING IN WAVES +
%CURRENT AROUND A LARGE VERTICAL PILE WHEN THE INITAL HOLE WAS
%GENERATED BY A CURRENT. THE TIME SCALE IS CALCULATED FOR DIFFERENT
%VALUES OF THE CURRENT WAVE VELOCITY (Ucwrms).
```

```
%The time scale is shown for 2 different values of (KCrms, trms).
%Since trms is given, the grain  size (z0,d50) will change for each
%value of KCrms. To find T when knowing T*, z0 must be calulated.

%DESCRIPTION OF SYMBOLS
%x: The normalized second-order wave crest.
%F1: D=0.50 m - The expected values of the time scale T*
%(col 1-5) and T(min) (col 6-9).
%F2: D=0.75 m - The expected value of the time scale T*
%(col 1-5) and T in minutes (col 6-9).
%F3: D=1.00 m - The expected value of the time scale T*
%(col 1-5) and T(min) (col 6-9).

%Et: The expected value of t  [-].
%ET: The expected value of T* [-].

syms x;

[n Hs h g s d50 arms c d]=Parameters();
[x1]=wc1();

s1=2.38;

KCrms1=0.7;
trms1=0.101;

KCrms2=1.5;
trms2=0.105;

for D=3:1:5

    for i=1:2
        if i==1;
        KCrms=KCrms1;
        else
        KCrms=KCrms2;
        end

        kp=1/h*asinh(2*pi*arms/(D*KCrms));
        wr=sqrt(g*kp*tanh(kp*h));
        Urms=wr*arms/(sinh(kp*h));

            j=0;
        for Ucwrms=0:0.01:0.7
            j=j+1;

            Uc=Ucwrms*Urms/(1-Ucwrms);
            wp=Uc*kp+sqrt(g*kp*tanh(kp*h));
            Tp=2*pi/wp;
```

```
z0_1=(24/(wp^d)*trms1*g*(s-1)/(c*Urms^(2-d)))^(1/(d-1));
z0_2=(24/(wp^d)*trms2*g*(s-1)/(c*Urms^(2-d)))^(1/(d-1));

S1=2*pi*Hs/(g*Tp^2);
Ur=Hs/(kp^2*h^3);

%parameters 2D model
alpha2=0.3536+0.2892*S1+0.1060*Ur;
beta2=2-2.1597*S1+0.0968*Ur^2;

%parameters 3D model
alpha3=0.3536+0.2568*S1+0.0800*Ur;
beta3=2-1.7912*S1-0.5302*Ur+0.284*Ur^2;

for y=1:2
    if y==1
    alpha=alpha2;
    beta=beta2;
    else
    alpha=alpha3;
    beta=beta3;
    end

    x1n=sqrt(8)*alpha*((x1(j)/(sqrt(8)*alpha))^...
    (beta)+log(n))^(1/beta);
    x=(x1n:0.001:5);

    pd=(n*(1/(sqrt(8)*alpha))^(beta)*beta.*x.^...
    (beta-1).*exp((x1(j)/(sqrt(8)*alpha))^(beta)).*...
    exp(-(x./(sqrt(8)*alpha)).^beta));

    ET=trapz(x,pd.*(-15.15./((KCrms.*x).^(s1))).*...
    (Ucwrms./(x.*(1-Ucwrms)+Ucwrms)-0.7));

    %RESULTING DATA
    F1(j,1)=Ucwrms;
    F2(j,1)=Ucwrms;
    F3(j,1)=Ucwrms;

    if D==3
       if y==1; % Data for 2D
          if i==1
             F1(j,2)=ET;
             F1(j,6)=ET*D^2/(sqrt(g*(s-1)*(12*z0_1)^3))/60;
          else
             F1(j,4)=ET;
             F1(j,8)=ET*D^2/(sqrt(g*(s-1)*(12*z0_2)^3))/60;
          end
```

```
            else     % Data for 3D
               if i==1
                  F1(j,3)=ET;
                  F1(j,7)=ET*D^2/(sqrt(g*(s-1)*(12*z0_1)^3))/60;
               else
                  F1(j,5)=ET;
                  F1(j,9)=ET*D^2/(sqrt(g*(s-1)*(12*z0_2)^3))/60;
               end
            end

         elseif D==4
             if y==1; % Data for 2D
                if i==1
                   F2(j,2)=ET;
                   F2(j,6)=ET*D^2/(sqrt(g*(s-1)*(12*z0_1)^3))/60;
                else
                   F2(j,4)=ET;
                   F2(j,8)=ET*D^2/(sqrt(g*(s-1)*(12*z0_2)^3))/60;
                end
             else     % Data for 3D
                 if i==1
                    F2(j,3)=ET;
                    F2(j,7)=ET*D^2/(sqrt(g*(s-1)*(12*z0_1)^3))/60;
                 else
                    F2(j,5)=ET;
                    F2(j,9)=ET*D^2/(sqrt(g*(s-1)*(12*z0_2)^3))/60;
                 end
             end

         else
             if y==1; % Data for 2D
                if i==1
                   F3(j,2)=ET;
                   F3(j,6)=ET*D^2/(sqrt(g*(s-1)*(12*z0_1)^3))/60;
                else
                   F3(j,4)=ET;
                   F3(j,8)=ET*D^2/(sqrt(g*(s-1)*(12*z0_2)^3))/60;
                end
             else     % Data for 3D
                if i==1
                   F3(j,3)=ET;
                   F3(j,7)=ET*D^2/(sqrt(g*(s-1)*(12*z0_1)^3))/60;
                else
                   F3(j,5)=ET;
                   F3(j,9)=ET*D^2/(sqrt(g*(s-1)*(12*z0_2)^3))/60;
                end
             end
         end
      end
```

```
        end
    end
end
end
```

Plot

```
function P=Plot(x)
%CASE 6: THIS FUNCTION USES PLOTS THE TIME SCALE FOR BACKFILLING IN
%WAVES + CURRENT AROUND A LARGE VERTICAL PILE WHEN THE INITAL HOLE
%WAS GENERATED BY A CURRENT, FOR DIFFERENT VALUES OF Ucwrms.

%Retrieving data from the Rayleigh distibution
[R R1 R2 R3]=Rayleigh();
% R:  Data for of E[T*].
% R1: D=3 m - Data for E[T].
% R2: D=4 m - Data for E[T].
% R3: D=5 m - Data for E[T].

%Retrieving data from the Forristall distibution
[F1 F2 F3]=Forristall();
% F1: D=3 m - Data for E[T*] (Col 1-5) and E[T] (Col 6-9).
% F2: D=4 m - Data for E[T*] (Col 1-5) and E[T] (Col 6-9).
% F3: D=5 m - Data for E[T*] (Col 1-5) and E[T] (Col 6-9).

%T* for ex 1 and 2 for D=3 m
h1=figure;
set(h1, 'Position', [5 5 700 500],'Visible','off')
h=plot(R(:,1),R(:,2),'b',F1(:,1),F1(:,2),'b--',...
                         F1(:,1),F1(:,3),'b:',...
       R(:,1),R(:,3),'k',F1(:,1),F1(:,4),'k--',...
                         F1(:,1),F1(:,5),'k:');
hleg=legend('Rayleigh       KC_{rms}=0.7',...
            'Forristall 2D  KC_{rms}=0.7', ...
            'Forristall 3D  KC_{rms}=0.7',...
            'Rayleigh       KC_{rms}=1.5',...
            'Forristall 2D  KC_{rms}=1.5', ...
            'Forristall 3D  KC_{rms}=1.5');
set(hleg,'Fontsize',12)
set (h, 'LineWidth', 2.5)
axis([0 0.7 0 7])
u = [0 0.1 0.2 0.3 0.4 0.5 0.6 0.7];
set(gca,'XTick',u,'Fontsize',12);
xlabel('U_{cwrms}','Fontsize',22)
ylabel('E[T*]','Fontsize',22)
title('D=3 m','Fontsize',17);
hgexport(gcf,'../../Figures/CASE6/CASE6D3.png',...
```

```
    hgexport('factorystyle'), 'Format', 'png')


%T* for ex 1 and 2 for D=4 m
h1=figure;
set(h1, 'Position', [5 5 700 500],'Visible','off')
h=plot(R(:,1),R(:,2),'b',F2(:,1),F2(:,2),'b--',...
                         F2(:,1),F2(:,3),'b:',...
       R(:,1),R(:,3),'k',F2(:,1),F2(:,4),'k--',...
                         F2(:,1),F2(:,5),'k:');
hleg=legend('Rayleigh       KC_{rms}=0.7',...
            'Forristall 2D  KC_{rms}=0.7', ...
            'Forristall 3D  KC_{rms}=0.7',...
            'Rayleigh       KC_{rms}=1.5',...
            'Forristall 2D  KC_{rms}=1.5', ...
            'Forristall 3D  KC_{rms}=1.5');
set(hleg,'Fontsize',12)
set (h, 'LineWidth', 2.5)
axis([0 0.7 0 7])
u = [0 0.1 0.2 0.3 0.4 0.5 0.6 0.7];
set(gca,'XTick',u,'Fontsize',12);
xlabel('U_{cwrms}','Fontsize',22)
ylabel('E[T*]','Fontsize',22)
title('D=4 m','Fontsize',17);
hgexport(gcf,'../../Figures/CASE6/CASE6D4.png',...
    hgexport('factorystyle'), 'Format', 'png')


%T* for ex 1 and 2 for D=5 m
h1=figure;
set(h1, 'Position', [5 5 700 500],'Visible','off')
h=plot(R(:,1),R(:,2),'b',F3(:,1),F3(:,2),'b--',...
                         F3(:,1),F3(:,3),'b:',...
       R(:,1),R(:,3),'k',F3(:,1),F3(:,4),'k--',...
                         F3(:,1),F3(:,5),'k:');
hleg=legend('Rayleigh       KC_{rms}=0.7',...
            'Forristall 2D  KC_{rms}=0.7', ...
            'Forristall 3D  KC_{rms}=0.7',...
            'Rayleigh       KC_{rms}=1.5',...
            'Forristall 2D  KC_{rms}=1.5', ...
            'Forristall 3D  KC_{rms}=1.5');
set(hleg,'Fontsize',12)
set (h, 'LineWidth', 2.5)
axis([0 0.7 0 7])
u = [0 0.1 0.2 0.3 0.4 0.5 0.6 0.7];
set(gca,'XTick',u,'Fontsize',12);
xlabel('U_{cwrms}','Fontsize',22)
ylabel('E[T*]','Fontsize',22)
title('D=5 m','Fontsize',17);
```

```
hgexport(gcf,'../../Figures/CASE6/CASE6D5.png',...
    hgexport('factorystyle'), 'Format', 'png')


%T for all D for ex 1.
h1=figure;
set(h1, 'Position', [5 5 700 500],'Visible','off')
h=plot(R1(:,1),R1(:,2),'c',F1(:,1),F1(:,6),'c--',...
                           F1(:,1),F1(:,7),'c:',...
       R2(:,1),R2(:,2),'k',F2(:,1),F2(:,6),'k--',...
                           F2(:,1),F2(:,7),'k:',...
       R3(:,1),R3(:,2),'m',F3(:,1),F3(:,6),'m--',...
                           F3(:,1),F3(:,7),'m:');
hleg=legend('Rayleigh      D=3 m','Forristall 2D  D=3 m',...
                                  'Forristall 3D  D=3 m',...
            'Rayleigh      D=4 m','Forristall 2D  D=4 m',...
                                  'Forristall 3D  D=4 m',...
            'Rayleigh      D=5 m','Forristall 2D  D=5 m',...
                                  'Forristall 3D  D=5 m');
set(hleg,'Fontsize',11)
set (h, 'LineWidth', 2.5)
u = [0 0.1 0.2 0.3 0.4 0.5 0.6 0.7];
set(gca,'XTick',u,'Fontsize',14);
xlabel('U_{cwrms}','Fontsize',22)
ylabel('E[T]','Fontsize',22)
title('KC_{rms}=0.7','Fontsize',17);
hgexport(gcf,'../../Figures/CASE6/CASE6_T1.png',...
    hgexport('factorystyle'), 'Format', 'png')


%T for all D for ex 2
h1=figure;
set(h1, 'Position', [5 5 700 500],'Visible','off')
h=plot(R1(:,1),R1(:,3),'c',F1(:,1),F1(:,8),'c--',...
                           F1(:,1),F1(:,9),'c:',...
       R2(:,1),R2(:,3),'k',F2(:,1),F2(:,8),'k--',...
                           F2(:,1),F2(:,9),'k:',...
       R3(:,1),R3(:,3),'m',F3(:,1),F3(:,8),'m--',...
                           F3(:,1),F3(:,9),'m:');
hleg=legend('Rayleigh      D=3 m','Forristall 2D  D=3 m',...
                                  'Forristall 3D  D=3 m',...
            'Rayleigh      D=4 m','Forristall 2D  D=4 m',...
                                  'Forristall 3D  D=4 m',...
            'Rayleigh      D=5 m','Forristall 2D  D=5 m',...
                                  'Forristall 3D  D=5 m');
set(hleg,'Fontsize',11)
set (h, 'LineWidth', 2.5)
u = [0 0.1 0.2 0.3 0.4 0.5 0.6 0.7];
set(gca,'XTick',u,'Fontsize',14);
```

```
xlabel('U_{cwrms}','Fontsize',22)
ylabel('E[T]','Fontsize',22)
title('KC_{rms}=1.5','Fontsize',17);
hgexport(gcf,'../../Figures/CASE6/CASE6_T2.png',...
    hgexport('factorystyle'), 'Format', 'png')
end
```